
DEVELOPMENT AND CHARACTERIZATION OF ETHYLENE PROPYLENE DIENE MONOMER RUBBER/STYRENE BUTADIENE RUBBER BLENDS

Thesis submitted to
Mahatma Gandhi University, Kottayam
Kerala, India

in partial fulfilment of the requirements
for the award of the degree of

Doctor of Philosophy

in

Chemistry

under the

Faculty of Science

by

Muraleedharan Nair T.



Rubber Research Institute of India, Kottayam
Kerala, India

July 2006

To my Wife and Daughter

Mrs. Lakshmi K. Nair & Ms. Parvathy M. Nair

*whose constant encouragement and
inspiration made this work possible*

Certificate

This is to certify that the thesis entitled '**Development and Characterization of Ethylene Propylene Diene Monomer Rubber/Styrene Butadiene Rubber Blends**' is a bonafide record of the research work carried out by **Mr. Muraleedharan Nair T.** under our joint supervision and guidance in partial fulfilment of the requirements for the award of the degree of **Doctor of Philosophy in Chemistry** under the Faculty of Science of Mahatma Gandhi University, Kottayam. The work presented in this thesis has not been submitted for any other degree or diploma earlier. It is also certified that **Mr. Muraleedharan Nair T.** has fulfilled the course requirements and passed the qualifying examination for the Ph.D. degree of Mahatma Gandhi University.



Dr M. G. Kumaran

Joint Director (Rtd.)
Rubber Board
Kottayam
Kerala
India



Dr G. Unnikrishnan

Assistant Professor in Chemistry
National Institute of Technology
Calicut
Kerala
India


Kottayam

15. 07. 2006

Declaration

I hereby declare that the thesis entitled '**Development and Characterization of Ethylene Propylene Diene Monomer Rubber/Styrene Butadiene Rubber Blends**' is a bonafide record of the research work carried out by me under the joint supervision and guidance of **Dr M.G. Kumaran**, Joint Director (Retd.), Rubber Board, Kottayam and **Dr G. Unnikrishnan**, Assistant Professor in Chemistry, Polymer Science & Technology Laboratory, National Institute of Technology Calicut. No part of the thesis has been presented for any other degree or diploma earlier.

Kottayam
15.07. 2006


Muraleedharan Nair T.

Acknowledgements

I bow my head before **God Almighty** for the blessings showered upon me throughout this research programme.

I would like to express with great pleasure, my deep sense of gratitude and respect to my supervising teachers **Dr M. G. Kumaran**, Joint Director (Retd.), Rubber Board, Kottayam, Kerala, India and **Dr G. Unnikrishnan**, Assistant Professor of Chemistry, National Institute of Technology Calicut, Kerala, India for their excellent guidance and constant encouragement throughout my work.

I take this opportunity to express my sincere thanks to **Dr N.M. Mathew**, Director, Rubber Research Institute of India, Kottayam for providing me with the facilities to carry out the work.

I have great pleasure to express my sincere gratitude to **The Director of Industries and Commerce**, Govt. of Kerala, for granted no objection certificate for utilising the laboratory facilities and for doing research.

I am deeply indebted to **Prof. (Dr) K. E. George** and **Prof. (Dr) Rani Joseph**, of Department of Polymer Science and Rubber Technology, CUSAT, Kerala, India for their cooperation and encouragement.

I am awfully grateful to **Dr V.B. Pillai**, Scientist and **Dr N.R. Manoj**, Technical Officer of NPOL, Cochin for their invaluable help and support.

I am Thankful to **Dr K.T. Thomas**, Dy. Director, **Dr Rosamma Alex**, Scientist, **Mr. Madusoodhanan**, Rubber Chemist, of RRII for their invaluable help.

I take this opportunity to express my gratitude to **Dr Peter Koshy**, Dy. Director, Regional Research Laboratory, Thiruvananthapuram. for getting scanning electron micrographs of test samples.

I am gratefully indebted to **Dr C.K. Radhakrishnan**, Head, Department of Chemistry, MAMO College, Makkam and **Dr A. Sujith**, National Institute of Technology Calicut for the support given to me.

I express my sincere gratitude to **Dr Sam Kunchandy**, Reader, S. N. College, Chengannur for his constant encouragement and help throughout this work.

I convey my indebtedness to my wife **Mrs. Lakshmi. K. Nair**, Senior Lecturer, N.S.S. Training College, Changanassery and my daughter **Ms. Parvathy M. Nair** for their unwavering moral support.

I would also like to offer my sincere gratitude to **Mr. T. Venugopal**, Reference Librarian, High Court of Kerala and **Dr. Gem Mathew**, Lecturer, St. Thomas College, Palai.

I express my sincere thanks to **Mr. Harish Kumar V. K.**, Angel DTP & Photostat for his initial helps.

I express my gratitude to **Mr. Shibu K. V.**, Minitek Computers, Athirampuzha for applying skill and experience for preparing the final layout and printing work of the thesis in time.

I am also thankful to all my relatives, friends and well wishers for their encouragement throughout this work.

Kottayam
15.07.2006

Muraleedharan Nair T.

Glossary of Terms

ABS	–	Acrylonitrile butadiene styrene copolymer
AFM	–	Atomic force microscopy
ACM	–	Polyacrylic rubber
BR	–	Polybutadiene rubber
CR	–	Chloroprene rubber
CRI	–	Cure rate index
C_a	–	Capillary number
d_e	–	Particle size at equilibrium
DCP	–	Dicumyl peroxide
DSC	–	Differential scanning calorimetry
DMA	–	Dynamic mechanical analysis
DTA	–	Differential thermal analysis
DIPDIS	–	Bis (diisopropyl) thiophosphoryl disulphide
DTG	–	Differential thermogravimetry
E'	–	Storage modulus
E''	–	Loss modulus
E_{dk}	–	Bulk breaking energy
ENR	–	Epoxidised natural rubber
ENB	–	5-ethylidene-2-norbornene
EPDM	–	Ethylene propylene diene monomer rubber
EPR	–	Ethylene propylene monomer rubber
EVA	–	Poly (ethylene-co-vinyl acetate)
EPDMSH	–	Mercapto-modified EPDM
GPF	–	General purpose furnace black
HAF	–	High abrasion furnace
HDPE	–	High density polyethylene
IPN	–	Interpenetrating network
IR	–	Polyisoprene rubber
LLDPE	–	Linear low density polyethylene
M	–	Mixed system

M_1	–	Mechanical property of component 1
M_2	–	Mechanical property of component 2
MPa	–	Mega pascal
MBTS	–	Mercaptobenzothiazyl disulphide
NBR	–	Acrylonitrile-co-butadiene rubber/Nitrile rubber
NR	–	Natural rubber
NMR	–	Nuclear magnetic resonance spectroscopy
PA6	–	Polyamide 6
PBPC	–	Polymer bound predispersed chemicals
PC	–	Polycarbonate
PDMS	–	Poly dimethyl siloxane
PE	–	Polyethylene
PMMA	–	Poly methyl methacrylate
PP	–	Polypropylene
PS	–	Polystyrene
PU	–	Polyurethane
PVC	–	Poly vinyl chloride
PET	–	Polyethylene terephthalate
R	–	Universal gas constant
S	–	Sulphur
SAN	–	Styrene acrylonitrile copolymer
SBR	–	Styrene butadiene rubber
SEM	–	Scanning electron microscopy
SMR	–	Standard Malaysian rubber
t	–	Time
t_c	–	Critical coalescence time
t_2	–	Scorch time
$\tan \delta$	–	Dissipation factor
TMA	–	Thermomechanical analysis
TEM	–	Transmission electron microscopy
T	–	Temperature
T_g	–	Glass transition temperature

TGA	–	Thermogravimetric analysis
t_{90}	–	Temperature of 90 % curing
TMTD	–	Tetramethyl thiuram disulphide
ϕ_1	–	Volume fraction of component 1
ϕ_2	–	Volume fraction of component 2
ν	–	Crosslink density
ρ	–	Density
σ	–	Modulus
τ_{12}	–	Shear stress
η	–	Viscosity
ϕ_d	–	Volume fraction of dispersed phase
ΔG_{mix}	–	Free energy change during mixing
ΔH_m	–	Enthalpy change
ΔS	–	Entropy change
λ	–	Extension ratio
γ	–	Shear rate
ψ	–	Packing fraction

Contents

Preface

Chapter 1

Introduction	1
1.1 Polymer blends	2
1.2 Types of polymer blends	2
1.2.1 Classification on the basis of miscibility.....	2
1.2.2 Classification on the basis of constituents.....	3
1.3 Blending techniques	3
1.3.1 Mill mixing.....	3
1.3.2 Chemical and mechano-chemical blending.....	3
1.3.3 Melt blending technique.....	4
1.3.4 Solution blending	4
1.3.5 Latex blending.....	5
1.3.6 Freeze-drying	5
1.3.7 Blending techniques-Merits and demerits.....	5
1.4. Polymer compatibility and miscibility	6
1.4.1 Compatibility.....	6
1.4.2 Miscibility	8
1.4.3 Thermodynamics of polymer miscibility	9
1.5 Properties of polymer blends.....	11
1.6 Theoretical considerations of blend phase morphology and Technological acceptability.....	12
1.6.1 Polymer ratio	12
1.6.2 Phase morphology	12
1.6.2.1 Phase morphology development	13
1.6.2.2 Dispersed morphology	17
1.6.2.3 Co-continuous morphology.....	19
1.6.2.4 Nanostructured polymer blends	21
1.6.3 Interfacial adhesion/crosslinking.....	23
1.6.4 Distribution of fillers.....	23
1.6.5 Distribution of plasticizers between the elastomers.....	24
1.6.6 Distribution of cross-links between the polymers.....	25
1.7 Characterisation of polymer blends.....	25
1.7.1 Microscopy.....	25
1.7.1.1 Optical microscopy	25
1.7.1.2 Scanning electron microscopy	26

1.7.1.3	Transmission electron microscopy.....	27
1.7.1.4	Atomic force microscopy	27
1.7.2	Thermo gravimetric analysis.....	27
1.7.3	Differential scanning calorimetry.....	29
1.7.4	Dynamic mechanical analysis	30
1.7.5	Spectroscopic techniques	32
1.7.5.1	Nuclear magnetic resonance (NMR).....	32
1.7.5.2	Fourier transform infrared spectroscopy (FTIR).....	32
1.8	Review of literature	32
1.9	Scope and Objectives	42
	References	45

Chapter 2

Materials and Experimental Techniques	56
2.1. Materials	57
2.1.1 Ethylene propylene diene monomer rubber (EPDM)	57
2.1.2 Styrene butadiene rubber (SBR)	58
2.1.3 Rubber chemicals and fillers	59
2.2 Blend preparation	61
2.3 Characterisation of blends	62
2.3.1 Mechanical properties	62
2.3.2 Morphology	64
2.3.3 Thermal analysis	64
2.3.3.1 Thermogravimetric analysis (TGA)	64
2.3.3.2 Differential scanning calorimetry (DSC)	64
2.3.4 Dynamic mechanical analysis (DMA)	64
2.3.5 Ageing studies	65
References	66

Chapter 3

Mechanical Properties of EPDM/SBR Blends.....	67
3.1 Introduction	68
3.2 Results and Discussion	69
3.2.1 Cure characteristics	69
3.2.2 Mechanical properties	71
3.3 Morphology	81
3.4 Model fitting.....	83
3.5 Conclusion.....	85
References	87

Chapter 4	
Mechanical Properties of Filled EPDM/SBR Blends	89
4.1 Introduction	90
4.2 Results and Discussion	91
4.2.1 Cure characteristics	91
4.2.2 Mechanical properties	93
4.2.3 Conclusion	99
References	100
Chapter 5	
Thermal Analysis of EPDM/SBR Blends	102
5.1 Introduction	103
5.2 Results and Discussion	104
5.2.1 Thermogravimetric analysis (TGA)	104
5.2.1.1 Effect of blend composition	104
5.2.1.2 Effect of cross-linking systems	110
5.2.1.3 Effect of fillers	113
5.3 Differential scanning calorimetry (DSC)	117
5.3 Conclusion	120
References	121
Chapter 6	
Dynamic Mechanical Analysis of EPDM/SBR Blends	122
6.1 Introduction	123
6.2 Results and Discussion	124
6.2.1 Storage modulus	124
6.2.1.1 Effect of blend ratio	124
6.2.1.2 Effect of curing agents	126
6.2.1.3 Effect of fillers	127
6.2.2 Loss modulus	129
6.2.2.1 Effect of blend ratio	129
6.2.2.2 Effect of curing agents	131
6.2.2.3 Effect of fillers	131

6.2.3 Loss tangent.....	133
6.2.3.1 Effect of blend ratio.....	134
6.2.2.2 Effect of curing agents	136
6.2.3.3 Effect of fillers	137
6.2.4 Effect of frequency.....	139
6.2.5 Theoretical modelling	140
6.3 Conclusion.....	142
References	143

Chapter 7

Ageing Studies on EPDM/SBR Blends.....	145
7.1 Introduction	146
7.2 Results and Discussion	148
7.2.1 Thermal ageing.....	148
7.2.2 Ozone ageing.....	153
7.2.3 Gamma irradiation.....	156
7.2.4 Water ageing	160
7.3 Conclusion.....	160
References	162

Chapter 8

Conclusion and Future Outlook	165
8.1 Conclusion.....	166
8.2 Future outlook.....	168
8.2.1 Use of compatibilisers.....	168
8.2.2 Examination of electrical properties	168
8.2.3 Effects of other types of fillers.....	168
8.2.4 Oil resistant and heat resistant polymer	169
8.2.5 Fabrication of useful products.....	169

List of Publication

Curriculum Vitae

Preface

Polymer blends attract interest due to the fact that new molecules are not always required for the preparation of materials with desirable macroscopic properties and that the blending is more rapid and economical than the development of a completely new polymer.

Ethylene propylene diene monomer rubber (EPDM) is used for various purpose in industry because of its excellent resistance to heat, ozone and weather. EPDM is unique for its efficiency in higher filler and oil loading. Styrene butadiene rubber (SBR) is a general purpose elastomer having high filler loading capacity, good flex resistance, crack-initiation resistance and abrasion resistance. The goal of the present work is to develop and characterize a blend system based on EPDM and SBR. The background, objectives and the results of the investigation have been presented in eight chapters, in this thesis.

Chapter 1 contains the fundamentals of blending, different blend characterization techniques and a review of the earlier works on different polymer blend systems. This Chapter also highlights the scope and objectives of the present investigation. The details of the materials used and experimental techniques adopted are given in Chapter 2.

Chapter 3 deals with the cure characteristics, morphology and mechanical properties of EPDM/SBR blends with respect to the blend ratio and crosslinking systems. In Chapter 4, the effects of black and non black fillers on the cure

characteristics and mechanical properties of the present blend system have been discussed.

Chapter 5 contains the results of the thermal analysis of the present blend system. The thermal behaviour has been followed by thermogravimetry (TG) and differential scanning calorimetry (DSC).

The dynamic mechanical analysis (DMA) was carried out to examine the viscoelastic behaviour of the blends. The results on storage modulus, damping characteristics and glass transition temperature at varying temperatures and frequencies are presented in Chapter 6. Chapter 7 gives the results of the examination of the ageing characteristics of the blend systems after exposing them to various degrading agents such as heat, ozone, water and gamma radiation.

Chapter 8 presents a general conclusion based on the results obtained from the above studies and the scope of future work.

Chapter 1

Introduction

Abstract

Polymer blends become versatile materials of polymer industry today since their properties can satisfy a wide spectrum of customer demands. In this chapter, the fundamentals of blending, reasons for blending, blend classification and characterization are presented. A review of the recent works on different polymer blend systems has been included. The scope and objectives of the present investigation are also discussed.

1.1 Polymer blends

The concept of physical blending of two or more existing polymers to obtain new products has gained significant attention over the years [1-5]. The aim of polymer blending is to develop products with attractive properties, which cannot be attained with individual components. The blending technique is quite attractive due to the fact that the already existing polymers can be used for it and thus the costly development of new polymers via polymerization or by the copolymerization of new monomers can be avoided. Another attraction of blending technology is the opportunities for the reuse and recycling of polymer wastes.

1.2 Types of polymer blends

Blends are broadly classified on the basis of miscibility and the constituents present.

1.2.1 Classification on the basis of miscibility

On the basis of miscibility, blends are of three types.

1. Completely miscible blends for which $\Delta H_m < 0$ due to specific interactions; homogeneity is observed at least on a nanometer scale, if not on the molecular level. This type of blends exhibit only one glass transition temperature (T_g), which is in between the T_g s of both the blend components in a close relation to the blend composition.
2. Partially miscible blends in which a part of one blend component is dissolved in the other. This type of blends with satisfactory properties are referred to as compatible. Both blend phases are homogeneous, and the T_g s are shifted from

the value for one blend component towards the T_g of the other component. In this case, the interphase is relatively wide and the interfacial adhesion is good.

3. Fully immiscible blends in which the interface is sharp and have a coarse phase morphology. These types of blends are having poor adhesion between the blend phases.

1.2.2 Classification on the basis of constituents

On the basis of constituents present in the blend, polymer blends are classified as:

1. Rubber/rubber blends
2. Plastic/plastic blends
3. Rubber/plastic blends

Among these the rubber/rubber blends have drawn considerable attention due to their wide range properties and applications.

1.3 Blending techniques

1.3.1 Mill mixing

Polymer blends, particularly those of elastomers, can be prepared in two-roll mixing mills. Roll mills are completely open to air and dust, a disadvantage, but they are the easiest mixing devices to clean. The mixing effectiveness of a two-roll mixing mill can vary from good to very poor depending upon the rheology of the components and the skill of the operator.

1.3.2 Chemical and mechanochemical blending

A chemical polyblend is given by polymeric systems in which long monomer sequences of one kind are chemically linked to similar monomer sequences of different kind in

either the axial direction or in the cross direction giving block copolymer or graft copolymer structures respectively. Selective or random cross-linking of mechanical blends may ultimately lead to mutual grafting, co-cross-linking or intercross-linking resulting in the formation of mechanochemical polyblends which may often appear as an interpenetrating polymer network (IPN) of structurally different polymers [6]. Such polyblends are commonly characterized by relatively uniform phase morphology with remote chance for gross phase separation, improved mechanical strength, thermal stability, chemical resistance and durability.

1.3.3 Melt blending technique

Blends can be prepared by melt mixing the ingredients in an internal mixture. Melt blending avoids contamination, solvent or water removal etc. The primary disadvantages of melt mixing are the chance for degradation and the high cost of the equipment. In most cases, a large difference in the melt viscosity of the components explains the difficulty. Cleaning of the mixer between each mixing is difficult. Mixing of small quantities below 5 g is also practically impossible [7].

1.3.4 Solution blending

Casting of a blend from a common solvent is the simplest mixing method available and is widely practiced. The method requires that the component polymers could be dissolved in a common solvent. Very small quantities of experimental polymers can be handled easily. In this case degradation is not a problem. There are certain limitations to this method. Not all polymers are readily soluble in common solvents. Residual solvents can influence the results of an analysis. It is difficult to make thick films.

1.3.5 Latex blending

Emulsion polymerization is employed for the preparation of rubber toughened plastic blends. The polymers should be in the latex or emulsion form. The mixing process of these micro-size latices and the subsequent removal of water produce excellent dispersion and distribution of discrete phase.

1.3.6 Freeze-drying

With freeze-drying, a solution of the two polymers is quenched down to a very low temperature and the solvent is frozen. Ideally, the polymers will have little chance to aggregate and will collect randomly in regions throughout the frozen solvent. Thus the state of the dilute solution is somewhat preserved. Solvent is removed by sublimation; no changes can occur because of the solid nature of the mixture. To a large extent, therefore, the resulting blend will be independent of the solvent, if the solution is single phase before freezing and the freezing occurs rapidly. Freeze drying seems to work best with solvents having high symmetry.

1.3.7 Blending techniques- Merits and demerits

Mill mixing or melt blending of the constituent polymers results in mechanical polyblends. Chemical polyblends formed by the chemical linkage of long monomer sequences of one kind to similar long monomer sequences of different kind give block co polymers or grafted co polymers. The random cross-linking of mechanical blends forms the mechano-chemical polyblends, which ultimately leads to mutual grafting, and co cross-linking. In solution blending, selected diluents are used to dissolve the component polymers and in latex blending, different latices are blended to form the polyblends.

The preparation of mechanical polyblends by mill mixing or melting is problem free compared to blending by other methods. High shearing forces for the mechanical blending of high molecular weight elastomers necessitate the use of open roll mills, internal mixers, etc. Comparable polymer viscosities at the mixing temperature are desirable for the ease of dispersion in open roll mills [8]. In solution casting, the removal of the diluents may lead to uncertain changes in the phase morphology, thus weakening the blend. Latex blending offers the possibility of finer scale dispersion than solution and melt blending. Latex blending does not have any major technical advantages over other methods, although some claims have been made of more homogeneous dispersion of carbon black in cis - BR latex, blended with NR or SBR latex. The mechano chemical blending technique is more widely used for elastomer- plastic blends.

1.4 Polymer compatibility and miscibility

1.4.1 Compatibility

Compatibility in technological sense is used to describe whether the result occurs as desired when two materials are combined together. Compatibility does not mean complete miscibility. Most polymer pairs are not miscible but are compatible as the polymer pairs achieve the desired properties. Marsh et al. [9] showed that among the three blends studied, viz; poly isoprene rubber (IR)-styrene butadiene rubber (SBR), IR-polybutadiene rubber(BR) and SBR-BR, only SBR-BR appeared homogeneous and the others behaved as micro-heterogeneous. According to some researchers, compatibility does not necessarily imply one-phase mixtures but kinetically stabilized mixtures with desirable properties and good adhesion between the phases. For many purposes, miscibility in polymer blends is neither a

requirement nor desirable, however, adhesion between the components is an essential requirement for better blend performance.

The practical utility of a blend is determined by its compatibility. The blends may be miscible or immiscible depending on thermodynamic requirements. Miscible blends are thermodynamically stable molecular level mixtures. Immiscible blends are separated into macroscopic phases with very minimum interfacial adhesion and unstable phase morphology. The interface between immiscible polymers in polymer blends can be schematically represented as in Figure 1.1. Generally, an interface is considered as a region having a finite distance neighbouring the dispersed phase. The properties of the interfacial region can differ from those of pure components. Lack of strong interface between polymer pairs limits the stress transfer across the phase boundaries. It is clear from this figure that the interaction between polymers A and B are very weak resulting in a very thin interface [10].

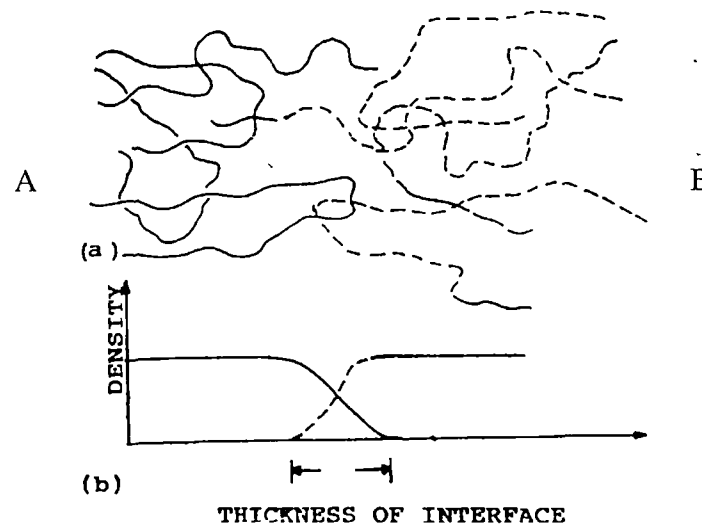


Figure 1.1. (a) Interface between immiscible polymers and (b) interfacial density profile between immiscible polymers. [J. Noolandi, *Polym. Eng. Sci.* 24, 70 (1984)]

Most of the blends are immiscible and incompatible due to lack of favourable interactions between the component polymers at the interfaces. This will result in a high interfacial tension between the phases, which leads to a coarse and unstable morphology. In addition, a high interfacial tension results in a narrow interface, poor physical and chemical interactions across the phase boundaries and, as a consequence, a poor interfacial adhesion between the phases. For a multiphase system like elastomer-elastomer blend, the mechanical behaviour depends critically on two demanding structural parameters; a proper interfacial tension leading to a phase size small enough to allow the material to be considered as macroscopically homogeneous and an interface adhesion strong enough to assimilate stresses and strain without disruption of the established morphology.

The rubber compounders faced problems when they tried blends from polar and non-polar rubbers. Polymer bound pre-dispersed chemicals (PBPC) are the first remedy to address these issues. It is techno-economic sense to use a single binder system for the full range of chemicals. The favoured binder system is based on the non-polar EPDM due to its good ageing and heat resistance and its slow curing characteristics. Manufacturers of PBPCs make use of various processing aids including compatibilizers in the EPDM binder so that the PBPCs offered are compatible with either polar or non-polar formulation components.

1.4.2 Miscibility

Miscibility, according to Stein et al [11] is more observed in blends those showed a single glass transition temperature (T_g). Normally the glass transition temperature of a polymer blend will be intermediate between the T_g s of the component

elastomers. Yuen and Kinsinger[12] showed that blends made from incompatible polymers are usually translucent or opaque and weak. Obviously, besides film clarity, blends of compatible polymers exhibit good mechanical properties, especially tensile strength while the performance of blends of incompatible polymers have been reported to exhibit a broad minimum in tensile strength.

The better performance of the final product depends on the extent of miscibility or compatibility of the component polymers in a rubber-rubber blend. Prediction of miscibility of polymer pairs is considerably complicated because the polymer molecules in general are associated with large molecular weight, of the order of hundreds of thousands and because the segments are constrained by their neighbouring segments. As a result they cannot be moved to fill any available site in a lattice model, often used for estimating thermodynamic parameters. This is only one example of the complicating differences between polymer molecules and small molecules that must be worked out in achieving successful prediction of polymer-polymer miscibility. The other factors are the small entropy change on mixing, the volume change for mixing, the polydispersity of molecular weight, the heterogeneity in molecular composition, the complex morphology, the slow relaxation of stress and strain and the influence of processing parameters on miscibility.

1.4.3 Thermodynamics of polymer miscibility

The thermodynamics of polymer miscibility can be explained by Gibb's free energy of mixing (ΔG_{mix}). It is a well accepted theory that for two polymers to be miscible, the (ΔG_{mix}) must be negative as given by the thermodynamic equation,

$$\Delta G_{\text{mix}} = \Delta G_{\text{mix}} - T\Delta S_{\text{mix}} \quad (1.1)$$

where ΔH_{mix} is change in enthalpy, ΔS_{mix} is change in entropy and T the temperature in absolute scale. ΔG_{mix} gives negative values only when ΔH_{mix} has a negative value or ΔS_{mix} has a higher value. A low value of ΔS_{mix} for high molecular weight polymers indicates that the polymers are miscible and that the thermodynamic factor contributing to the miscibility of polymers is enthalpy of mixing. The important criteria for a complete miscibility of a polymer blend at constant pressure and temperature are

$$\Delta G_m < 0, \quad \text{and} \quad (1.2)$$

$$\frac{\partial^2 \Delta G_m}{\partial \phi_2^2} > 0 \quad (1.3)$$

However the change in free energy of a binary mixture (ΔG_m) can vary with composition as shown in Figure 1.2.

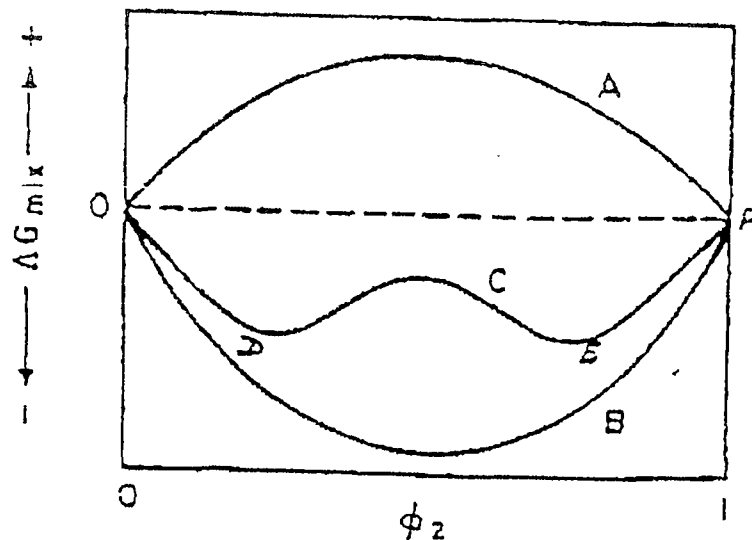


Figure 1.2 Possible free energy of mixing diagrams for binary mixtures

In Figure 1.2, the curve OBP satisfies both conditions for all ϕ values and represents a completely miscible binary system. The compositions OD and PE of

the curve OCP satisfy both the conditions, but the compositions DCE, although satisfying the first condition, fails to satisfy the second. Hence they represent immiscible states and separate into two phases having different compositions with different volume fractions of components A and B. The system represented by curve OAP is immiscible for all compositions because $\Delta G_m > \text{zero}$.

1.5 Properties of polymer blends

The behaviour of two polymers in a mixture or blend is not necessarily the same as expected from the behaviour exhibited by them in their isolated forms. The ultimate polyblend properties are dependent on:

1. Extent of phase separation
2. Nature of the phase provided by the matrix material
3. Properties of the component polymers [13, 14]
4. Interaction between the component polymers
5. Morphology [15-18], compatibility or miscibility between polymers [19, 20]

It has been noted that the different physical properties of all miscible polyblends follow an arithmetical semi empirical rule [21, 22] by the following equation;

$$P = P_1 \phi_1 + P_2 \phi_2 + I \phi_1 \phi_2 \quad (1.4)$$

where P is the property of interest, ϕ is the concentration and I is an interaction term that can be positive, negative or zero. Depending upon these values, polyblends may behave like mixtures when I is zero, exhibit higher polyblend property (synergistic effect) when I is positive and show lower polyblend properties (antisynergistic effect) when I is negative.

In the case of an immiscible polyblend giving a continuous phase (P_1) and a dispersed phase (P_2), Eq.1.2 is not feasible for property analysis. Hence another semi-empirical relationship is used to analyze the physical properties, given by

$$\underline{P_2} = \frac{1 + AB\phi_2}{P_1 - B\psi\phi_2} \quad (1.5)$$

where ϕ_2 is the concentration of the dispersed phase, 'A' the shape and orientation of the dispersed phase, 'B' the relative values of the properties P_1 , P_2 and A, ' ψ ' a reduced concentration term (packing fraction).

1.6 Theoretical considerations of blend phase morphology and technological acceptability

1.6.1 Polymer ratio

In general, the polymer with higher fraction and, if assisted with a lower Mooney viscosity usually (but not necessarily so), forms the continuous phase with another polymer dispersed in it. Technologically this is important as the continuous phase gives the desired main vulcanizate properties e.g. EPDM for better ozone protection, NBR for better oil resistance and BR for better wear resistance.

1.6.2 Phase morphology

Fine phase sizes of $\leq 10 \mu\text{m}$ are technologically desired and this can be achieved by using high mixing shear forces [23, 24, 25] even without the use of processing aids or compatibilisers. For a non-polar and a highly polar rubber blend such as natural rubber (NR)/acrylonitrile butadiene rubber (NBR), interfacial tension imposes a limit on the phase size that can be attained without the use of a compatibiliser, and the phase sizes may even increase with prolonged mixing.

1.6.2.1 Phase morphology development

The control of phase morphology is the key issue when desired properties have to be imparted to polymer blends. The shape, size, and spatial distribution of the phases result from a complex interplay between viscosity (and elasticity) of the phases, interfacial properties, blend composition and processing parameters. The investigations made by Scott and Macosko [26], in the case of model polystyrene (matrix)-amorphous nylon (dispersed phase) blends, showed how and to what extent was the blend morphology developed during the short reactive processing. The morphology development at short mixing times can be summarized as follows:

- The dispersed phase forms sheets or ribbons in the matrix
- Holes appear in these sheets or ribbons as a result of interfacial instability
- Size and number of holes increase which leads to lace structure
- Lace breaks down into irregularly shaped pieces of diameter close to the ultimate particle size
- Break-up of drops and cylinders lead to the final spherical droplets (Figure 1.3) At intermediate mixing times, thus in the melt state, mixing affects only the size of the largest particles which are transformed into smallest ones, so leading rapidly to an almost invariant morphology governed by the dynamic equilibrium between domain break-up and coalescence

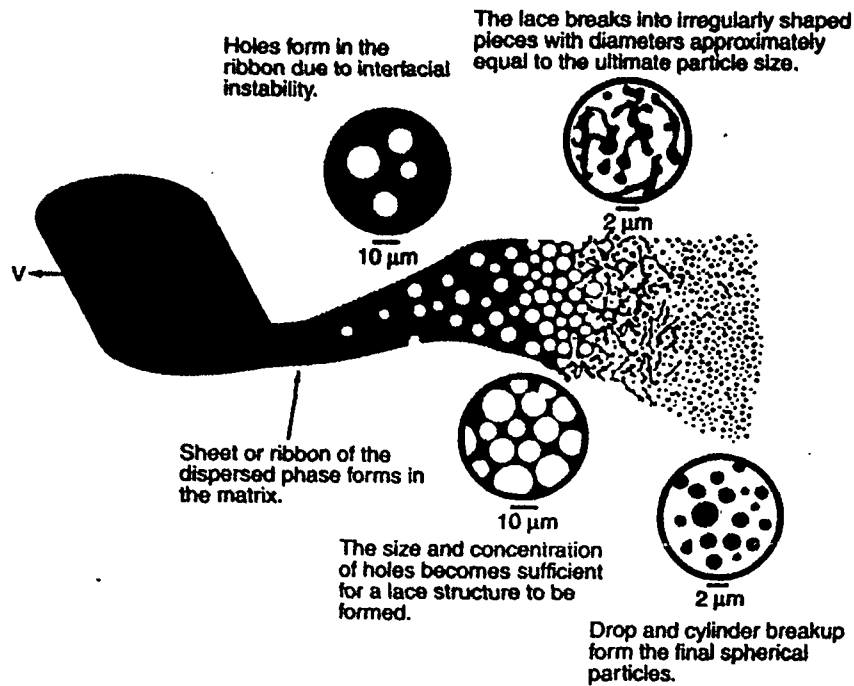


Figure 1.3. Mechanism proposed for the initial morphology development in polymer blends [C.E.Scott and C.W. Macosko, *Polymer*, 35, 5422 (1994)]

Morphology of an elastomer blend explains how the rubber phase is dispersed as domains in another continuous rubber matrix. Since the size distribution changes with composition, the dispersed phase dimension increases with increasing concentration of the rubber phase due to coalescence.

Coalescence process, may arise from several types of interactions such as:

- Van der waals forces between neighbouring particles
- Capillary forces
- Buoyancy resulting from the different gravities of the two components and
- Friction resulting from viscous flows.

Tokita's equation [27], explains the dependence of concentration of the dispersed phase on the coalescence rate.

$$d_e \cong 24P_r\sigma/\pi\tau_{12}\{\phi_d + (4P_rE_{dk}/\pi\tau_{12})\phi_d^2\} \quad (1.6)$$

Where d_e is the particle size at equilibrium, τ_{12} is the shear stress, σ is the interfacial tension, E_{dk} is the bulk breaking energy, ϕ_d is the volume fraction of the dispersed phase and P_r is the probability that a collision to result coalescence. From the equation it is clear that as the volume fraction of the dispersed phase increases, d_e increases. When the lower viscosity component forms the dispersed phase, due to the restricted diffusion of the dispersed particles in more viscous medium, the rate of coalescence decreases. The critical coalescence time t_c is given as:

$$t_c = (3\eta_m R/2\sigma) \ln(R/2h_c) \quad (1.7)$$

Where η_m is the matrix viscosity, R is the radius of particle and h_c is the critical separation distance between the particles.

Favis and Chalifoux [28] investigated the influence of composition on the morphology of polypropylene (PP)/polycarbonate (PC) blends. They studied the size and size distribution of the minor phase in the melt blended state as a function of composition and reported that composition had a marked effect on the dispersed phase size particularly at intermediate concentrations where the region of dual phase co-continuity was observed. Wu [29] studied the notched impact toughness of nylon-rubber blends and found that a sharp tough-brittle transition occurred at a critical particle size when the rubber volume fraction and rubber-matrix adhesion were held constant.

Another important factor, which influences the phase morphology, is the viscosity ratio. The relative importance of the applied viscous forces and the counter rotating

interfacial forces can be expressed in terms of a dimensionless number called capillary number (Ca), which is given by;

$$Ca = \frac{\eta_m \dot{\gamma} R}{\tau} \quad (1.8)$$

where η_m is the viscosity of the matrix, $\dot{\gamma}$ is the shear rate, R is the droplet radius and τ is the interfacial tension. When Ca exceeds a critical value, the droplet will deform and subsequently break up under the influence of the interfacial tension. However one should note that the critical Ca value for breakup of the droplet strongly depends on the viscosity ratio, P .

Favis and Chalifoux [28] reported that lowering the viscosity ratio of the blends from 7 to 2 has a significant impact on the phase size/composition relationship and the region of dual phase continuity is found to shift to a higher composition. However, the position and shift of the region of dual phase continuity are not consistent with predictions based exclusively on composition and viscosity ratio.

Recently a number of researchers have attempted to incorporate the viscoelastic effects into general models related to the morphology of polymer blends. These include the studies of Scholz et al. [30], Graebbling and Muller [31], Palierne [32] and Lee and Park [33]. In their studies on the rheological properties of immiscible polymer blends in the melt stage, a pronounced appearance of elasticity due to the interfacial tension was reported at low frequency. The morphological state of the blends was strongly influenced by the elastic properties of the system. The model due to Palierne [32] accounts for the linear viscoelastic nature of the component phases and the particle size distribution in non-dilute emulsions. This interesting

model takes into account the size of the viscoelastic droplets dispersed in a viscoelastic matrix and the interfacial tension between the components

The Palierne approach has been used successfully to predict the interfacial tension between several polymers. For example, Asthana and Jayaraman [34] used the Palierne model to estimate the interfacial tension in reactively compatibilised blends. On the other hand, Utracki [35] has successfully tested the constitutive equation to describe the morphology generation in immiscible polymer blend systems developed by Lee and Park, using the experimental results obtained on linear low density polyethylene (LLDPE)/polystyrene (PS) blends.

1.6.2.2 Dispersed morphology

The commonly accepted mechanism by which a dispersed morphology is controlled involves particle elongation in the imposed flow field and then its successive break-up into smaller particles until critical conditions are reached at which the equilibrium size is attained. The morphological parameters such as size, shape, interfacial area, uniformity and distribution and the interparticle distance of dispersed particle affect the ultimate properties of the blends.

The dispersed phase morphology of polymer blends is also strongly influenced by the composition of the blends. Increasing the fraction of the dispersed phase results in an increase in the particle size due to coalescence. Indeed, by increasing the concentration of the second phase, the number of particles in the system increases leading to an enhanced number of particle-particle collisions, which accounts for the increased coalescence. The influence of the elasticity ratio on the dispersed phase morphology of binary polymer/polymer blends is still not well understood. Several

factors are yet to be explored in this area. Van Oene [36] performed a classical study in this area to understand the effect of the elasticity ratio. According to this, there are two modes of dispersion in capillary flow: the stratification and droplet–fiber formation. The generation of these microstructures is controlled by the particle size, the interfacial tension, and the difference in viscoelastic properties between the two phases. For blends of polymethyl methacrylate (PMMA) and polystyrene (PS), which showed high stress, was observed to form particles of PMMA in PS matrix. Addition of low molecular weight PMMA to the same system resulted in stratification. When the dispersed particle size is smaller than 1 μm , the difference in morphology (droplets vs stratification) vanished showing that the elastic contribution to the interfacial tension was no longer dominant. The elastic contribution to the interfacial tension can lead to the encapsulation of the lower elasticity component by the higher elasticity component. The studies by Migler [37] and Hobbie and Migler [38] clearly demonstrated that due to the high droplet elasticity, the droplet could align in the vorticity direction rather than in the flow direction. This behaviour was related to the high normal forces in the droplets and the presence of closed strain lines that form in the flow gradient plane. Elmendorp and Van der Vegt [39] had suggested that molecular weight of the matrix might have an influence on the coalescence process. The role of the molecular weight on the coalescence process has been examined by Park et al. [40]. They carefully monitored the droplet trajectories during glancing collisions. The influence of shear on the phase morphology has also been investigated. It was suggested based on Taylor's analysis, the dispersed phase size should be inversely proportional to the applied

shear stress. Min et al. [41] found that for poly ethylene (PE)/ polystyrene(PS) blend system, a fine morphology was created by the application of a high shear stress. In this blend system, the shear stress appears to predominate over the viscosity ratio. However, other authors [42-44] showed that varying the shear stress by a factor of 2 to 3 had little effect on the particle size. Favis [45] pointed out that the dispersed phase morphology has not highly sensitive to changes in shear stress and shear rate in an internal mixer. These results suggest that the Taylor's theory overestimates particle size. The studies performed by Sundararaj and Macosko [46], and Cigana et al. [47] also came to the same conclusion and they related this to the viscoelastic nature of the droplet.

1.6.2.3 Co-continuous morphology

Conventionally, a co-continuous phase structure is defined as the coexistence of at least two continuous structures within the same volume in which each component is a polymer phase with its own internal network like structure from which its properties result. It can also be defined the co-continuous structure as one in which at least a part of each phase forms a coherent continuous structure that permeates the whole volume. Contrary to dispersed type morphology, the mechanism and the key control of the co-continuous type are still not well understood. The complexity arises mainly from the ambiguous effect of the visco-elastic characteristics of the components, their composition, and the magnitude of interfacial tension.

The co-continuous phase morphology has been intensively investigated by various researchers [48-57]. The concept of co-continuity was first introduced as a narrow range of compositions where phase inversion occurs. Most of the studies have

focused on the prediction of the composition of this phase inversion. An important challenge in the study of co-continuous polymer blends is the accurate determination of their morphology. A variety of methods have been used for detecting co-continuity including solvent extraction, microscopy with image analysis, electrical conductivity measurements, and rheological measurements. Although there exist a large number of techniques, solvent extraction has been the most common choice for the characterisation of the co-continuity. The effect of sample size on the results of solvent extraction for detecting co-continuity in polymer blends has been examined by Galloway and co-workers [48]. It has been demonstrated that the co-continuity is clearly affected by the interfacial tension between the phases, by the processing conditions such as mixing time and type of flow, and by the rheological characteristics of the blend components. Modified theories of phase inversion have also been proposed in which the effect of elasticity of the blend components on phase inversion, accounted satisfactorily [58-59]. Such studies are based on the work of Van Oene [36] who proposed a relation for the elastic contribution to the effective interfacial tension under dynamic conditions. In fact Bourry and Favis [60] suggested an elastic contribution in the encapsulation phenomena and proposed a model based on the elasticity ratio. According to this model, the more elastic phase tends to encapsulate the less elastic one.

Willemsse et al. [51,53] introduced a semi-empirical model based on geometrical and microrheological considerations. This model implies a range of compositions within which fully co-continuous structures can exist. Combination of the geometrical requirements with micro-rheological considerations for stability of extended

structures leads to the development of the new model describing the critical volume fraction for the minor phase as a function of matrix viscosity, interfacial tension, shear rate, and phase dimensions. Li and Favis [61] reported the role of the blend interface type on the co-continuous morphology. These authors proposed a classification of the blend interfaces, which provides a general framework for the role of the interfaces on co-continuous morphology development.

In recent years, several strategies have been developed to form well-defined and predictable multi-component polymer structures with phase separation at the nano scale [62]. The most straightforward approach is to use linear block copolymers with components A and B. However the most important drawback of this approach is that both components A and B with their different chemical and electronic structures have to be connected by a covalent bond, which limits the availability of bond possible between A and B pairs.

1.6.2.4 Nanostructured polymer blends

Nanostructured polymer morphologies have been reported by several researchers. Typically, Hu et al. [63] developed a concept of in-situ polymerization and in-situ compatibilisation for obtaining stabilized nanoblends and showed their feasibility by using PP and PA6. Their method consists of polymerizing a monomer of PA6, ϵ -caprolactam, in the matrix of PP. A fraction of the PP bears 3-isopropenyl- α , α dimethyl benzene isocyanate (TMI), which acts as growing centers to initiate PA6 chain growth. The polymerization of PA6 and the grafting reaction between PA6 and PP took place simultaneously in the matrix of PP leading to the formation of compatibilized nano blends.



Figure 1.4 Morphology of PP-g-TMI/εCL/NaCL/microactivator system.
[Hu G.H., Cartier H., Plummer C., *Macromolecules*, 32, 4713, (1999)]

The size of the dispersed phase was between 10 and 100 nm, as shown in Fig.1.4. Pernot et al. [64] also adopted a similar methodology to produce a co-continuous nano morphology. In this approach, one component bears reactive groups along the backbone and the second component possesses complementary reactive moieties only at the end. Eventhough this novel strategy is expected to be versatile, it has yet to be proven that this technique could be applied to the different ranges of polymers including semiconducting or fluorescent materials and that it can be used in thin layers. Kietzke et al. [62] developed two new approaches to synthesize nanoscale polymer blend systems. In both cases, thin spin coated layers are used. In the first approach, two dispersions of single component nanospheres have mixed and processed into thin layers. In the second approach, the nanospheres were prepared from a mixture of two polymers in a suitable solvent.

In this case, both polymers were contained in individual nanoparticles, with the upper limit of the dimension of phase separation given by the particle size.

1.6.3 Interfacial adhesion/cross-linking

Cross-linking is affected in blends due to the inadequate miscibility of the blend components. The discrete particles/fillers of the polymer blend may reduce the opportunity for cross-linking at the interface and as a result the tensile properties of the system is lowered. Silica is polar whilst BR or NR/ IR is non-polar and therefore high interfacial tension or poor interfacial adhesion can be expected. If silica particle surfaces are not properly wetted by the polymer/s then one can expect weakness at the interfaces, which ultimately leads to excessive heat build-up during flexing, or dynamic fatigue as two silica particle surfaces can abrade during dynamic fatigue resulting in excessive heat generation and possible crack/tear failures.

The dramatic improvements in vulcanizate properties with high dispersible silicas illustrate the above point[65]. The use of silane coupling agents whereby the polar entities can chemically react with the polar silica hydroxyl groups and the polysulphidic, mercapto or thiocynato entities can chemically cross-link with non-polar polymer main chains suggests that silanes are not only coupling agents but as compatibilisers as well for rubber-silica and may be even for polymer blends themselves.

1.6.4 Distribution of fillers

The filler distribution in a polymer blend can be uneven due to the differences in polymer properties such as viscosity, polarity and other structural features. Earlier

studies on filler distribution showed that in the blend of polybutadiene (PB) and natural rubber (NR), more filler was preferentially absorbed in the low viscosity rubber, PB[66]. However, the studies by other researchers showed that though the filler first penetrate the soft rubber, as the mixing continues, the viscosity of the softer rubber increases because of the higher filler content, after which the second polymer shares in the filler uptake [67].

Considerable research works has been done on the distribution and partitioning and migration of carbon black in NR/ SBR/ BR blends [68]. Since carbon black is non-polar, little problems encountered. However carbon black has lower affinity for the polar rubbers e.g. NBR or CR. When blending e.g. NBR-black masterbatches with NR/BR, black migration to NR/ BR has been observed. Relatively little research work has been reported for silica. In NR/ BR/ NBR blends, silica filled, one would expect the silica to partition/ migrate more to the NBR phase. With silane treatment, this tendency should be reduced especially during and after curing as the silica is coupled to the polymer main chain by a chemical reaction.

1.6.5 Distribution of plasticizers between the elastomers

In the blend, the distribution of plasticizer depends upon its compatipility with the blend components. For eg. paraffinic oils are most compatible plasticizer for low polarity polymers such as ethylene propylene rubbers (EPR), but this plasticizer is replaced by dioctyl phthalate in polar rubber like acrylonitrile butadiene rubber (NBR) because the later being incompatible in paraffinic oil. In the blends, to avoid partitioning of the plasticizer to one polymer component alone, mixed plasticizers suitable for the blend components is usually applied [69].

1.6.6 Distribution of cross-links between the polymers

The degree of co-vulcanization primarily depends on the cure rate of the individual polymers and secondly on the distribution of the curatives between the two polymers. This is due to the differences in their solubility in the two polymers. Accelerators are usually polar materials and if NR/IR and NBR constitutes a blend, accelerators will be distributed more to the NBR phase. Sulphur, the vulcanizing agent being non polar form a rubber soluble sulfurating agent, which again is polar, and hence we can expect the NBR phase to have more cross-links. In any case initial good dispersion and distribution of sulphur and accelerators must be a pre-requisite for good distribution of cross-links in elastomer blend. For immiscible elastomeric blends, it is considered that the best co-vulcanised technological properties will be equal to the sum of the properties of the individual components [70].

1.7 Characterization of polymer blends

The characterization of polymer blends becomes easier, due to the availability of adequate number of modern techniques known today. The various techniques used for characterization include different types of microscopies, thermogravimetric analysis dynamic mechanical analysis, calorimetric methods, scattering techniques, X-ray analysis, spectroscopes, rheological analysis etc.

1.7.1 Microscopy

1.7.1.1. Optical microscopy

Walters and Keyte [71] extensively used optical microscopy in their studies to differentiate the components of polymer blends, by applying phase-contrast technique. Though this microscopy was useful for gum and lightly compounded elastomers it was not suitable for investigations on filled elastomers. In optical

microscopy, thin samples of the blends are viewed under the microscope for magnified images with a resolution of the order of $1\mu\text{m}$ [72]. The transmitted and reflected light microscopies are considered for analysis in optical microscopy. The optical micrographs of a blend in transmission mode depend up on the optical properties of the material. In other words, in samples where the absorption coefficient varies from place to place, the contrast in final image becomes more specific.

1.7.1.2 Scanning electron microscopy

The scanning electron microscope (SEM) is one of the most versatile and widely used tools of modern science as it allows the study of both morphology and composition of different materials. The attraction of this microscopy is the high resolution images of the morphology or topography of a specimen, with great depth of field, at very low or very high magnifications. The scanning electron micrographs also help to analyse the composition of a material by monitoring secondary X-rays produced by the electron-specimen interaction. Characterisation of fine particulate or blended matter in terms of size, shape, and distribution is the uniqueness of this technique. A variety of scanning electron microscopes are available for the high resolution imaging and characterization of beam sensitive materials. Jeol- 6400F, Jeol JSM-5600LV, XL30 etc are some of the SEMs of this category available today. Since SEM studies are limited to surface features only, for more accurate information about the internal structure of polymer blends, cryogenically fractured surfaces are viewed under the microscopes [73,74].

1.7.1.3 Transmission electron microscopy

In Transmission electron microscopy (TEM), a test specimen is bombarded with electrons and the number of electrons that travel through the specimen is measured as a function of position. The number of electrons that pass through the sample is proportional to the sample thickness and electron density. The electron density may not be identical for each phase in the blend and the number of electrons passing through the two phases may be different. In this technique, a staining material OsO_4 or RuO_4 with a high electron density that will preferentially migrate to one of the two phases is used to locate the position of each phase. The sample on keeping in the staining material is diffused in to the sample and a thin section is cut (10-100 nm thick) and viewed in the TEM. The region of specimen that reacts readily with the stain easily appears dark and the other regions appear light.

1.7.1.4 Atomic force microscopy

The recently introduced Atomic force microscopy (AFM) [74] has the potential for atomic resolution on certain samples including polymers. In this method samples need not be stained but cryosectionised and the cyosectionised surface of the specimen block is analysed [75]. The main feature of AFM over other microscopical methods includes higher resolution, easiness of specimen preparation and greater versatility in varying the mechanisms for achieving image contrast.

1.7.2 Thermo gravimetric analysis

The degradation behaviour of polymers and polymer blends has been studied extensively by thermogravimetry (TG) [76-80]. The standard test method for

compositional analysis by TG] describes a general technique to determine the quantity of four arbitrarily defined components [81,82], viz., (1) highly volatile matter, (2) matter of medium volatility, (3) combustible material, and (4) ash left after oxidative decomposition of inorganic components. The definition of each component is based on its relative volatility or involatility. The high volatile matter refers to moisture, polymers, diluents oil, plasticizer, emulsifiers, curatives (sulphur, accelerator), antioxidants, antiozonants and other low boiling components (approx. 300°C or lower). Materials such as processing oils, processing aids, elastomers, resins etc are referred to as 'medium volatile matters' (degrade at 300 to 750°C). The oxidisable materials, which are not volatile at 750°C, are referred as 'combustible materials' (e.g. carbon black, graphite etc.). The 'ash' refers to nonvolatile residues in oxidizing atmosphere, which may include metallic oxides and fillers (e.g. silica). In the absence of non-black fillers, the ash may also be composed of zinc oxide, which is a component in many vulcanizates. A small amount of ash may be due to elastomer residue (< 1 %). Besides compositional analysis, TGA has been used for determining thermal stability and for the evaluation of thermal decomposition kinetics in order to predict long- term as well as short-term thermal stability. A schematic TG/ DTG curve of elastomer vulcanizates is presented in Figure 1.5

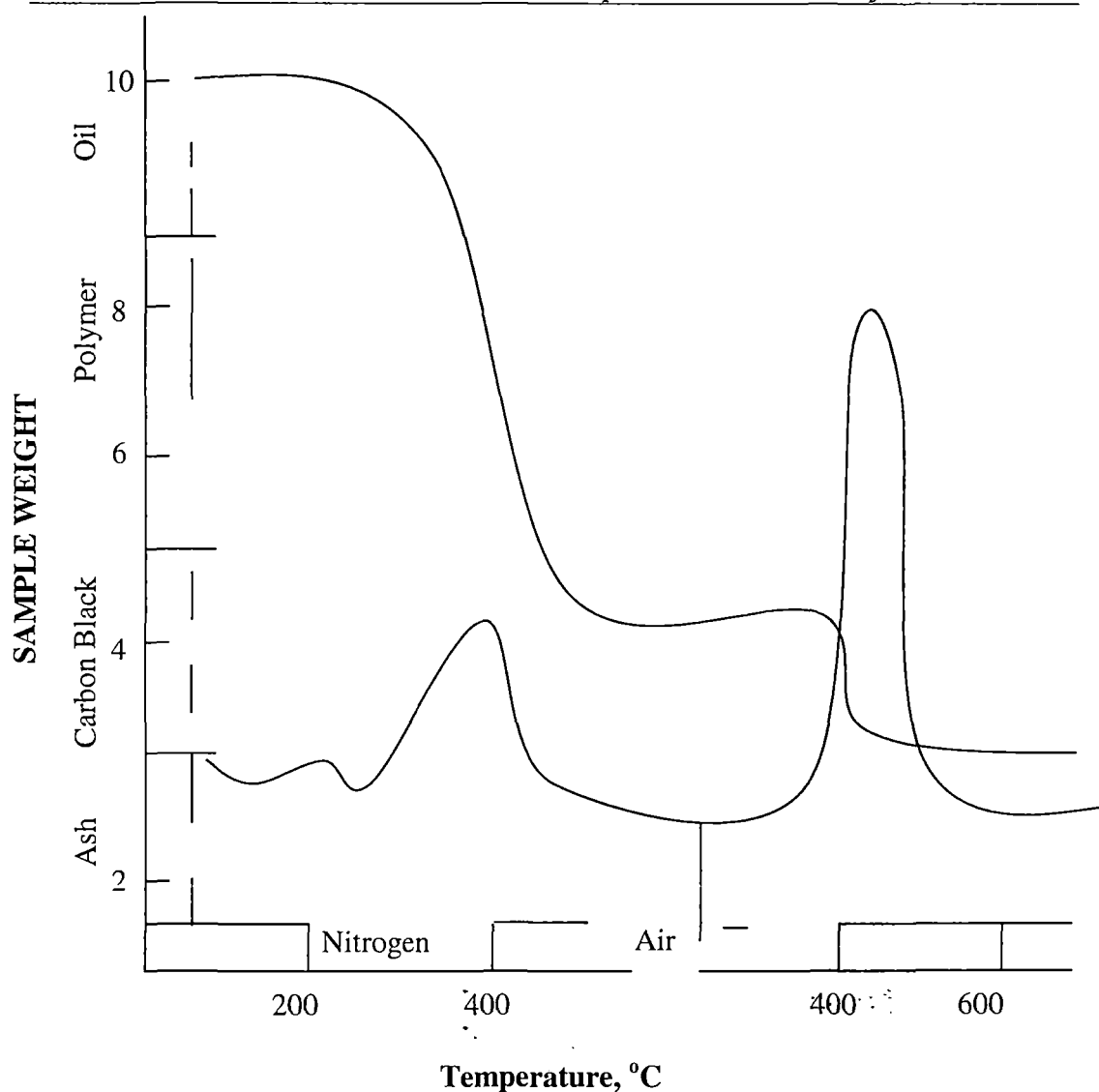


Figure 1.5. Schematic TG and DTG curves of elastomer vulcanizates

1.7.3 Differential scanning calorimetry

Differential scanning calorimetry (DSC) is another research tool used to investigate the thermal properties such as heat flow rate, glass transition temperature (T_g), melting point (T_m) etc. The most unambiguous criterion of polymer compatibility is the detection of a single glass transition whose temperature is intermediate between those corresponding to the two component polymers. The glass transition temperature (T_g) correlates to the low temperature limit before elastomers stiffen and lose their elastomeric properties. It is the

temperature region where the physical transition from a rubbery to a brittle state takes place. A typical DSC transition is shown in Figure 1.6

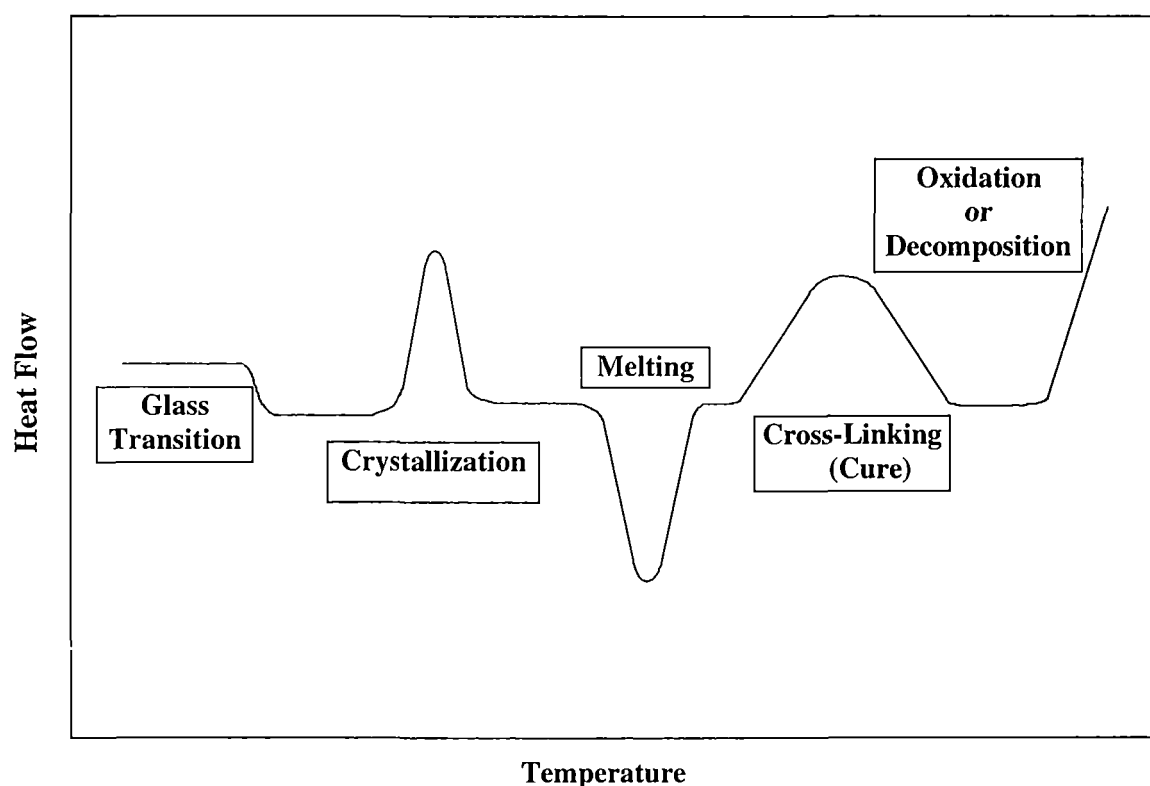


Figure 1.6. Typical DSC transition.

1.7.4 Dynamic mechanical analysis

Dynamic mechanical analysis (DMA) at a selected frequency over a range of temperatures has grown as a useful technique for the characterization of polymeric materials- homopolymers, copolymers, blends and composites-and their evaluation for consideration in stress and safety sensitive applications [83-85]. A typical DMA demonstration curve for PET tape is shown in Figure 1.7.

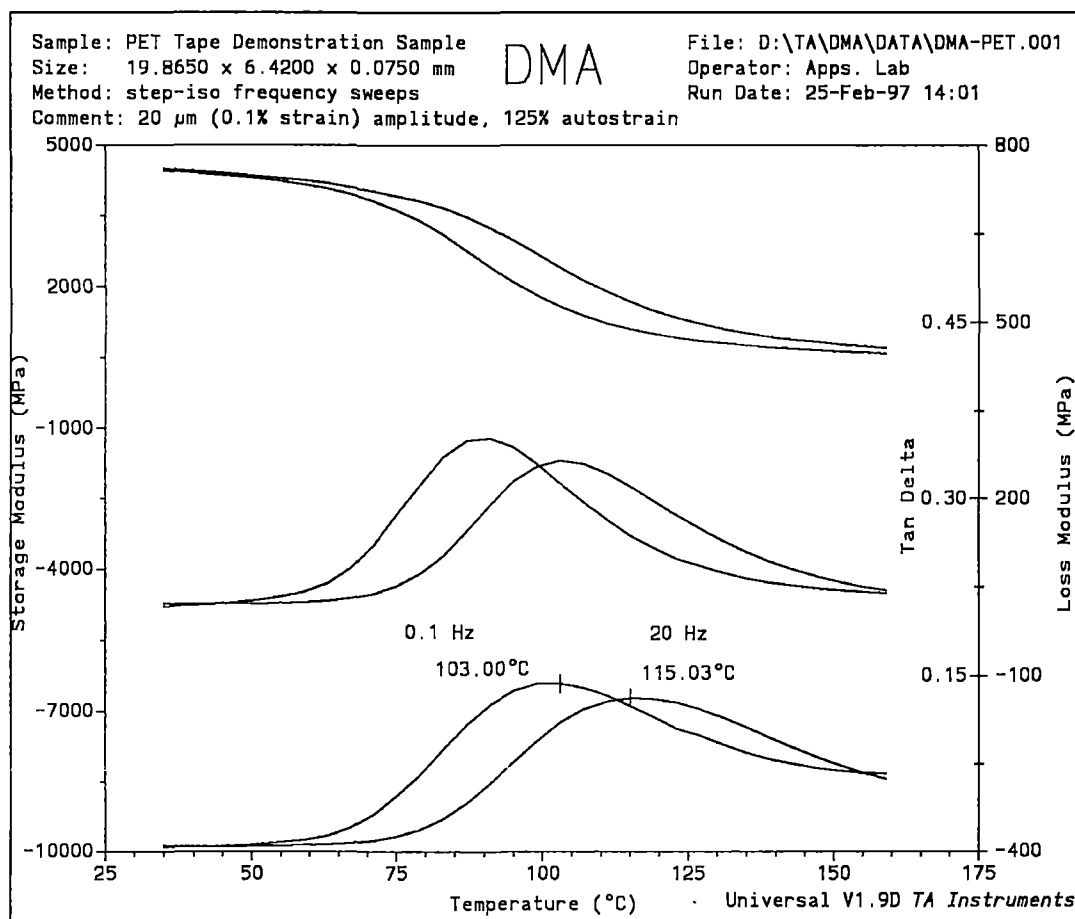


Figure 1.7 Typical DMA demonstration curves

Dynamic mechanical analysis is a technique that helps us to evaluate glass transition temperature (T_g) of the blends and the individual components from which we can assess the miscibility of the blends. The dynamic mechanical properties like storage modulus (E'), loss modulus (E'') and loss tangent ($\tan \delta$) of polymer blends depend on structure, crystallinity, extent of cross-linking etc [86]. The data and information generated may then be employed as a means of fingerprinting polymer systems and for locating glass transition and related properties.

1.7.5 Spectroscopic techniques

1.7.5.1 Nuclear magnetic resonance (NMR)

The NMR technique on polymers is generally confined to studying the spin-spin and spin-lattice relaxation processes as a function of temperature and composition. This spectroscopy has been applied effectively to crystalline systems where the spin-spin relaxation time for the protons in the amorphous phase is much greater than that for the protons in the crystalline phase. The phase separation in poly styrene/poly(vinyl methyl ether) [87] and the compositional variations of poly(vinyl chloride)/Hytrel have been studied using NMR[88]. Elmqvist and Svanson coworkers [89] showed that broad line NMR is a sensitive tool for the detection of small amounts of a soft phase embedded in a hard matrix.

1.7.5.2 Fourier transform infrared spectroscopy (FTIR)

FTIR has proved to be a valuable technique for characterising polymers, over the past few decades. With this technique the identification of many polymeric materials is easy and quick. From infrared data, it is feasible to determine many qualitative and semi-quantitative polymeric features, such as stereochemistry [90], types of additives, degree of degradation, presence of a co-polymer, chain length, orientation, and crystallinity [91-92].

1.8 Review of Literature

The fundamental concepts in polymer blending have been described systematically in literature[1-5]. Other interesting studies are also being done on them. For example, the effect of blend ratio on the cross-linking characteristics and dynamic elastic properties of high-density polyethylene/ethylene-propylene diene monomer

(HDPE/EPDM) blends was examined by Chandra et al.[93]. They found that the cross-link density first increased and then decreased with increase in EPDM content. Chough and Chang [94] showed the relationship between vulcanization reactivity and chemical structure of NR and blends of BR/ SBR. Their studies revealed that the rate of vulcanization was highest in NR compared to BR and SBR. The studies on EPDM/silicon rubber blends by Geerts et al. [95] described the melt mixing of the blends, cross-linking by gamma radiation and the permeability of the blends in methanol vapour. Mishra and Naik [96] investigated the internal mixing of ethylene-vinyl acetate (EVA)/EPDM blends in the temperature range of 80-230°C. They found that the extent of degradation of EVA and EPDM was minimum at the temperature ranges of 110-120°C and 150-160°C. A conductive rubber composite was developed by Sau et al.[97] from different blends of EPDM and acrylonitrile-butadiene rubber (NBR) containing acetylene black. They observed that the conductivity rose with increasing temperature and the activation energy of the conduction increased with a decrease in the loading of conductive fillers. Studies on the cure characteristics of SBR/epoxidised NR (ENR) blends by Ismail and Suzamah [98] and investigations on the highly filled EPDM rubber for the effect of curative systems, grafted rubber, cure rate, temperature etc by Markovic[99]and coworkers are some of the recent works in polymer blend research. Chough et al [100] studied the relationship between vulcanization reactivity and chemical structure using rheometer and DSC for natural rubber (SMR 5CV), butadiene rubber (BR 01), SBR 1501, and their blends. Choudhary et al.[101] investigated the shrinkability and micro structural properties

of composites based on low-density polyethylene (LDPE) and polyurethane (PU) rubber by rheometric and DSC studies. They found from high temperature DSC that with increase in PU content, stability of composites increased, and further high temperature processing decreased the initial degradation temperature but enhanced the rate of degradation. Sirqueira and Soares[102]demonstrated the decrease of the curing time with the addition of 2.5 phr of EPDMSH (ethylene-propylene-diene functionalized with mercapto groups), mainly in NR/EPDM (70:30 wt %) blend, indicating the accelerator effect of this functionalized copolymer. The reactive compatibilization of EPDMSH was shown by the presence of insoluble material in non-vulcanized/compatibilized blends and by its thermogravimetric analysis.

Go and Ha [103] studied the morphological behaviour of EPDM and butadiene rubber (BR) blends. They found that EPDM and BR were incompatible and the addition of a mixture of aliphatic and aromatic hydrocarbon (AAHC) effectively enhanced the compatibility of these elastomers. Ashalatha et al.[104] worked on the morphological properties of polypropylene (PP)/EPDM/NR blends and found a double-layered morphological structure in the blends. Laokijcharoen and Coran [105] also worked in this area and were successful in studying the method for determining phase morphology of unvulcanized NR/HDPE blends.

Sabbagh[106] showed that the poor compatibility of NR and EPDM could be enhanced by the addition of compatibilizers such as poly butadiene (BR), chlorinated rubber, PVC, etc. A similar work by Soares et al.[107] indicated that reactive compatibilization of EPDM-based dissimilar elastomer blends could be performed using mercapto-functionilised co-polymers. Soares et al. [108] studied

the reactive compatibilization of EPDM based dissimilar elastomer blends in terms of mechanical properties and swelling degree using mercapto-functionalised copolymers which resulted in an improvement of mechanical properties.

Sakr et al [109] investigated the effects of carbon black and temperature on the mechanical properties of styrene butadiene rubber (SBR) and natural rubber (NR) at various temperatures. They identified the optimum carbon black concentration as 95 parts per hundred (phr) for unblended samples. Younan et al.[110] made an extensive study on the dielectric and mechanical properties of EPDM-chloroprene blends loaded with white and black fillers and with PVC as a compatibilizer. In their studies, the effective blend ratio of EPDM and chloroprene was identified as 50:50. They highlighted the improvements in the mechanical properties of the blends with the addition of black and non-black fillers. The work by Ghoneim and Ismail [111] on EPDM/NR blends showed that the effective blend ratio for carbon black dispersion was 75:25 and that at this blend ratio the mechanical properties and stability against ageing were good. Ramesan et al.[112] studied the influence of carbon black on uncompatibilized and compatibilized SBR/NBR blends. Their studies revealed that compatibilized blends showed enhanced mechanical properties in the presence of high-abrasion furnace (HAF) black in comparison with uncompatibilized samples. Oliveira and Soares [113] investigated the effect of vulcanizing system on the cure and mechanical properties of NBR/EPDM blends. The studies on SBR/ENR blends by Ismail et al[114] showed that the increasing composition of ENR in the blend enhanced the mechanical properties and reduced the scorch and cure time. Ghosh and Basu [115] were successful in developing

filled co-vulcanizates of elastomer blends comprising of NR and EPDM of commercial importance using a multifunctional rubber additive, bis(diisopropyl) thiophosphoryl disulphide (DIPDIS). Corish and Powell [116] observed that blending of natural rubber and poly butadiene exhibited various advantages such as heat stability and abrasion resistance.

The degradation behaviour of polymers and polymer blends has been studied extensively by thermogravimetry (TG)[117-121]. There are several interesting studies reported on the thermal stability and polymer compatibility of blends and individual polymers based on their degradation behaviour. Ghosh et al.[122] investigated the thermal and oxidative degradation of poly ethylene/ethylene propylene diene monomer rubber (PE/EPDM) blends vulcanized by using sulfur accelerator systems. Manchado et al.[123] applied TGA to evaluate the effect of the components on the thermal stability, degradation kinetics etc. of PP/EPDM blends of different compositions in isothermal and constant heating rate conditions in an environment of pure nitrogen. Gamlin et al.[124] used high resolution TGA and modulated TGA to study the effect of ethylene content and maleated EPDM content on the thermal stability and degradation kinetics of EPDM. Modulated TGA showed that EPDM degradation is complex, with activation energy of degradation increasing throughout the degradation.

The crystallization behaviour and thermal properties of 'toughened polypropylene with balanced rigidity' (TRPP), were investigated by Jhang et al. [125] by DTA and TGA. They noted that the melting point, thermal oxidation temperature and thermal oxidation onset temperature of the TRPP's were all a little lower than

those of PP. The feasibility of using TGA and pyrolysis to estimate the blend composition of SBR/NBR blends was investigated by Shield et al.[126]. They estimated the blend compositions by TGA from the linear correlation between the polymer composition and the temperature required to pyrolyze a sample to specific “% weight loss”. In addition, there exist different investigations on the thermal degradation, heat flow rate and T_g of different polymer blends[127-130].

Differential scanning calorimetry (DSC) is another research tool used to investigate the thermal properties such as heat flow rate, glass transition temperature (T_g), melting point (T_m) etc. The most unambiguous criterion of polymer compatibility is the detection of a single glass transition whose temperature is intermediate between those corresponding to the two component polymers. The glass transition temperature (T_g) correlates to the low temperature limit before elastomers stiffen and lose their elastomeric properties. It is the temperature region where the physical transition from a rubbery to a brittle state takes place. Besides DSC, other thermal analyses such as derivative DSC, thermo mechanical analysis (TMA) and dynamic mechanical analysis (DMA) are generally used to determine T_g . T_g values determined by different thermal methods may be slightly different. T_g of an elastomer produced by different manufacturers can be different depending on the composition and microstructure. The effect of blend ratio on the cross-linking characteristics of EVA and the EPDM copolymer was studied by Mishra et al. [131] by differential scanning calorimetry (DSC) and a torque rheometer. They found that the cure rate increased whereas the optimum cure time and energy consumption for curing decreased with an increase in the

EVA/EPDM blend ratio. Phase morphology is an important factor in the determination. In a study by Ha et al. [132] on poly propylene-g- maleic anhydride and EPDM blends, it was found that the T_g of both PP and EPDM phases were shifted to higher temperatures as the EPDM content was increased. of properties of polymer blends. Sabbagh[106] evaluated the compatibility of NR/EPDM blends with and without different compatibilizers by DSC, viscosity measurements and scanning electron microscopy (SEM). The study showed that the addition of small percentage of compatibilizer enhanced the blend properties.

Dynamic mechanical analysis is used as an effective tool for characterizing the miscibility between two polymers in blend systems. The viscoelastic properties [133]. like storage modulus, loss modulus and loss tangent of polymer depend on structure, crystallinity, extent of cross-linking, etc. Bandyopadhyay and coworkers[134] studied the dynamic mechanical properties of the blends of NR/EVA in terms of storage modulus and loss tangent. Ramesan et al. [135] carried out the DSC and DMA test of compatibilized SBR/acrylonitrile butadiene copolymer rubber (NBR) blends to examine the miscibility of the blends. Manchado et al.[136] studied the crystallinity of isotactic propylene (iPP) in its blends with EPDM reinforced with different fibres. They analysed the effects of both fibres and EPDM on the crystallization kinetics and morphology of iPP, using DSC and optical microscopy. Xiao et al[137]investigated the miscibility between EPDM (terpolymer) and PP by means of dynamic mechanical thermal analysis (DMT) and DSC. The results showed that a decrease in the PP content and an increase in the cross-link density of EPDM in the EPDM/PP blends caused the

glass transition temperature peaks of EPDM to shift from a lower temperature to higher one. Wippler [138] reported the dynamic mechanical properties of polycarbonate (PC)/ polyethylene (PE) blends. The Takayanagi model was used to predict the behaviour of experimental storage moduli. The effect of poly chloroprene (CR) content on the storage moduli of acrylonitrile butadiene styrene copolymer (ABS) was reported by Kang et al.[139]. They found that the storage moduli of the blends increased with increase in CR content. Studies on the influence of blend composition on the viscoelastic properties of NR/EVA and NBR/EVA blends have been reported [140,141]. It was found that the damping factors of these blends increased with increase in rubber content, and this behaviour has been correlated with the phase morphology of the blend system. Karger-Kocsis and Kiss [141] studied the effect of morphology on the dynamic mechanical properties of PP/EPDM blends. The presence of a two phase morphology and two separate damping peaks for blend components remaining at their original positions in the dynamic mechanical plots indicated the incompatibility of the system. McLaughlin [142] and Guest and Daly [143] studied the influence of microstructure on the viscoelastic behaviour of PC/ styrene acrylonitrile copolymer (SAN) blend. Li et al. [144] investigated the compatibility of polycarbonate with polystyrene and polyester. Single glass transition temperatures of blends indicated the miscibility of the system. Varghese et al.[145] studied the miscibility of poly (vinyl chloride) (PVC) with 50% epoxidised natural rubber (ENR). These blends showed a single T_g , intermediate between the T_g s of the pure components, indicating the miscibility of the system. Several studies have

been reported on the effect compatibilization on the dynamic mechanical properties of various polymer blends [146-151]. Brahim et al.[147] indicated that the addition of pure and tapered diblock copolymers into PE/PS blends enhanced the phase dispersion and interphase interactions. Investigations on the effect of carboxylated nitrile rubber (ENBR) as a compatibiliser in PVC/ENR blends were done by Ramesh and De [148]. The DMA results showed that an immiscible composition of PVC/ENR became progressively miscible by the addition of XNBR. The addition of ethylene- methyl acrylate copolymer as a compatibiliser in LDPE/PDMS blends was found to shift the T_g values corresponding to the homopolymers[151]. Zaharescu and Mihalcea [152] studied the degradation effect of EPDM/ethylene-propylene rubber (EPR) blends in different environmental conditions such as oxygen, distilled water, and salt water. The studies showed that in contrast, chloride ions promote degradation of the blends. Excellent reports on the ageing characteristics of rubbery systems exist. Bhowmick and White[153] investigated the thermal, UV- and sunlight ageing of thermoplastic elastomeric natural rubber-polyethylene blends. They found that thermal ageing of the blends of two polymers caused the tensile properties to deteriorate, especially at longer times, or higher temperatures of ageing after an increase of properties in the initial stage.

The reasons for the deterioration during ageing may be the action of heat, oxygen, ozone, weather or radiation on vulcanizates. It is well known that for many unsaturated rubbers, the hydrogen atom of α -methylenic carbon is abstracted in the presence of oxygen and an oxidative reaction chain is initiated which propagates

auto-catalytically and ends in chain scission. Besides scission of the main chain and of the cross-links, depending upon polymers, ageing causes the formation of more cross-links of the same type as those already present or of a different type, which may be inactive to further scission. Introduction of antioxidants and antiozonents helps to reduce the property loss of rubber vulcanizates due to ageing though these chemicals have limitations in performance. With the introduction of weather resistant rubbers such as ethylene propylene diene monomer rubber (EPDM), hypalon and polysulfide, the efforts to modify the ageing characteristics of highly unsaturated rubbers gained a new momentum through blending techniques[154]. Malhotra and Saran [155] observed the weather resistance of compression moulded EPDM/poly vinyl chloride (PVC) blends by accelerated weathering in Xenostst 150 S weatherometer under controlled temperature and relative humidity for 720 h of exposure. Their studies showed that the blends with 50 phr of EPDM had shown better retention on accelerated weather tests. The demands for high temperature, ozone and weather resistant rubber materials have increased during the last decade. Emmet[156] showed that the addition of polyvinyl chloride to nitrile rubber enhanced the thermal, ultraviolet and ozone resistances. In another work, Noland et al [157] found that the ultraviolet degradation of polymethyl methacrylate/poly vinylidene fluoride blends was consistent with that of the component elastomers when considered separately. The photo degradation of ethylene vinyl acetate copolymer /poly vinyl chloride and nitrile rubber/ poly vinyl chloride blends has been studied by Skowronsky et al

[158]. Many other interesting works have also been reported on the ageing characteristics of polymeric systems [159-164].

1.9 Scope and Objectives

Styrene butadiene rubber (SBR) is a synthetic rubber extensively used in industry. SBR is commonly used in wire/cable insulations, shoe soles, passenger tire treads and extruded industrial products. It has got high electric resistance, low permanent set, controlled plasticity, good abrasion resistance, and smooth extrusions. However, it lacks resistance to ozone, heat, radiations and weather. This disadvantage of SBR can be overcome by blending it with a suitable elastomer.

Ethylene Propylene Diene Monomer (EPDM) rubbers have unsaturation dangling from the main backbone and, hence, are more resistant to ozone attack. The unsaturation levels are usually in the 2-10% range. EPDMs with high unsaturation are more cure compatible with diene rubbers (e.g. NR, BR etc.) and are generally used to improve ozone resistance. They can generally tolerate higher loadings of filler and oil. EPDMs can be cured using sulphur and peroxide-accelerator systems. EPDM rubbers are generally amorphous type polymers. However, as ethylene content increases, crystallinity develops above 55-65%. This crystallinity usually melts in the range of 30-90°C. Therefore, EPDM has a strong influence on compound processability below 90°C, yielding good green strength and shape retention. The high ethylene content in EPDM increases the tensile stress for both broad and narrow molecular weight polymers (molecular weight distribution of EPDM ranges from narrow to broad). Ethylene propylene molecules have long, flexible, and mobile chain segments which allow for easy penetration of filler

particles. Hence, significantly large volumes of carbon black and/or mineral fillers can be incorporated into the polymer. This approach coupled with the inherent low density of ethylene propylene polymers, compared to other rubbers, permits compound cost to remain relatively low. High tensile strength and good tear resistance are indicative of good reinforcement. Applications utilizing ethylene-propylene diene monomer rubber span a broad range of technologies and industries. Traditional rubber market segments include automotive (coolant hoses; weather stripping for doors, windows; brake components; engine mounts etc.), building and construction (roof sheeting; pond & reservoir liners; seals & gaskets), electrical (power cable insulation; cable jacketing), tire products (tire sidewall components; tire valves; inner tube blending) etc.

The goal of the present work is to develop and characterize blends from SBR and EPDM. The processing characteristics and physical properties have been evaluated in terms of blend ratio, three cross-linking systems and different fillers.

The following are the main objectives of this work:

- To develop blends based on ethylene propylene diene monomer rubber (EPDM) and styrene butadiene rubber (SBR),
- To study the morphology of the blend systems,
- To investigate the effects of blend ratio and cross-linking systems on the mechanical properties of the blend systems,
- To study the effects of black and non-black fillers on the mechanical properties of the blends,

- To study the effect of filler concentration on the mechanical properties of blend systems,
- To evaluate the thermal stability, degradation behaviour, and phase transitions of the blends by using thermogravimetric analysis (TGA) and differential scanning calorimetry (DSC),
- To study the dynamic mechanical properties of the blend systems,
- To examine the ageing characteristics of the blend systems under the influence of heat, γ -radiation, ozone and water.

References

1. D.R.Paul, in Polymer Blends, D.R.Paul, S. Newman, Eds, *Academic Press*, New York, (1978).
2. Polymer Blends, Volume 1- Formulation, Volume II- Performance, D.R. Paul, C.B. Bucknall, Eds, *John Wiley & Sons*, Inc, New York, (2000).
3. Encyclopedia of Polymer Science and Engineering, Second Ed., H.F. Mark, M. Bikales, C.G.Overberger, G. Menges, J.I. Kroschwitz. , Eds, *John Wiley & Sons*, Inc., New York,(1987).
4. C.W. Macoscko, *Macromol. Symp.* **149**, 171 (2000).
5. L.A. Utracki, Introduction to Polymer Blends, In Polymer Blends Handbook, L.A. Utracki, Ed., Volume 1, *Kluwer Academic Publishers*, Dordrecht, (2002).
6. P.Ghosh, Polymer Science and Technology, plastics, Rubbers/Blends and Composites, Second edition, *Tata Mc Graw-Hill Publishing Company Ltd. New Delhi* (2002).
7. M.T.Shaw in Polymer blends and mixtures, D.J.Walsh, J.S.Higgins, A. Maconnachie Eds. *Imperial college*, London, U.K. (1984).
8. *JSR News* **5**(6),1(1967).
9. P.A. Marsh, A.Voet and L. D. Price, *Rubber Chem. Technol.* **40**,359(1967); **41**,344(1968).
10. M.L. Di Lorenzo and M.Friguire, *J. Polym. Eng. Sci.***17**, 429 (1997)
11. D. J. Stein, R. H. Jung, K. H. Illers, and H. Hendus, *Angew, Macromol. Chem.***36**,89 (1974).
12. H.K. Yuen and J.B. Kinsinger, *Macromolecules* **7**(3), 329(1974).
13. D.I.L. Kang, C.S. Ha and W.J. Cho, *Eur. Polym.J.*, **28**, 565 (1992).
14. K.T.Varughese, *J.Appl. Polym. Sci.*, **39**, 205 (1990).

15. B.D. Favis, *J.Appl. Polym Sci.*, **39**, 285 (1990).
16. S.Danesi and R.S. Porter, *Polymer*, **19**, 448 (1978).
17. K.T. Varughese, G.B.Nando, P.P. De and S.K.De, *J.Mater. Sci.*,**23**, 3894 (1988).
18. B. Ohlsson, H. Hassander and B. Tornell, *Polym. Eng. Sci.*, **36**, 501(1996).
19. B.K. Kim, G.S. Shin, Y.T. Kim and T.S. Park, *J.Appl. Polym Sci.*, **47**, 1581 (1993).
20. T.Noumura, T. Nishio, T. Fujiii, J. Sakai, M. Yamamoto, A.Uemura and M. Kakugo, *Polym. Eng. Sci.*, **35**, 1261 (1995).
21. L. E. Nielson, Predicting the properties of mixtures, *Marcel Dekker*, New York, p.13, (1978).
22. R.Hill, *J. Mech Phys., Solids*, **13**, 189(1965).
23. K. G. Karnika de Silva, & M. V. Lewan, Blends of Natural Rubber. Publd. Chapman & hall. Chp.6(1998).
24. K.Kongsin, & M. K. Lewan, Blends of Natural Rubber Publd. Chapman & hall. Chp. 7(1998)
25. Bernhard Schwaiger and Anke Blume , Silica/Silane- a winning reinforcement formula. *Rubber world* Apr.pp. 32 (2000).
26. C.E. Scott and C.W. Macosko, *Polym. Bull* 26, 341(1991).
27. N. Tokita, *Rubber Chem. Technol.*, **50**, 292, (1977).
28. B.D.Favis, J.P.Chalifoux, *Polymer*, **29**,1761 (1988).
29. S. Wu, *Polym. Eng. Sci.* **27**, 335 (1987).
30. P. Scholz, D. Froelich, R. Muller, *J.Rheol*, **33**, 481 (1989).
31. D. Graebing and R. Muller, *J.Rheol*, **34**, 193 (1990).

32. J.F. Palierne, *Rheol. Acta*, **29**, 204 (1990).
33. H.M. Lee and O.O. Park, *J. Rheol.*, **38**, 1405 (1994).
34. H. Asthana and K. Jayaraman, *Macromolecules*, **32**, 3412 (1999).
35. L.A. Utracki, The Rheology of Multiphase Systems, In *Rheological Fundamentals of Polymer Processing*, Covas, J.A., Ed., Kluwer Academic Press, Dordrecht, (1995).
36. H.J. Van Oene, *J. Colloid Interface Sci.*, **40**, 448, (1972).
37. K.B. Migler, *J. Rheol.* **44**, 277 (2000).
38. E.K. Hobbie and K.B. Migler, *Phys. Rev. Lett.* **82**, 5393 (1999).
39. J.J. Elmendorp and A.K. Van der Vegt, *Polym. Eng. Sci.*, **26**, 1332 (1986).
40. C.C. Park, F. Baldessari, L.G. Leal, *J. Rheol.* **47**, 911 (2003).
41. K. Min, J.L. White, J.F. Fellers, *J. Appl. Polym. Sci.*, **29**, 2117 (1984).
42. B.D. Favis, *J. Appl. Polym. Sci.*, **39**, 285 (1990).
43. S. Thomas and G. Groeninckx, *J. Appl. Polym. Sci.* **71**, 1405 (1999).
44. S. Joseph and S. Thomas, *Eur. Polym. J.* **39**, 115 (2003).
45. B.D. Favis, Factors Influencing the Morphology of Immiscible Polymer Blends in Melt Processing, In "Polymer Blends Volume 1, Formulation, D.R. Paul, C.B. Bucknall, Eds, *John Wiley & Sons*, New York, 501-537 (2000).
46. U. Sundararaj and C.W. Macosko, *Macromolecules*, **28**, 2647 (1995).
47. P. Cigana, B.D. Favis, R. Jérôme, *J. Polym. Sci. Polym. Phys.*, **34**, 1691 (1996).

48. J.A. Galloway, K.J. Koester, B.J. Paasch, C.W. Macosko, *Polymer*, **45**,423 (2004).
49. J. Lyngaae-Jorgensen and L.A. Utracki, *Polymer*, **44**,1661 (2003).
50. R.C. Willemse, *Polymer*, **40**, 2175 (1999).
51. R.C. Willemse, A. Posthuma de Boer, J. Van Dam, A.D.Gotsis, *Polymer*, **40**, 827 (1999).
52. J.K. Lee and C.D. Han, *Polymer*, **40**, 2521 (1999).
53. R.C. Willemse, A.Posthuma de Boer, J. Van Dam, A.D. Gotsis, *Polymer*, **39**, 5879 (1998).
54. R.T. Rol, G. Groeninckx, I. Vinckier, P. Moldenaers, J. Mewis, *Polymer*, **45**, 2587 (2004).
55. N. Marin and B.D. Favis, *Polymer*, **43**, 4723 (2002).
56. J. Li and B.D. Favis, *Polymer*, **42**, 5047 (2001).
57. S. Joseph and S. Thomas, *J. Polym. Sci. Polym. Phys*, **40**,755 (2002).
58. S. Steinmann, W. Gronski, C. Friedrich, *Polymer*, **42**, 6619 (2001).
59. N. Mekhilef and H. Verhoogt, *Polymer*, **37**, 4069 (1996).
60. D. Bourry and B.D. Favis, *J. Polym. Sci., Part B: Polym, Phys*, **36**, 1889 (1998).
61. J. Li and B.D. Favis, *Macromolecules*, **35**, 2005 (2002).
62. T. Kietzke, D. Neher, K. Landfester, R. Montenegro, R. Guntner, A.U. Scherf, *Nature Mater.* **2**, 48 (2003).
63. G.H. Hu, H.Cartier, C.Plummer, *Macromolecules*, **32**,4713 (1999)
64. H. Pernot, M. Baumert, F.Court, L. Leibler, *Nature Mater.* **1**,54 (2002).

65. A. J. Tinker, A.J. Blends of Natural Rubber, Publd. By Chapman & hall .
Chp.1 (1998)
66. W. M. Hess and V. E Chirico, *Rubb. Chem. Technol.*, **50**, 301, (1977).
67. C. M. Blow C.M, Hepburn C. Rubber Technology and Manufacture,
Second edition, p.45, 243, Butterworths, London, (1981).
68. J. L. White, Rubber processing: Technology, Materials and Principles.
Publd. by Hansar/Gardner. Chp. 7.7, (1995).
69. Jianhe Liao & Sally Groves Blends of Natural Rubber. Publd. Chapman &
Hall. Chp. 11(1998).
70. G.Kerruth, H. Blumel, & H.Weber, *Gummi Kunst.***22**, 413 (1969).
71. M. H. Walters and D. N. Keyte, *Trans. Inst.Rubber Ind.***38**,40(1962).
72. Hima Varghese, Ph.D Thesis, M.G. *University*, Kerala, 6,(1998).
73. Soney C. George, K. N. Ninan, Gabriel Groeninckx, Sabu Thomas, *J.Appl.*
Polym. Sci. **78**, 1281, (2000).
74. Hima Varghese, S.S. Bhagavan, S.Thomas, *J. Appl. Polym. Sci.*,**71**, 2343
(1999)
75. G. Binning, H. Rehren, C.Gerber and E. *Weibel*, *Phys. Rev. Lett.*, **49**, 57 (1982).
76. Y Wang, Q Fu, QJ Li, G Zhang, KZ Shen,YZ Wang, *J. Polym. Sci. Part B-*
Polymer Physics, **40**, pp 2086(2002).
77. J Arranz Andres, R Benavente, B Pena, E Perez, ML Cervada, *J. Polym.*
Sci. Part B-Polymer Physics, **40**, pp 1869 (2002).
78. BG Soares, FF Alves, MG Oliveira, ACF Moreira, *J Appl. Polym. Sci.*, **86**,
239 (2002).

79. G Lachenal, I Stevenson, N Celette, *Analyst*, 2201, (2001).
80. RS Rajeev, SK De, AK Bhowmick, B John, *Polym. Degrad. Stab.*, **79**,449 (2003).
81. Annu. Book *ASTM Stand.* Pt. 37, D-297-81 (1982).
82. C. Earnest, Ed., "*Compositional Analysis by Thermogravimetry*", (ASTM Spec. Tech. Publ. N. 997 (1988).
83. C.D. Wingard and C.L. Beatty, *J Appl. Polym. Sci*; **41**, 2539 (1990).
84. B. Harris, O.G. Braddel, D.P. Almond, C. Lefebvre, J. Verbist, *J Mater Sci*; **28**,3353 (1993).
85. J. Das, S. Bandyopadhyay, S. Blairs, *J Mater Sci*; **29**, 5680 (1994).
86. T.M. Murayama, Ed., *Dynamic mechanical analysis of polymeric materials*, Elsevier, New York (1978).
87. T.Nishi, T.T. Wang, T.K. Kewie, *Macromolecules*, **8**,227 (1975).
88. T.Nishi, T.K. Kwei and T.T. Wang, *J. Appl. Phys.*, **46**, 4157 (1975).
89. C.Elmqvist and S.E Svanson, *Eur. Polym. J.*, **11**, 789 (1975).
90. J.L. Koenig, *Spectrochimica Acta*, **22**, 1223 (1966).
91. L. E. Wolfram, and J. G. Grasselli, *Applied Spectroscopy*, **24**, 263 (1970).
92. P. A. Flournoy, *Spectrochimica Acta*,**22**, 15 (1966).
93. R. Chandra , S. Mishra and T.R. Parida, *Polym. Inter.*, **37**, 141 (1995).
94. S.H. Chough and D.H. Chang, *J. Appl. Polym. Sci.*, **61**, 449 (1996).
95. Y. Geerts, S. Gillard and G. Genskens, *Eur. Polym. Jnl.*, **32**, 143 (1996).
96. S. Mishra and J.B. Naik, *Polym. Plast. Technol. Eng.*, **36**, 231 (1997).
97. K.P. Sau, T.K. Chaki and D. Khastgir, *J. Mater. Sci.*, **32**, 5717 (1997).

98. H. Ismail and S. Suzamah, *Polym. Test.*, **19**, 879 (2000).
99. M.G. Markovic, N.R. Choudhary, M. Dimopoulos, J.G. Matisons, N.K. Dutta and A.K. Bhattacharya, *Polym. Eng.Sci.*, **40**, 1065(2000).
100. SH Chough and DH Chang, *J. Appl. Polym. Sci.*, **61**,449 (1996).
101. SR Choudhury, JK Mishra, CK Das, *J. Thermoplastic Composite Materials*,**13**, 400(2000).
102. AS Sirqueira, BG Soares, *J Appl. Polym. Sci.*, **83**,2892 (2002).
103. J.H. Go and C.S. Ha, *J. Appl. Polym. Sci.* , **62**, 509 (1996).
104. P.V.Ashalatha, K.E. George and D.J. Francis, *J. Elast. Plast.*, **29**, 92 (1997).
105. P. Laokijcharoen and A.Y. Coran, *Rubber Chem. Technol.*, **71**, 966 (1998).
106. S.H. EI Sabbagh, *Polym. Test.*, **22**, 93 (2003).
107. B.G. Soares, A.S. Sirgueira, M.G. Oliveira and M.S.M. Almeida, *Kaut. Gummi Kunstst.*, **55**, 454 (2002).
108. B.G. Soares, A.S. Sirgueira, M.G. Oleveira and M.S.M. Almeida, *Macromol. Symp.*, **189**, 45 (2002).
109. E.M. Sakr, H.A. Zayed, S.A. EI Mawla, M. Kenawy, M.R. Nagy and Czechoslovak, *J. Phys.*, **45**, 275 (1995).
110. A.F. Younan, S.L. Abd-el-Messieh and A.A. Gasser, *J. Appl. Polym. Sci.* **70**, 2061 (1998).
111. A.M. Ghoneim and M.N. Ismail, *Polym. Plast. Technol. Eng.*, **38**, 979 (1999).

112. M.T. Ramesan and C.K. Premalatha, R. Alex, *Plast. Rubber Comp.*, **30**, 355 (2001).
113. M.G. Oliveira and B.G. Soares, *Polym. Polym. Comp.*, **9**, 459 (2001).
114. H. Ismail, S. Suzaimah and H.M. Hainezam, *J. Elast. Plast.*, **34**, 119 (2002).
115. A.K. Ghosh and D.K. Basu, *J. Appl. Polym. Sci.*, **84**, 1001 (2002).
116. P. J. Corish and B. D. W. Powell, *Rubber Chem. Technol.* **47**, 481 (1974).
117. Y Wang, Q Fu, QJ Li, G Zhang, KZ Shen, YZ Wang, *J. Polym. Sci. Part B- Polymer Physics*, **40**, 2086 (2002).
118. J Arranz Andres, R Benavente, B Pena, E Perez, ML Cervada, *J. Polym. Sci. Part B- Polymer Physics*, **40**, 1869 (2002).
119. BG Soares, FF Alves, MG Oliveira, ACF Moreira, *J Appl. Polym. Sci.*, **86**, 239 (2002).
120. G Lachenal, I Stevenson, N Celette, *Analyst*, **126**, 2201 (2001).
121. RS Rajeev, SK De, AK Bhowmick, B John, *Polym. Degrad. Stab.*, **79**, 449 (2003).
122. P Ghosh, B Chattopadhyay, AK Sen, *European Polymer Journal.*, **32**, 1015 (1996).
123. M Lopez Manchado, L Torre, JM Kenny, *Rubber Chem. Technol.*, **73**, 694 (2000).
124. C Gamlin, MG Markovic, NK Dutta, NR Choudhury, JG Matison, *J Thermal Analysis and Calorimetry*, **59**, 319 (2000).

125. HJ Jhang, JW Wang, SK Cao, Y Wang, *J. Appl. Polym. Sci.*, **79**, 1351 (2001).
126. SR Shield, GN Ghebremeskel, C Hendrix, *Rubber chem.. Technol.*, **74**, 803 (2001).
127. NC Das, TK Chaki, D Khastgir, *J. Polymer Engineering*, **22**, pp 115 (2001).
128. SH Botros and AF Monstafa, *J. Elastomers and Plastics* , **34**, 15 (2002).
129. S Ilisch, R Androsch, HJ Radhusch, E Spirk, I Hudec, *Kautschuk Gummi Kunststoffe*, **55**, 48(2002).
130. J Peng, XH Zhang, JL Qiao, GS Wei, *J. Appl. Polym. Sci.*, **86**, 3040 (2002).
131. S. Mishra, B. Baweja and R. Chandra, *J. Appl. Polym. Sci.*, **74**, 2756 (1999).
132. CS Ha, YW Cho, JH Cho, *J Appl. Polym. Sci.*, **77**, 2777(2000).
133. M. Patri, A.B Samui and P.C Deb, *J. Appl. Polym Sci.*, 1993, 48, 1709
134. G.G. Bandyopadhyay, S.S. Bhagawan, K.N. Ninan and S. Thomas, *J. Appl. Polym. Sci.* **72**, 165 (1999).
135. MT Ramesan, B Kuriakose, P Pradeep, R Alex, S Varghese, *International Polymer Processing*, **16**, 183(2001).
136. MAL Manchado, L Torre, JM Kenny, *J. Appl. Polym. Sci.*, **81**, (2001).
137. HW Xiao, SQ Huang, T Jiang, SY Cheng, *J. Appl. Polym. Sci.*, **83**, 315 (2002).
138. C.Wippler, *Polym. Eng. Sci.*, **30**, 17 (1990).
139. D.IL, Kang, C.S. Ha and W.J. Cho, *Eur. Polym. J.*, **28**, 6, 565, (1992).
140. M.A Kader, W.D Kim, S. Kaang and C.Nah, *Polymer Int.*, 2005, 54, 120

141. J. Karger – Kocsis and L. Kiss, *Polym. Eng. Sci.*, **27**,4, 254 (1987).
142. K.W. McLaughlin, *Polym. Eng. Sci.*, **29**, 22, 1560 (1989).
143. M.J.Guest and J.H. Daly, *Eur. Polym. J.*, **26**, 6, 603 (1990).
144. Y.Li and H.L. Williams, *J. Appl. Polym. Sci.*, **40**, 1891 (1990).
145. K.T. Varghese, G.B.Nando, P.P. De and S.K. De, *J. Mater, Sci.*, **23**, 3894 (1998).
146. T.M. Murayama (Ed.), *Dynamic Mechanical Analysis of Polymeric Materials*, Elsevier, New York, (1978).
147. B. Brahimi, A. Ait-Kadi, A. Ajji and R. Fayt, *J. Polym. Sci. Part B. Polym. Phys.*, **29**, 946 (1991).
148. P. Ramesh and S.K. De, *J. Appl. Polym. Sci.*, **50**, 1369 (1993).
149. R.N.Santra, B. K. Samantaray, A.K. Bhowmick, and G.b. Nando, *J. Appl. Polym. Sci.*, **49**, 1145 (1993).
150. R. M. Holsti-Miettinen, J. V. Seppala, O.T. Ikkala, and I.t Reima, *Polym. Eng. Sci.*, **34**, 5, 395 (1994).
151. R.E Cohen and A.R. Ramos, *J. Macromol. Sci. Phys.*, **B17(4)**, 625 (1980).
152. Zaharescu and I. Mihalcea, *Polym. Degrad. Stab.*, **50**, 39(1995).
153. A.K.Bhowmick and J. R. White, *J. of Material Science- Springer*-37, 5141(2002).
154. M. G. Oliveira, B. G. Soares, *Polymers & polymer composites*,9, **7**,459, (2001).
155. V.P. Malhotra and V. Saran, *J. Appl. Polym. Sci.*, **56**, 45 (1997).
156. R. A. Emmett., *Ind. Eng. Chem.* **36**, 730 (1944).

157. J. S. Noland., N.N.C. Hsu, R.Saxon ,and J.M. Schmitt, *Adv.Chem. Ser.*, **99**, 15 (1971).
158. T. Skowronsky T. F. Rabek and B. Ranby. *Polym. Eng. Sci.*, **24**, 278 (1984).
159. A. T. Koshy, B. Kuriakose, and S.Thomas, *Polym. Deg. Stab.***36**, 137 (1992).
160. A. Jha A and A. K. Bhowmick, *Polym Degrad Stab* **62**, 575 (1998).
161. K. Mequanint, R.Sanderson and H. Pasch. *Polym Degrad Stab* **77**,121 (2002).
162. I.Vieira, VLS. Severgnini, DJ. Mazera ,M.S. Soldi , EA Pinheiro, ATN.Pires and V. Soldi,. *Polym degrad Stab***74**, 151 (2001).
163. R.A. Correa, RCR Nunes and VL. Lourenco. *Polym Degrad Stab.* 52 (1996), p. 245.
164. J. Devenas., Stevenson, N.Celette. G. Vigier, and L.David.. Laboratoire des Materiaux Polymeres et Biomateriaux, Univ. Claude Bernard Lyon 1, 43 Bd du 11 November, 69100, VILLEURBANNE, France.

Chapter 2

Materials and Experimental Methods

Abstract

The materials used and the experimental methods followed for the present investigation are presented in this chapter. The physical properties of the elastomer components of the blend and compounding ingredients have been discussed. The experimental techniques used for compounding, curing and blend characterization have been described. The various characterization techniques include mechanical property measurements, scanning electron microscopy, thermal analysis, dynamic mechanical analysis, and ageing studies.

2.1 Materials

2.1.1 Ethylene propylene diene monomer rubber (EPDM)

There are two types of ethylene-propylene rubbers; EPM- copolymers of ethylene and propylene and EPDM terpolymers of ethylene, propylene, and a diene. In the present research work, EPDM has been selected as one of the component elastomers. In the designation EPDM, E stands for ethylene, P denotes propylene, M represents a polymethylene ($-\text{CH}_2-$) saturated backbone and D represents the third co-monomer, a nonconjugated diene which introduces pendant unsaturation into the polymer. The chemical structure of EPDM terpolymer is shown in Figure 1. The diene shown is 5-ethylidene-2-norbornene (ENB). ENB is the most widely used diene in EPDM terpolymers, mainly due to its ease of incorporation into the polymer and its higher reactivity towards sulphur vulcanization.

EPDM- 502 was used throughout this study, supplied by Herdillia Unimers Ltd., Mumbai, India. This elastomer is fast curing, light coloured, non-staining and capable of accepting large quantities of mineral black and oil. The physical properties of raw EPDM-502 rubber are given in Table-2.1.

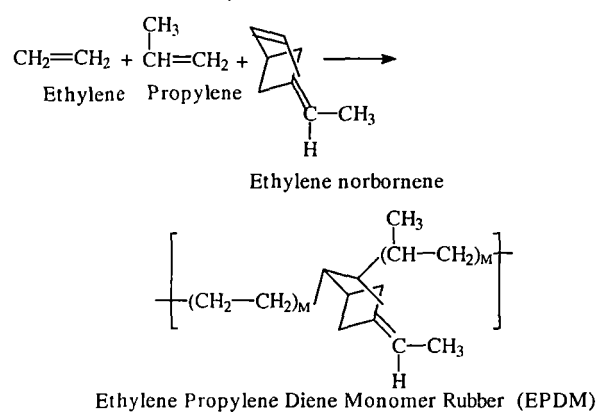


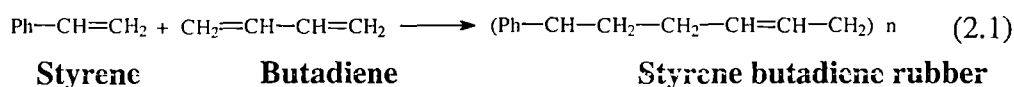
Figure 1 Structure of EPDM rubber

Table 2.1 Physical properties of EPDM-502

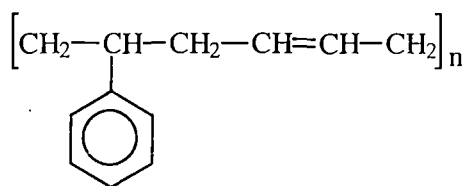
Property	Value
Mooney Viscosity: (ML 1+4)	55 at 125°C
Ethylene/Propylene ratio	62/38
Diene (%)	4.0
Density (mg/m ³)	0.86

2.1.2 Styrene butadiene rubber (SBR)

Styrene and butadiene are the co-monomers used in the manufacture of SBR according to the following reaction:



The chemical structure of SBR is given below:

**Figure 2** Structure of SBR rubber

The advantages of SBR are good abrasion resistance, high electric resistance, and low permanent set and good crack initiation resistance. SBR is cheaper than EPDM. However, its heat build up is high and the ozone resistance is poor. SBR-1502 supplied by India Rubber Chemicals, Kottayam, India was used in the present study. The main characteristics of SBR-1502 are given in Table 2.2.

Table 2.2 Physical properties of SBR-1502

Characteristics	Value
Mooney viscosity: ML 1+4	50 at 100°C
Bound styrene (%)	23.0
Organic acid content (%)	5-7
Density (mg/m ³)	0.93

2.1.3 Rubber chemicals and fillers

The rubber chemicals such as sulphur (S), dicumyl peroxide (DCP), zinc oxide, stearic acid, mercaptobenzothiazyl disulphide (MBTS), and tetramethyl thiuram disulphide (TMTD) used were of commercial grade. The fillers used were high abrasion furnace (HAF) black, general-purpose furnace (GPF) black, silica and clay. The physical properties of black fillers are given in Table 2.3.

Table 2.3 Physical properties of black fillers

Physical properties	HAF	GPF
ASTM 1765 Number	N-330	N-660
Particle Size (nm)	32	70
ASTM Iodine Number	80	35
Structure (cm ³ /BP/100g)	105	90

The characteristic features of the non-black fillers used in the present study viz; clay and silica are given in Tables 2.4 and 2.5 respectively.

Table 2.4 Characteristics of clay

Properties	Value
Brightness	90.0 ±1.0
Yellowness	2.0 ±1.0
2 micron w/w % (min)	60.0
+300 mesh w/w (max)	0.05
Moisture w/w % (max)	0.5
P ^H (10% solids)	4.5 – 5.5
Bulk density (Kg/lit)	0.4 – 0.5
Specific surface area (m ² /g) BET	10 – 12
Oil absorption (g/100g)	55 – 65
Specific gravity	2.6

Table 2.5 Specifications of silica

Physical properties	Value
Average particle size	400 mesh
Retention on 100 mesh	Nil
Bulk density (gm/ml)	0.087
Silica content, (%)	91
Loss on drying at 100°C (%)	0.5
P ^H of 5% solution	6.5 – 7
Loss on ignition at 1000° C (%)	9
Iron content (%)	0.02
Surface area m ² /gm (BET)	320 – 350
Specific gravity	1.9

2.2 Blend preparation

The blends of EPDM and SBR, with different cross-linking systems and fillers, were prepared on a two roll mixing mill (diameter 150 mm; speed of the slow roll 24 rev/min; gear ratio 1:16). The mastication of each polymer, and the subsequent blending and compounding were done between the hot rolls of the mill at 80°C. The basic recipes used for compounding are given in Table 2.7. The compounds have been designated as E₀S, E₂₀S, E₄₀S, E₆₀S, E₈₀S, E₁₀₀S, E₀P, E₂₀P, E₄₀P, E₆₀P, E₈₀P, E₁₀₀P, E₀M, E₂₀M, E₄₀M, E₆₀M, E₈₀M and E₁₀₀M, where E stands for EPDM rubber and the subscripts indicate the weight percentage of EPDM in the blends. The vulcanising systems sulphur, peroxide and mixed (sulphur + peroxide) are designated as S, P and M respectively. The designation E₀S represents pure SBR vulcanised by S. Fillers such as high abrasion furnace black (HAF), general purpose furnace black (GPF), silica and clay used in the study have been coded as HB, GB, SI and CL respectively. The filler loading has been indicated by prefixes. For instance, 10 HB shows 10 parts per hundred rubber (phr) of HAF black loaded system.

Table 2.7 Compounding Recipe (in phr^a)

Ingredients	Sulfur system (S)	Dicumyl peroxide System (DCP)	Mixed system (S+DCP)	10 HB	20 HB	30 HB	30 GB	30 SI	30 CL
Polymer ^b (blends)	100.0	100.0	100.0	100.0	100.0	100.0	100.0	100.0	100.0
Zinc Oxide	4.0	4.0	4.0	4.0	4.0	4.0	4.0	4.0	4.0
Stearic Acid	1.5	1.5	1.5	1.5	1.5	1.5	1.5	1.5	1.5
MBTS	1.25	1.25	1.25	1.25	1.25	1.25	1.25	1.25	1.25
TMTD	1.00	1.00	1.00	1.00	1.00	1.00	1.00	1.00	1.00
Sulfur	2.50	—	—	2.5	2.5	2.5	2.5	2.5	2.5
DCP	—	4	—	—	—	—	—	—	—
S+DCP	—	—	2.0+2.0	—	—	—	—	—	—
HAF	—	—	—	10.0	20.0	30.0	—	—	—
GPF	—	—	—	—	—	—	30.0	—	—
Silica	—	—	—	—	—	—	—	30.0	—
Clay	—	—	—	—	—	—	—	—	30.0

^a Parts per hundred of rubber by weight^b EPDM/SBR blends of varying composition

Rheometric parameters such as optimum cure (t_{90}), maximum and minimum torques (MH & ML) and scorch time (TS₂) of the blends were obtained by using a Scarabaeus GmbH Rheometer (Germany). The vulcanization of the blends was carried out on a hydraulic press (platen size 8' x 8') under a pressure of 1500 psi at a temperature of 160°C.

2.3 Characterization of blends

2.3.1 Mechanical properties

(a) Tensile strength, modulus and elongation at break

The tensile testing of samples was carried out on an Instron Universal Testing Machine (UTM Model 4411) according to ASTM D 412-98 test procedure, using dumb bell shaped test specimens at a crosshead speed of 500 mm/min. The failure properties were calculated using the following equations:

$$\text{Tensile strength (Mpa)} = \frac{\text{Load at failure}}{\text{Area of cross section}} \quad (2.1)$$

$$\text{Ultimate elongation (\%)} = \frac{\text{Displacement at failure}}{\text{Effective gauge length}} \times 100 \quad (2.2)$$

(b) Tear strength

The tear strength tests of un-nicked 90° angle test pieces were carried out as per ASTM D624-81 test method under the same experimental conditions of tensile strength testing. The tear strength was calculated by using the equation:

$$\text{Tear strength [dNm]} = \text{Load at failure/Thickness} \quad (2.3)$$

(c) Abrasion resistance

Abrasion tests were conducted using a Din Abrader as per DIN 53516. The abrasion resistance has been expressed as relative volume loss (mm³).

(d) Hardness

The hardness of the samples was measured by using a Durometer (Modex India Pvt.Ltd., Mumbai, India) as per ASTM 2240-86 test method and has been expressed in shore A unit.

2.3.2 Morphology

The morphology of the blends has been analysed by using both optical and scanning electron microscopes [1,2,3]. A JEOL JSM-5600 LV Scanning electron microscope and Jeol JFC-1200 Fine Coater (Jeol Ltd., Tokyo, Japan) were also used for the morphology study of the blends.

2.3.3 Thermal analysis

2.3.3.1 Thermogravimetric analysis (TGA)

Thermogravimetric analysis (TGA) and derivative thermogravimetric analysis (DTG) were carried out by using, TGA Q50 V2.34 Build 127 [TA Instruments, Germany]. Thin specimens of 10 to 20 milligram weight were scanned from 30-800°C at a heating rate of 20°C /min. The analyses were performed in an inert atmosphere of nitrogen. The mass loss profile has been expressed in percent of the original sample mass.

2.3.3.2 Differential scanning calorimetry (DSC)

The DSC measurements were done by using DSC Q100V3.5 Build175 [TA Instruments, Germany] to find the glass transition properties and blend compatibility. From the DSC plots of heat capacity (C_p) versus temperature (°C), glass transition temperature (T_g) has been obtained. The DSC experiments were carried out as per ASTM D 3418-82.

2.3.4 Dynamic mechanical analysis (DMA)

The viscoelastic properties of the blends were measured by using a Dynamic Mechanical Thermal Analyser, Q800 (TA Instruments, USA) in the frequency

range of 0.1-100 Hz. The temperature of the testing was in the range of -70 to 120⁰ C and the amplitude was 15 μ n. Single cantilever has been used for mounting the samples. Compression molded samples of dimension 25 x 8 x 3 mm³ were used for testing.

2.3.5 Ageing studies

Ozone ageing studies under static conditions were conducted as per ASTM D 518 method B in a Mast Model 700-1 Ozone Test Chamber at 40⁰C. Ozone concentration in the chamber was adjusted to 50 parts per hundred million (pphm). The thermal ageing characteristics of the vulcanizates were studied by ageing for 96 hrs at 100⁰C in a multi cell-ageing oven (Prolific Engineers, Indian). The influence of γ -radiation of different dose rates on the tensile strength and elongation at break of EPDM/SBR blends was investigated by aging the sample in a gamma chamber. The distilled water ageing of the blends was conducted on sulphur-cured specimens prepared from tensile pad as per ASTM D471-66 specifications.

References

1. Hima Varghese, S.S. Bhagavan and S. Thomas, *J. Appl. Polym. Sci.*, **71**, 2335 (1999).
2. A. P.Mathew, S. Packirisamy and S. Thomas, *J. Appl. Polym. Sci.*, **78**, 2327(2000).
3. S. C.George, K.N. Ninan, G. Groeninecx and S. Thomas, *J. Appl. Polym. Sci.*, **78**, 1280 (2000).

Chapter 3

Mechanical Properties of EPDM/SBR Blends

Abstract

The mechanical properties of EPDM/SBR blends were investigated with special reference to the effects of blend ratio and cross-linking systems. Among the blends, the one with 80/20 EPDM/SBR has been found to exhibit the highest tensile, tear, and abrasion properties at ambient temperature. The observed changes in the mechanical properties of the blends have been correlated with the phase morphology, as attested by scanning electron micrographs. The effects of three different cure systems, viz; sulphur (S), dicumyl peroxide (DCP), and a mixed system consisting of sulphur and peroxide (M), on the blend properties also were studied. The stress-strain behaviour, tensile strength, elongation at break and tear strength have been found to be better for the blends cured by mixed system.

A part of results of this chapter has been published in *J. Appl. Polym. Sci.*, **93**, 2606 (2004).

3.1 Introduction

The mechanical properties of polymer blends are highly dependent on blend ratio, characteristics of blend components, processing conditions, extent of interfacial adhesion between the components and phase morphology of the blends. Coran and Patel [1-4] conducted several studies on rubber/ thermoplastic blends to correlate their physical and mechanical properties with the characteristics of the blend components. The processing and mechanical properties of butyl-EPDM blends have been reported by Callan et al. [5]. Imoto [6], in the studies on EPDM/EPM compounds, showed that the physical properties of the blends were proportional to blend ratio. Oliveira and Soares [7] examined the effects of curing systems and curing parameters, on the mechanical properties and crosslink density of NBR/EPDM blends. They found that the accelerator type and the sulphur concentration affected the mechanical properties. Ghilarducci et al. [8] investigated the influence of blend composition on the internal friction of NR/SBR compounds. Utracki [9] discussed very interesting correlations between morphology and mechanical properties of different blend systems.

The present chapter describes the cure characteristics and mechanical properties of blends of EPDM and SBR. The cure time, scorch time, cure rate index, tensile strength, tear strength, elongation at break, hardness and abrasion resistance of the blends have been discussed with special reference to the effects of blend ratio and crosslinking systems.

3.2 Results and Discussion

3.2.1 Cure Characteristics

The cure characteristics of EPDM/SBR blends with different vulcanizing systems are given in Table 3.1. Typical rheographs of E₁₀₀S, E₈₀S, and E₆₀S are given in Figure 1. The optimum cure time (t_{90}) shows a gradual increase with increase in EPDM content in the blends for all the cross-linking systems used for this work. The t_{90} has been found to be highest for DCP cured systems compared to sulphur and mixed systems for a given blend ratio.

Among the sulphur cured blends, the scorch time and thus the scorch safety are higher for the blends E₆₀S and E₈₀S. The scorch safety has been found to be better for DCP cured system for a given blend ratio. The minimum torque (ML) values are found to be higher for sulfur cured systems for a given blend ratio than the DCP and Mixed systems. The maximum torque (MH), which is a measure of cross-link density, is higher for the blends vulcanized by S and Mixed systems than the DCP system.

Table 3.1 Cure Characteristics of EPDM/SBR blends

Sample Code	Blend Ratio	Optimum Cure time, t_{90} (min)	Scorch Time, TS_2 (min)	Min Torque, ML(dNm)	Max Torque, MH(dNm)	CRI (min^{-1})
E ₀ S	SBR100/EPDM0	4.61	2.70	2.55	15.88	52.36
E ₂₀ S	SBR80/EPDM20	4.62	2.75	2.65	13.19	58.48
E ₄₀ S	SBR60/EPDM40	4.92	2.77	2.73	13.23	46.51
E ₆₀ S	SBR40/EPDM60	5.68	2.83	2.91	12.69	44.44
E ₈₀ S	SBR20/EPDM80	5.90	3.48	3.47	12.85	45.05
E ₁₀₀ S	SBR0/EPDM100	7.40	4.76	2.25	17.00	37.88
E ₀ P	SBR100/EPDM0	11.20	2.18	0.81	16.69	11.09
E ₂₀ P	SBR80/EPDM20	12.26	3.17	0.53	13.08	11.00
E ₄₀ P	SBR60/EPDM40	13.71	3.46	0.38	13.03	08.88
E ₆₀ P	SBR40/EPDM60	13.80	3.43	0.25	11.96	09.64
E ₈₀ P	SBR20/EPDM80	13.96	3.88	0.65	11.86	10.19
E ₁₀₀ P	SBR0/EPDM100	14.96	5.19	1.13	9.57	10.24
E ₀ M	SBR100/EPDM0	4.11	2.44	1.68	16.29	59.88
E ₂₀ M	SBR80/EPDM20	6.22	2.95	1.64	13.14	30.67
E ₄₀ M	SBR60/EPDM40	6.41	3.12	1.60	13.13	43.67
E ₆₀ M	SBR40/EPDM60	8.56	3.13	1.58	12.33	18.42
E ₈₀ M	SBR20/EPDM80	8.73	3.68	2.06	12.36	24.69
E ₁₀₀ M	SBR0/EPDM100	8.90	4.97	1.69	12.28	51.81

Figure 3.2 shows the cure characteristics of E₈₀S, E₈₀P and E₈₀ Mix systems. It has been found that the rate of cure in mixed and sulphur systems is faster than the DCP system and the torque values are higher in mixed and sulphur systems. The cure rate index (CRI) was calculated using the equation;

$$CRI = 100/t_{90}-t_2 \quad (3.1)$$

where t_{90} is the cure time and t_2 is the scorch time. The CRI values are also given in Table 2.1. Cure rate index for the present blend systems has been found to increase with increase in SBR content for all the vulcanizing systems. The values have been found to be lowest for peroxide system.

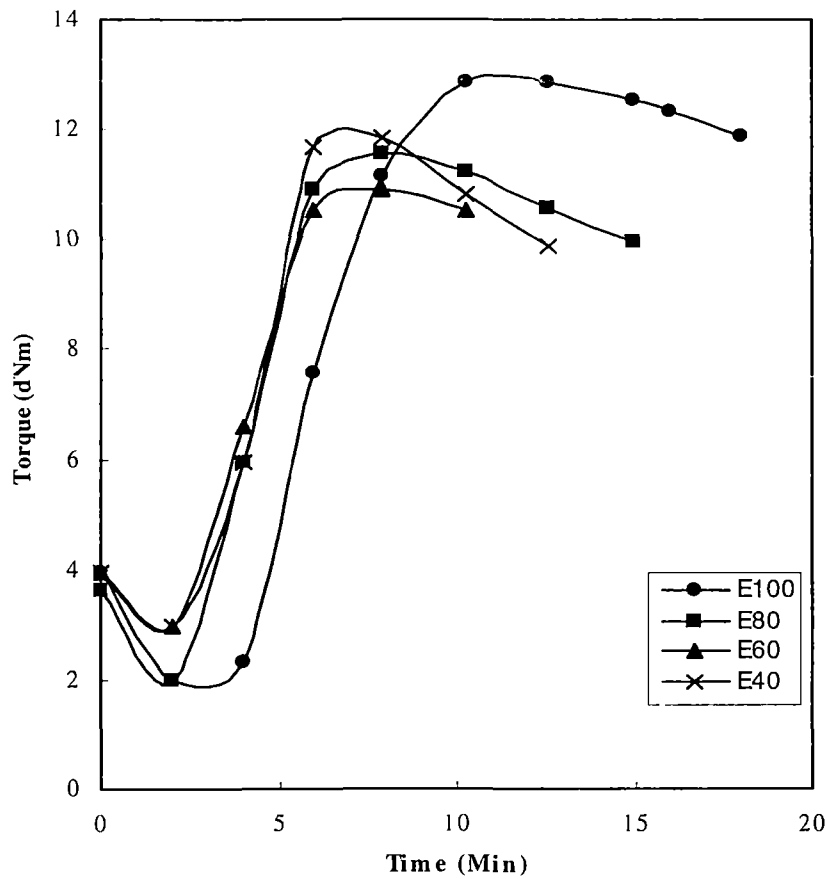


Figure 3.1 Rheographs of sulphur cured EPDM/SBR blends

A high CRI value shows higher vulcanization rate. Therefore, SBR is the cure-activating component for the systems. For a given blend ratio, the CRI is highest for blends cross linked by S and lowest for those with DCP curing systems.

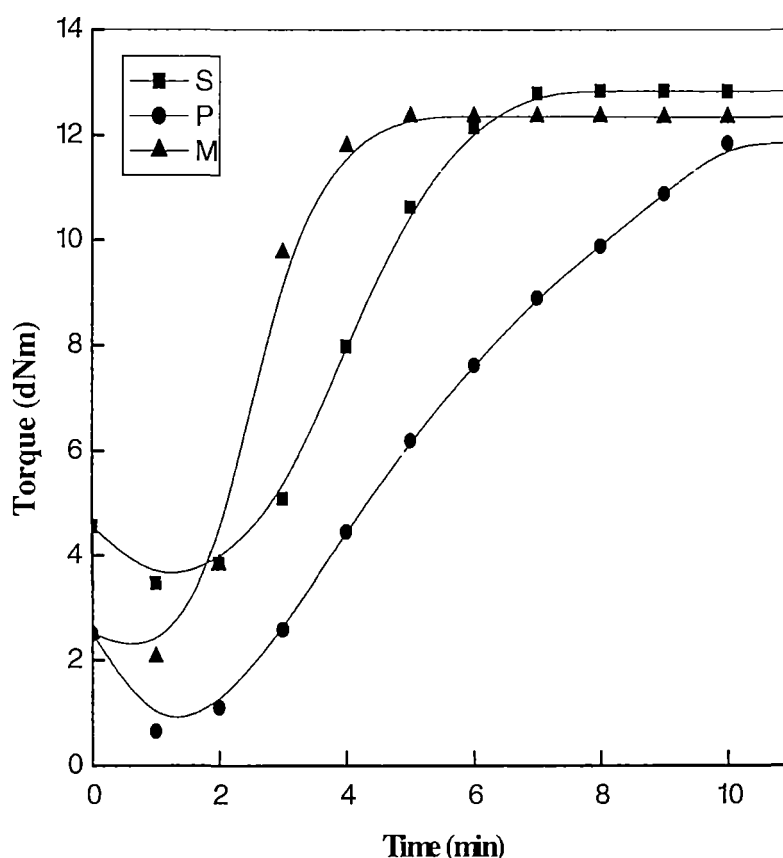


Figure 3.2. Rheographs of E₈₀ blend cured with different systems.

3.2.2 Mechanical properties

Figure 3.3 shows the stress- strain curves of sulphur cured EPDM/SBR blends. It is clear from the graphs that as the EPDM content of the blends increases, the % strain increases. This deformation behaviour is due to the orientation of crystalline regions of EPDM under the applied stress. The ultimate stress values are found to

be highest $E_{80}S$ blend system. Figure 3.4 represents tensile strength vs EPDM weight % of sulphur cured blend systems. Among different compositions, the blend, $E_{80}S$ (EPDM 80/SBR20) shows the highest tensile strength.

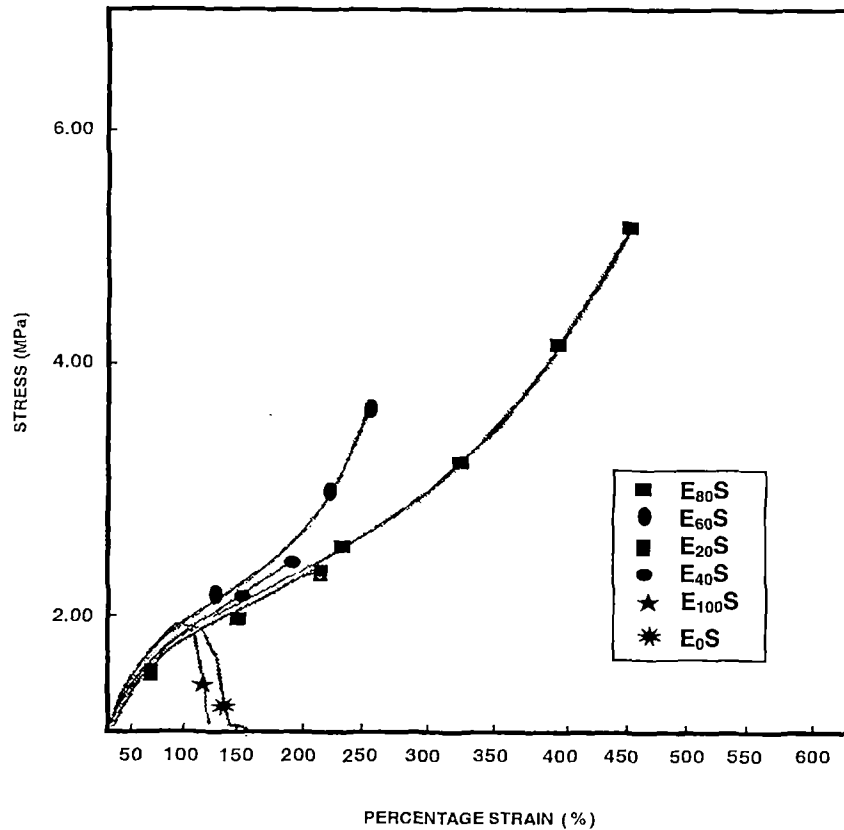


Figure 3.3. Effect of blend ratio on the stress-strain curves of sulphur cured EPDM/SBR blends.

The tensile strength values of the blends are found higher compared to that of the component elastomers. This positive deviation can be attributed to the mutual reinforcement of SBR and EPDM in the blends [10]. The synergism in tensile strength can also be attributed to strain hardening [11-14]. Materials, which undergo strain hardening, during stretching, have higher strength at break than materials those do not undergo it. During strain hardening both amorphous and

lamella r components attempt to orient along the drawing direction. These orientations cause close packing of chains, thereby increasing the intermolecular forces of attraction, which accounts for the higher stress at rupture. Due to stretching, EPDM in the present blend system undergoes deformation leading to high orientation of chains along with a reorganization of crystalline entities in the pull direction.

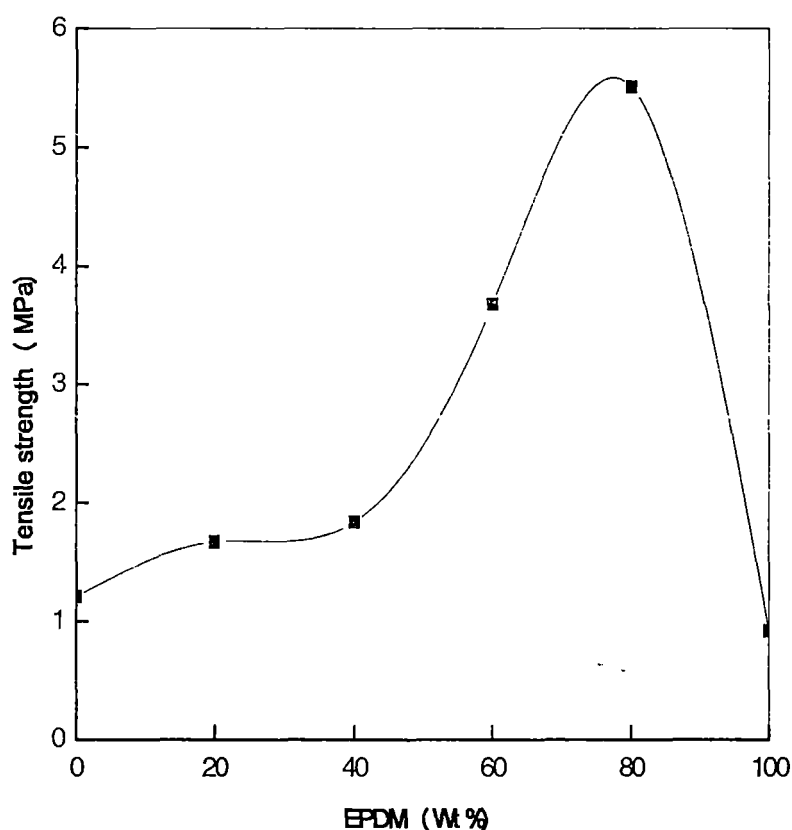


Figure 3.4 Effect of blend ratio on tensile strength

Figure 3.5 shows the effect of different cross-linking systems viz; sulphur, DCP and mixed on the tensile strength of EPDM/SBR blends. The graphs clearly show that the tensile strength increases in all the blends with increase in EPDM content. Among the different vulcanizing systems, for a given blend ratio, the tensile strength has been found to be highest for the mixed cure system (S+DCP) and the

lowest for the DCP system. The difference in the tensile strength with respect to curing systems can be attributed to the difference in the type of crosslinks introduced between the macromolecular chains during vulcanization. The 'S' vulcanization introduces polysulphidic linkages, the DCP cure, C-C linkages by a free radical mechanism and the mixed cure, both polysulphidic and rigid C-C linkages. A schematic representation of the network crosslinking is given in Figure 3.6.

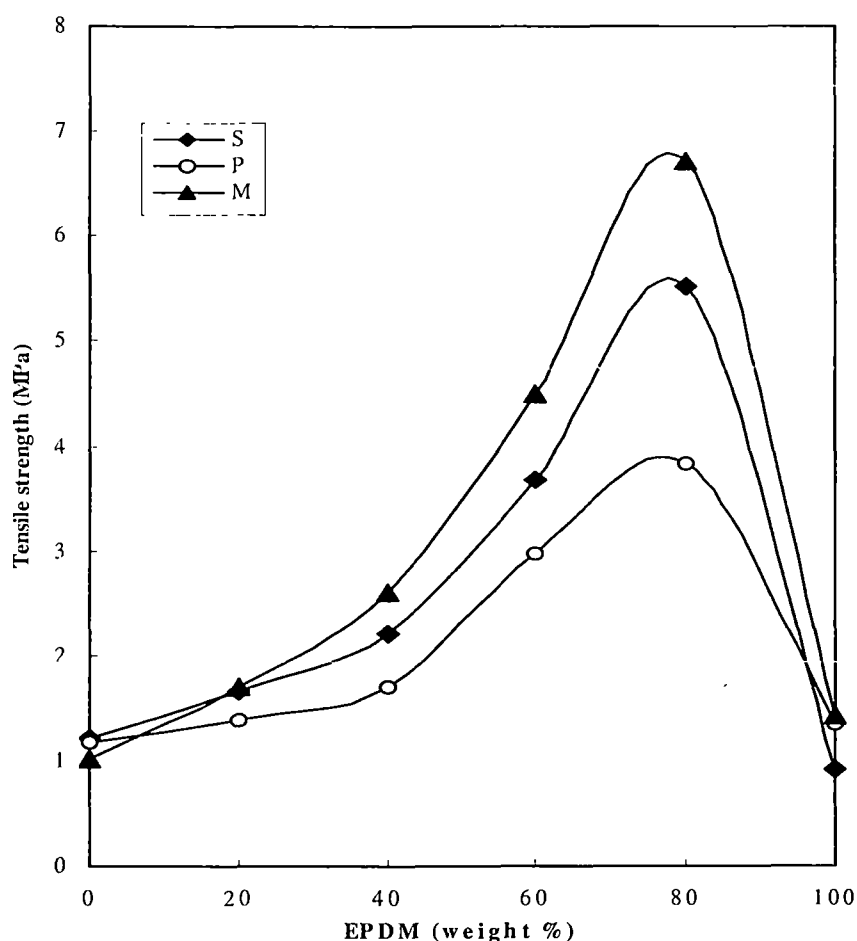


Figure 3.5 Effect of different cross-linking systems on the tensile strength

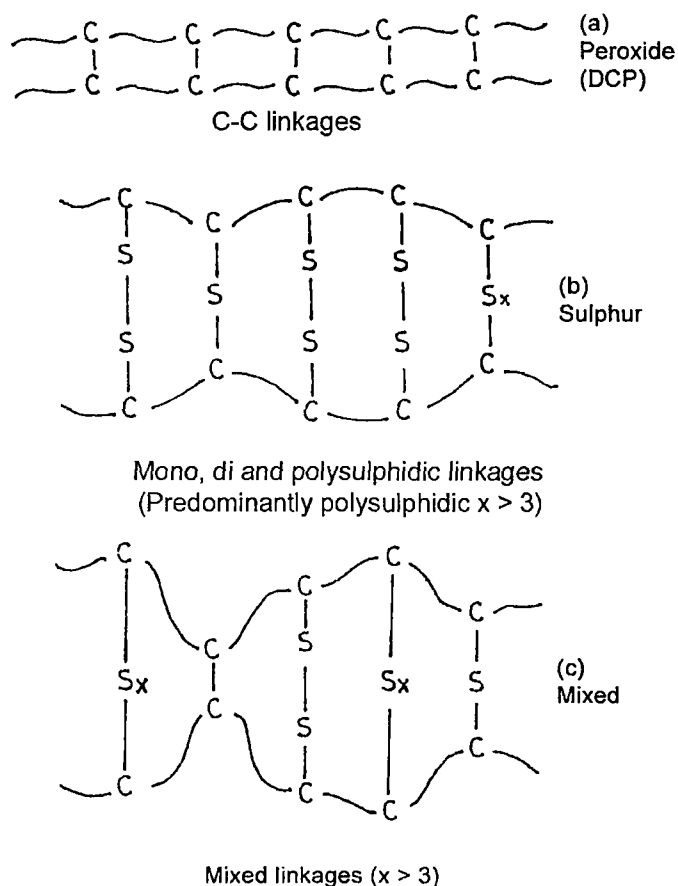


Figure 3.6 Schematic representation of crosslinking of EPDM/SBR blends cured by S, P and M systems.

The effect of blend ratio on elongation at break for the blends cured by sulphur, DCP and Mixed systems is presented in Figure 3.7. It has been found that the elongation at break increases with increase in EPDM content. The increase in EB can be correlated to the rearrangement of EPDM crystallites under an applied stress. In DCP and mixed cured blends, the elongation at break values has been found to be lower compared to sulphur cured systems. This is definitely associated with the higher flexibility of the molecular chains with polysulphidic linkages.

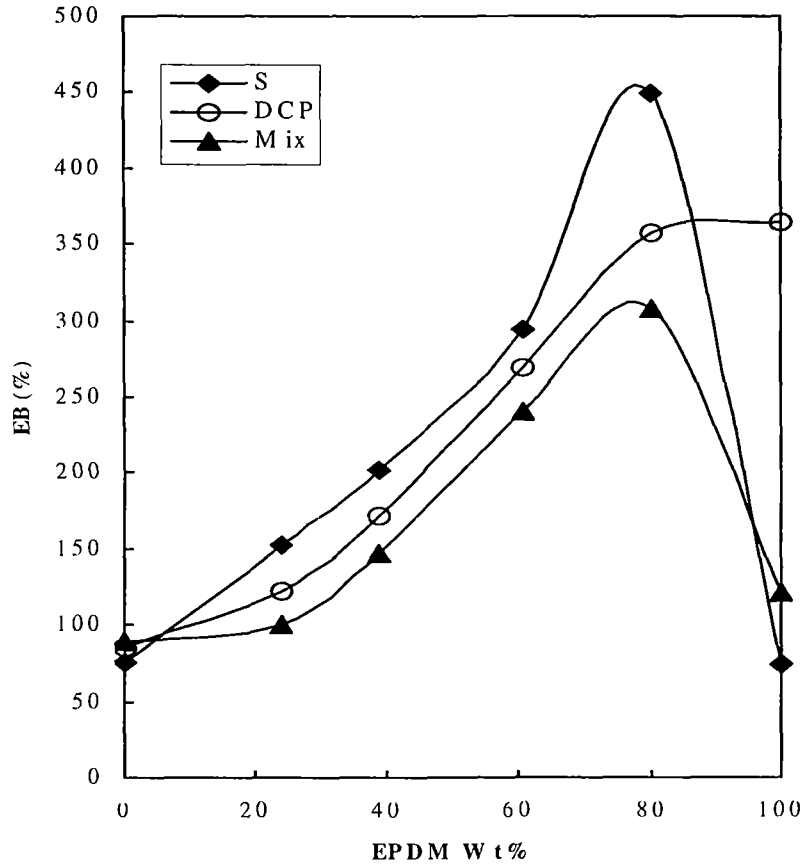


Figure 3.7 Effect of blend ratio on elongation at break

The cross-linked state of the blends has been measured in terms of cross-link density. The cross-link density of the blends was calculated from the tensile values using the kinetic theory of elasticity [15]

$$\nu = \sigma / (\lambda^{-1} \lambda^2) RT \quad (3.2)$$

where ν is the crosslink density (number of cross links per cc), σ is the modulus, λ is the extension ratio, R is the gas constant and T is the temperature on absolute scale. Figure 3.8 represents the effect of different crosslinking systems viz; S, P and M on the crosslink density of the blends. It is seen that the crosslink density of S and M cured blends increases with EPDM content for all the blend ratios.

However with increase the weight % of EPDM, the values have been found to decrease in peroxide cured systems. This can be due to uneven distribution of DCP in EPDM and SBR phases. It is interesting to note that the crosslink densities of the component elastomers are far lower compared to the blends, which complements the effect of blending on achieving better mechanical properties.

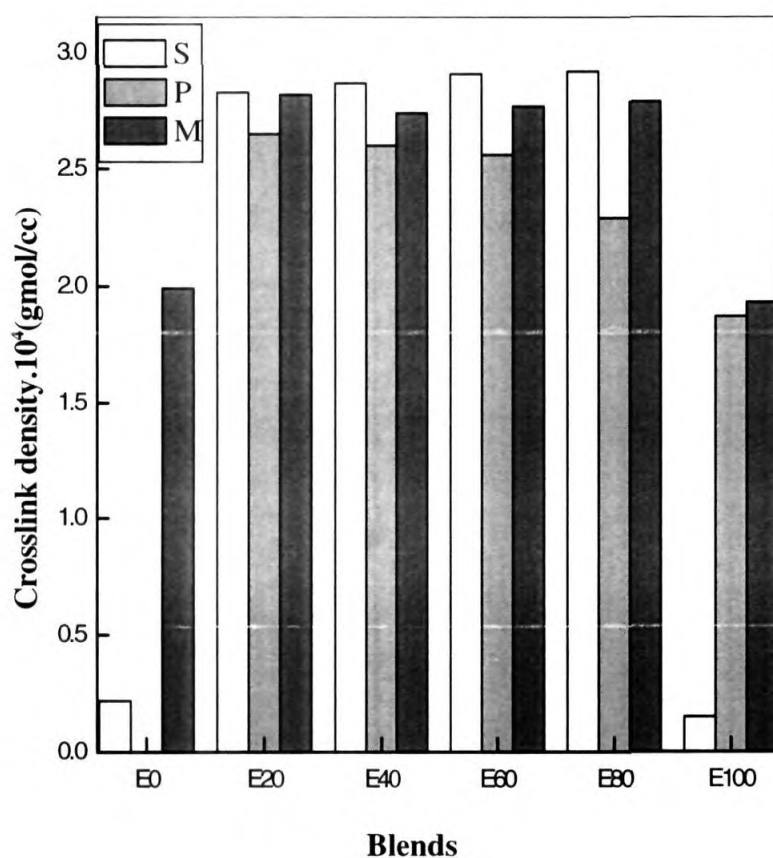


Figure 3.8 Effect of different crosslinking systems on crosslink density

Table 3.2 Young's Modulus and cross-link density of EPDM/SBR blends

Sample code	Young's Modulus (100%)
E ₀ S	0.09
E ₂₀ S	1.25
E ₄₀ S	1.27
E ₆₀ S	1.28
E ₈₀ S	1.29
E ₁₀₀ S	0.07
E ₀ P	-
E ₂₀ P	1.23
E ₄₀ P	1.22
E ₆₀ P	1.23
E ₈₀ P	1.01
E ₁₀₀ P	0.82
E ₀ M	0.88
E ₂₀ M	1.23
E ₄₀ M	1.24
E ₆₀ M	1.25
E ₈₀ M	1.23
E ₁₀₀ M	0.85

The Young's moduli for the blends are given in Table 3.2. It has been found that the Young's moduli are comparatively higher for sulphur and mixed cure systems than DCP. This can be attributed to the flexible polysulphidic crosslinks in sulphur system and a mixture of polysulphidic and C-C crosslinks in mixed system.

The dependency of tear strength on the weight percentage of EPDM is shown in Figure 3.9. Tear strength of the blends also shows synergism due to strain-induced crystallization. The tear strength has been found to increase with increased weight percentage of EPDM and the highest tear strength is for blend with 80 wt % of EPDM. Among the vulcanizations systems, the tear strength is highest for the mixed system.

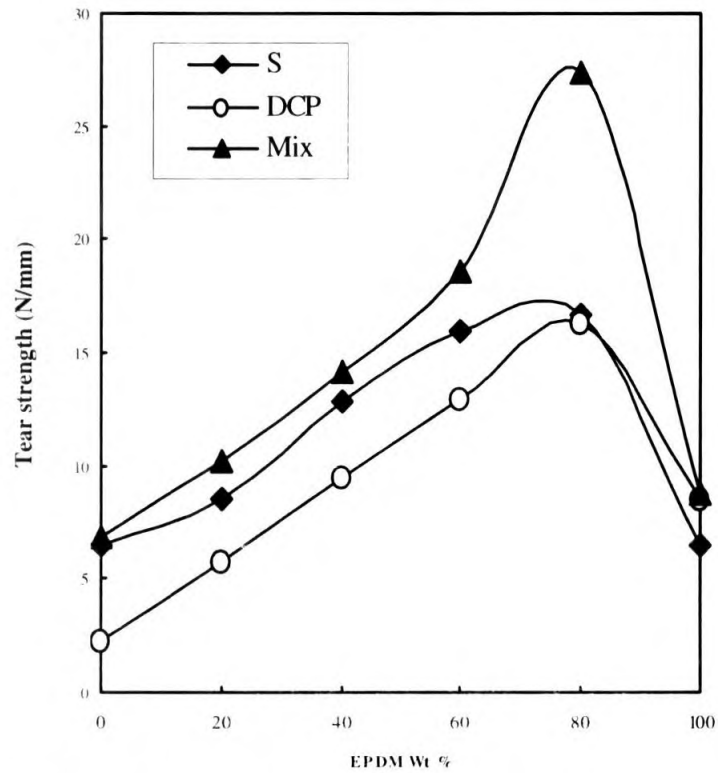


Figure 3.9 Effect of blend ratio and crosslinking systems on tear strength

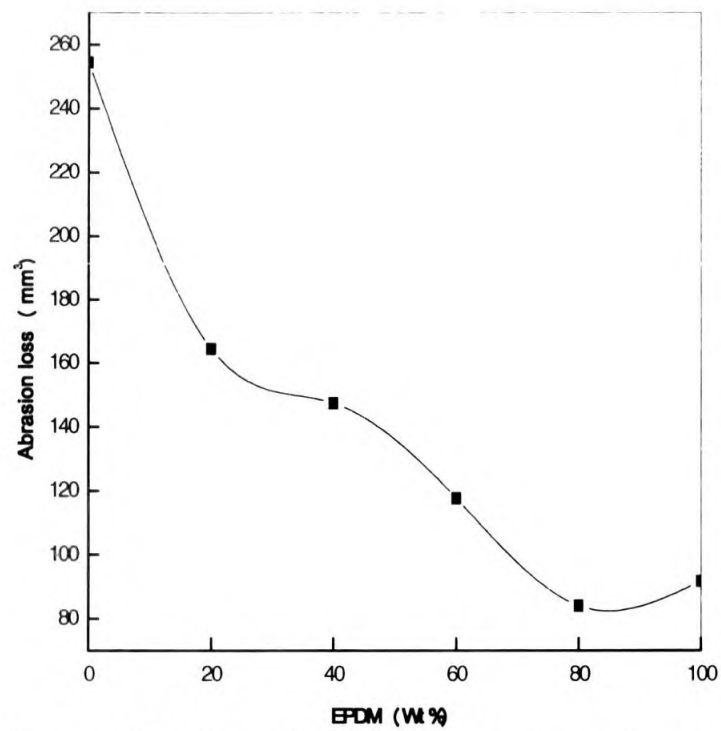


Figure 3.10 Effect of blend ratio on abrasion resistance

The abrasion resistance in terms of volume loss has been studied for sulphur cured blends. The change in abrasion resistance with weight percentage of EPDM is shown in Figure 3.10. The abrasion loss has been found to be minimum for the blend E₈₀S. A marginal increase in the hardness of the blends has also been noted with increase in weight percentage of EPDM in the blends except in DCP cured systems where the values are decreased as shown in Figure 3.11. This is definitely due to the rigid C-C crosslinks in DCP cured blends.

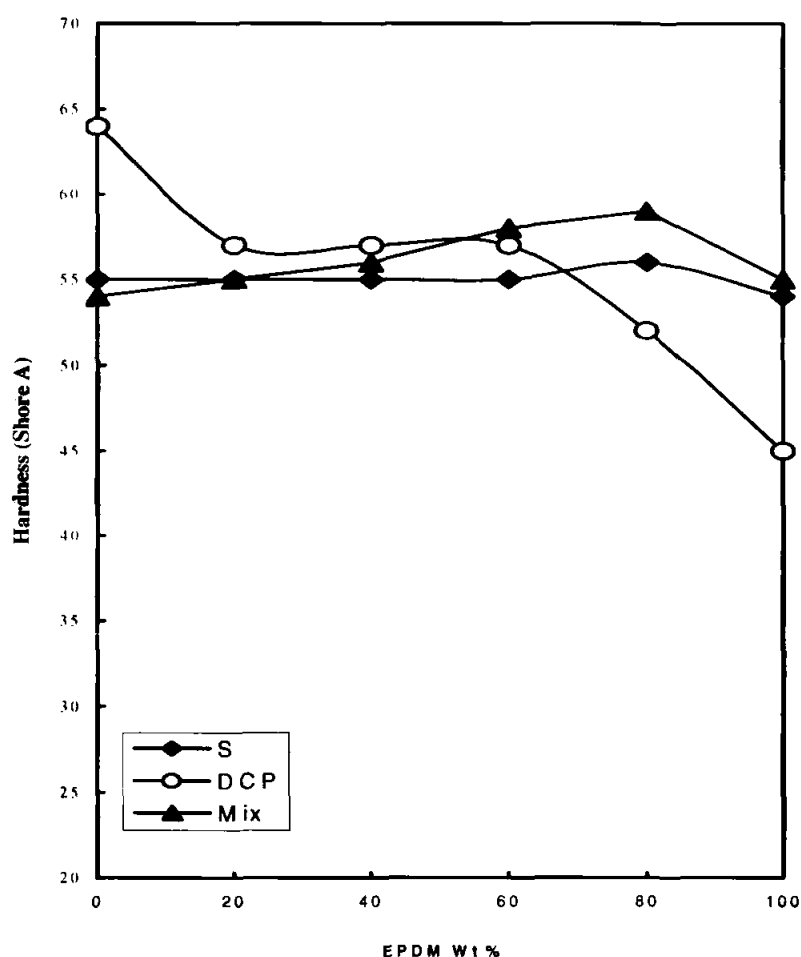


Figure 3.11 Effect of blend ratio on hardness

3.3 Morphology

SEM has been successfully used by researchers to study the morphology of polymer blends [16-19]. The SEM photographs of unfractured specimens of E_{80} blends cured with DCP, sulphur and mixed systems are presented in Figures 3.12a, 3.12b and 3.12c respectively. Figure 3.12a exhibits the SEM of DCP cured $E_{80}P$ blend having a flake like structure filled with pores which ultimately leads to lower mechanical properties. In Figure 3.12b it can be seen that the phase domains are globular shaped and are of relatively uniform size. The domains of SBR particles have been found to be dispersed in the EPDM matrix, which prevents crack growth in the blend during tensile stress. In the mixed system, $E_{80}M$ (Figure 3.12c), it has been found that the particles are more uniform in size and they are interwoven with the globular structure.

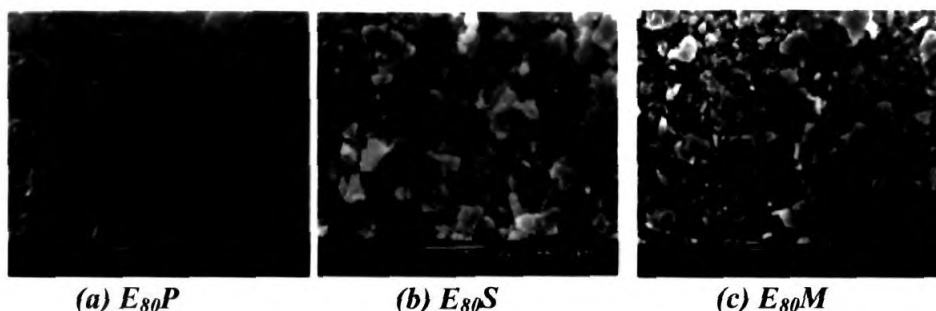


Figure 3.12 SEM photographs of cryogenically fractured specimens of EPDM/SBR blends

The SEMs shown in Figures 3.13a, 3.13b, 3.13c, 3.13d, 3.13e and 3.13f explain the morphology of tensile fractured surfaces of sulphur cured EPDM/SBR blends in different blend ratios. Figure 3.13a exhibits the SEM of pure EPDM, vulcanized by sulphur with a characteristic ductile failure and rough surface. The absence of a dispersed phase in it causes easy crack propagation and for poor tensile properties. Figure 3.13b shows the changes in morphology with the introduction of SBR in to EPDM. The SEM of blend $E_{80}S$ shows that small domains of the dispersed phase SBR is distributed relatively uniformly throughout the matrix. Earlier studies [20-22]

showed that crack bifurcation in blends can be prevented by small and uniformly distributed minor phase in the matrix. It can be noted that the particle size of the minor phase in blend E₈₀S is small and uniform which helped to toughen the matrix and prevent crack propagation. The miscibility of the blend was found increased.

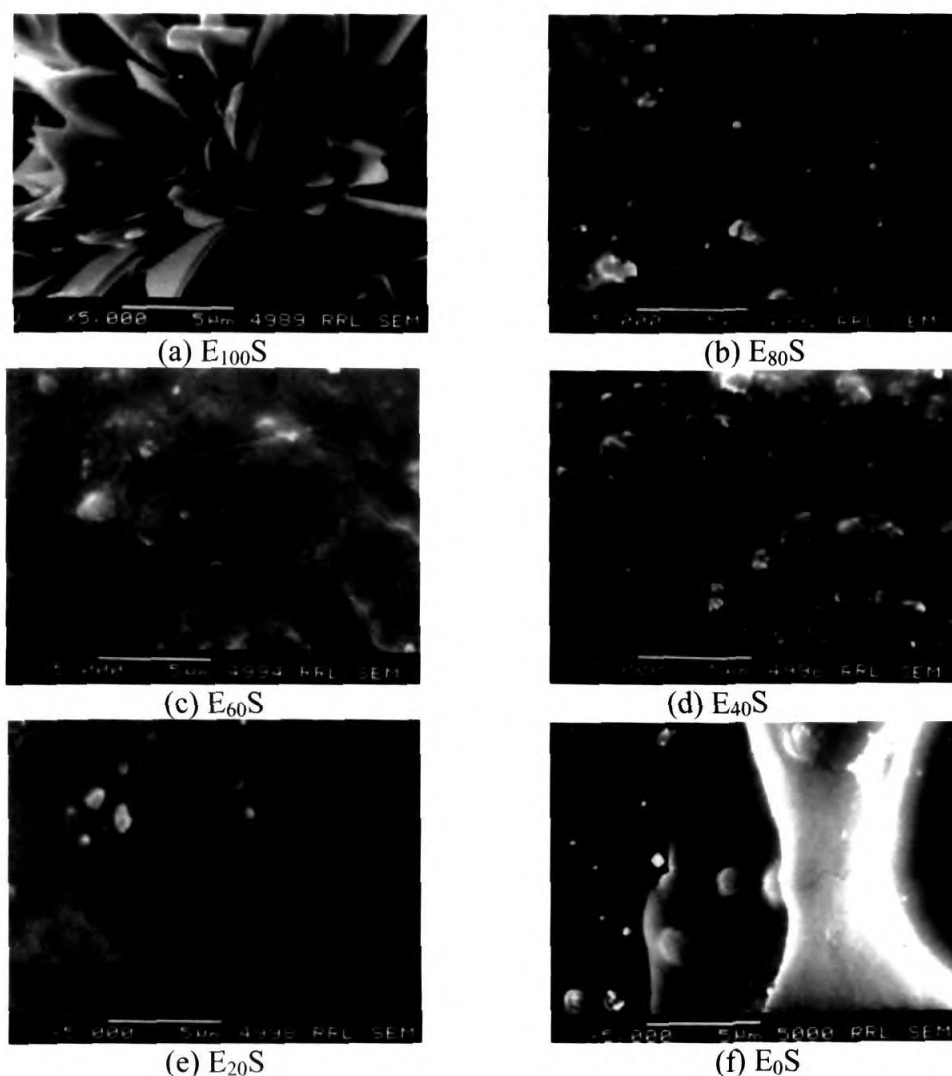


Figure 3.13 SEMs of tensile fractured specimens of EPDM/SBR blends:
(a) E₁₀₀S, (b) E₈₀S (c) E₆₀S (d) E₄₀S (e) E₂₀S & (f) E₀S

The results of DMA and DSC are complementary to this observation. It is noteworthy that the blend E₈₀S has given better tensile values. As SBR particles are agglomeration of the dispersed phase particles happen. Consequently,

miscibility of the blends decreases and the crack propagation increases in the blends E₆₀S, E₄₀S and E₂₀S as represented by Figures 3.13c, 3.13d and 3.13e. Figure 3.13f represents the SEM of pure SBR. The morphology studies show that a better distribution of dispersed phase exists in E₈₀ composition.

3.4 Model Fitting

The mechanical behaviour of EPDM/SBR blends has been modeled by using various composite models such as parallel, series and the Halpin-Tsai equation. The parallel model (highest upper-bound model) is given by the equation [23].

$$M = M_1\phi_1 + M_2\phi_2 \quad (3.3)$$

where M is the mechanical property of the blend and M_1 and M_2 are the mechanical properties of components 1 and 2, respectively and ϕ_1 and ϕ_2 are the volume fractions of the components 1 and 2 respectively. In parallel model, the components are considered to be arranged parallel to one another so that the applied stress elongates each of the components by the same amount. The arrangement of the components in the blend is in series with the applied stress in the lowest bound series model. The equation [24] used is,

$$1/M = \phi_1/M_1 + \phi_2/M_2 \quad (3.4)$$

The equation, according to Halpin-Tsai is

$$M_1/M = (1 + A_i B_i \phi_2) / (1 - B_i \phi_2) \quad (3.5)$$

where B_i is given as

$$B_i = (M_1/M_2 - 1) / (M_1/M + A_i) \quad (3.6)$$

In this equation, the subscript 1 and 2 represent the continuous and dispersed phase, respectively. The value of A_i for elastomer domains dispersed in hard continuous matrix is, 0.66. The experimental results are compared with the theoretical models in Figures 3.14 and 3.15. The graphs show that for tensile strength (Fig 3.13), the experimental value of E_{80S} lie relatively closer to the parallel model as the weight percentage of EPDM increases.

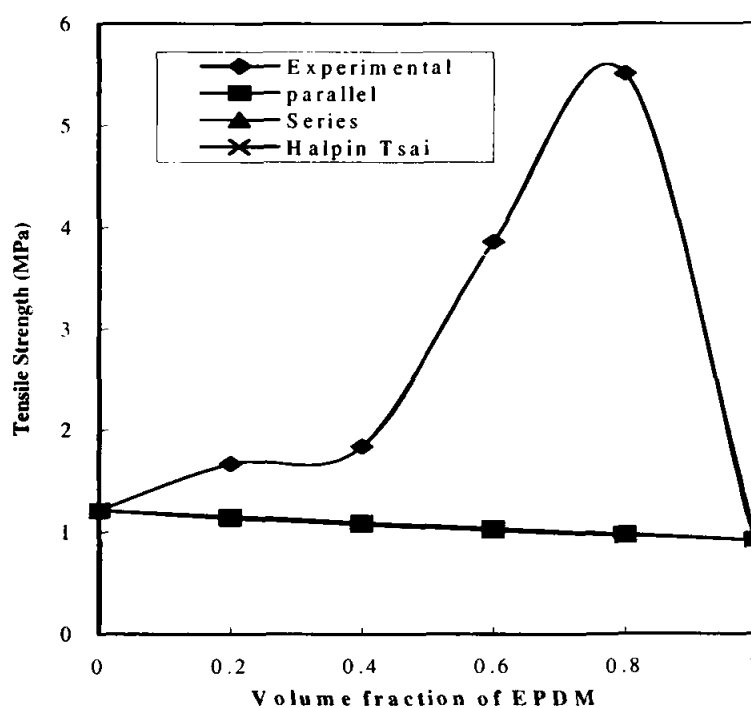


Figure 3.14 Comparison of experimental values with various models on the tensile strength of sulphur cured EPDM/SBR blends

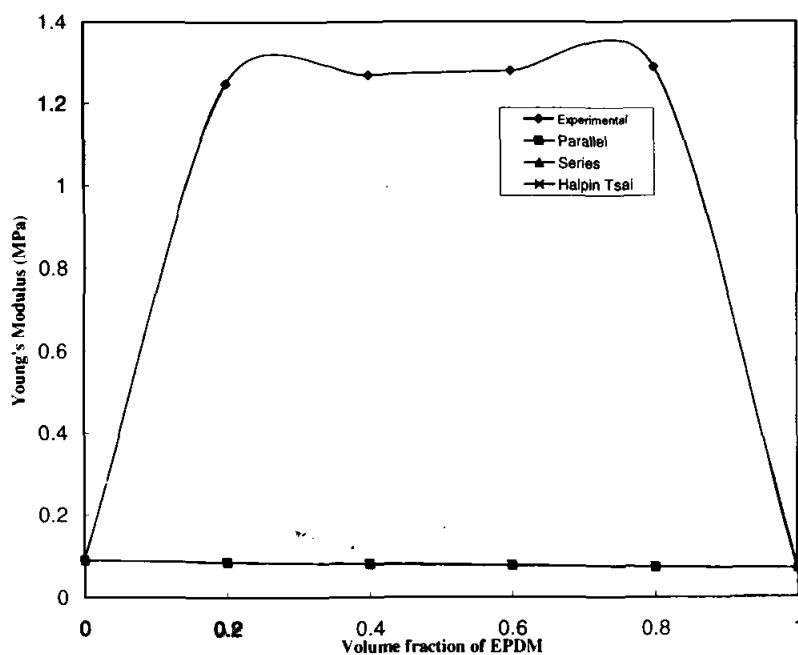


Figure 3.15 Comparison of experimental values with various models on the Young's modulus of sulphur cured EPDM/SBR blends.

3.5 Conclusion

The effects of blend ratio and three cure systems on the mechanical properties of EPDM/SBR blends were investigated. The properties such as elongation at break, tensile strength, tear strength and abrasion resistance increased with increase in EPDM content in the blends. A similar trend was also found for hardness in sulphur and mixed systems but in peroxide, the property was found to be decreased. Among the different vulcanizing systems, the tensile and tear strength were higher for the mixed systems compared to S and DCP systems. The elongation at break was higher for sulphur-cured blends due to the flexible polysulphidic linkages. The abrasion resistance of the blends was found to be increased with EPDM

content. The results have been interpreted in terms of the morphology of the blends as attested by SEM photographs. The experimental observation has been compared with different theoretical models.

References

1. A.Y. Coran and R. Patel, *Rubber Chem. Technol.* **53**,781 (1980).
2. A.Y. Coran and R. Patel, *Rubber Chem. Technol.* **54**,892 (1980)..
3. A.Y. Coran, R. Patel, *Rubber Chem. Technol.* **56**, 210 (1983).
4. A.Y. Coran and R. Patel, *Rubber Chem. Technol.* **56**, 1045 (1983).
5. J.E. Callan , B. Topcik, and F. P, Ford , *Rubber World* **151** (6) 60 (1965).
6. M. Imoto, *J. Soc. Rubber Ind. Jpn.* **42**, 439 (1969).
7. M.G. Oliveira and B.G. Soares, *Polymers and Polymer composites*, **9**,7,459 (2001).
8. A. Ghilarducci, S. Cervený, H. Salva, CL. Matteo, AJ. Marzocca, *Kautschuk GummiKunststoffe*, **54**, 382, (2001).
9. L.A. Utracki, *Two-phase polymer systems*. New York, Hanser Publishers (1991).
10. P. H. Poh and G.K Khok, *Polymer- Plastics Technology and Engineering*, **39**, 151, (2000).
11. M. Narkis, I. Reiter, S. Shkolnik, A. Siegmann, P. Eyerer, *J. Macromol. Sci.-Phys.* **B26** (1), 37 (1987).
12. S. Thomas, S.K. De, B.R. Gupta, *Kautschuk+Gummi Kunststoffe*, **40** (7), 665 (1987).
13. *Encyclopedia of Polymer Science and Technology*, Vol.6. Interscience publishers, New York, **399** (1967).
14. Krishna C. Bharanwal, *Basic Elastomer Technology*, The rubber Division, ACS, 2001.
15. C.M. Blow, C. Hepburn, *Rubber Technology and Manufacture*, Second Edition, p290, 299, Butterworths, London, 1981.
16. A.N.Gent and C.T.R. Pulford, *J. Mater. Sci.*, **19**, 3612, (1984).

17. B. Kuriakose and S.K. De , *J. Mater. Sci.*, **20**, 1864 (1985).
18. S.S.Bhagavan , D.K.Tripathy, and S.K. De, *J. Mater. Sci.* **6**,157(1987).
19. S.Thomas, B.Kuriakose, B.R. Gupta, and S.K.De, *J. Mater. Sci.* **21**, 711 (1986).
20. Hu.R.; Dimonic, V.L.; El-aasser, M.S.; Pearson, R.A; Hiltner, A; Mylonakis, S.G. Sperling, L.H., *J Polym. Sci Part B Polym. Phys*, **35**, 1501 (1997).
21. S.Thomas, BR.Gupta and S.K. de, *J. Vinyl Technol.*, **9**, 71 (1987).
22. Y. Fukahori, *Intl. Polym. Sci.Technol.*,T/76, **9**(1982).
23. S. Thomas and A. George, *Eur. Polym. Jnl.*, **28**,1451(1992).
24. L.E. Nielson, *Rheol. Acta*, **13**, 86 (1974)

Chapter 4

Mechanical Properties of Filled EPDM/SBR Blends

Abstract

The effects of fillers on the mechanical properties of EPDM/SBR blends were studied with special reference to the filler type and loading. The black fillers used for the study were high abrasion furnace (HAF) black and general-purpose furnace (GPF) black; and the nonblacks used were clay and silica. The mechanical properties such as modulus, elongation at break, tensile strength, tear strength and hardness were found to be better for HAF black filled blends compared to the other filler loaded systems. The optimum filler loading required for achieving higher mechanical properties was observed to be lowest for HAF black.

A part of the results of this chapter has been published in *J. of Appl. Polym. Sci.*, **93**, 2606 (2004).

4.1 Introduction

Fillers have been incorporated in rubbers for achieving properties, which can not be attained by vulcanization alone [1-5]. It was known to the technologists that rubbers could absorb substantial quantities of fine particle size fillers into their matrix for improved processibility, resistance to abrasion and tearing and enhanced hardness. Different types of carbon blacks and non-black fillers are used in rubber industry to achieve specific properties [6-9].

The effects of different carbon blacks on rubber properties are determined by their particle size, specific surface area and structure. In general, fillers with smaller particle size and higher surface area carbon blacks impart higher levels of reinforcement. Higher structure improves extrusion behaviour, compound modulus and compound viscosity [10]. Properties such as tensile strength and abrasion resistance are increased with increase in loading of carbon black to an optimum, beyond, which they could decrease. The performance, failure properties, and appearance of a rubber product are influenced by the dispersion of fillers in rubber compounds. There are several interesting works available in this regard to justify the role of black fillers in rubber compounds [11-15].

Reinforcing fillers such as silica and carbon black have a significant influence upon the properties of an elastomer, often increasing its mechanical durability and elastic properties [16]. The effects of filler reinforcement on elastomers further depend upon the polymer character. Danenberg [17] described the influence of different types of carbon blacks on SBR and found that small particle size black

fillers increased the tensile strength and abrasion resistance. There are several works available in literature studying the effect of different fillers on the vulcanizate properties of elastomers and their blends [18-26].

In this chapter, the mechanical properties of sulphur cured, filled EPDM/SBR blends have been discussed. The fillers used were HAF, GPF, clay and silica.

4.2 Results and Discussion

4.2.1 Cure characteristics

The cure characteristic of sulphur vulcanized, filled EPDM/SBR blends were determined. The blend ratio selected was 80/20 EPDM/SBR. The alkaline or acidic nature of fillers influences the cure rate of vulcanizates. The rheographs of filled blends are given in Figure 1. The p^H of furnace blacks used has been found to be between 7 and 9. It is clear from Table 4.1 that both HAF and GPF blacks have activated the cure rate and as a result the t_{90} values are found to decrease upon filler loading up to 80 phr. A delay of cure has been observed in blends filled with non-black fillers. Clay and silica are acidic fillers whose p^H values were noted as 5.5 and 3.5 respectively. Due to the higher acidic nature, the cure rate of silica filled blend has been found to be lowest. Among the different filled blends, the scorch time was found to be higher for the HAF black filled ones for given filler loading. This indicates the better scorch safety of HAF black filled compound compared to GPF filled system. The silica filled system exhibits better scorch safety among the non-black fillers.

Table 4.1 Cure characteristics of filled EPDM/SBR blends

Sample Code	Blend Ratio	Optimum Cure time, t_{90} (min)	Scorch Time, t_2 (min)	CRI
E ₈₀ S	SBR20/EPDM80	5.90	3.48	45.05
E ₈₀ S10HB	SBR20/EPDM80/HAF10	4.86	1.97	34.60
E ₈₀ S20HB	SBR20/EPDM80/HAF20	4.84	1.72	32.05
E ₈₀ S30HB	SBR20/EPDM80/HAF30	4.53	1.51	33.11
E ₈₀ S40HB	SBR20/EPDM80/HAF40	3.59	1.06	39.53
E ₈₀ S80HB	SBR20/EPDM80/HAF80	3.63	1.08	39.22
E ₈₀ S120HB	SBR20/EPDM80/HAF120	5.04	0.66	22.83
E ₈₀ S160HB	SBR20/EPDM80/HAF160	5.72	0.81	20.37
E ₈₀ S30GB	SBR20/EPDM80/GPF30	5.03	1.48	28.17
E ₈₀ S30SI	SBR20/EPDM80/SI30	8.18	2.19	16.69
E ₈₀ S30CL	SBR20/EPDM80/CL30	5.93	1.43	27.78

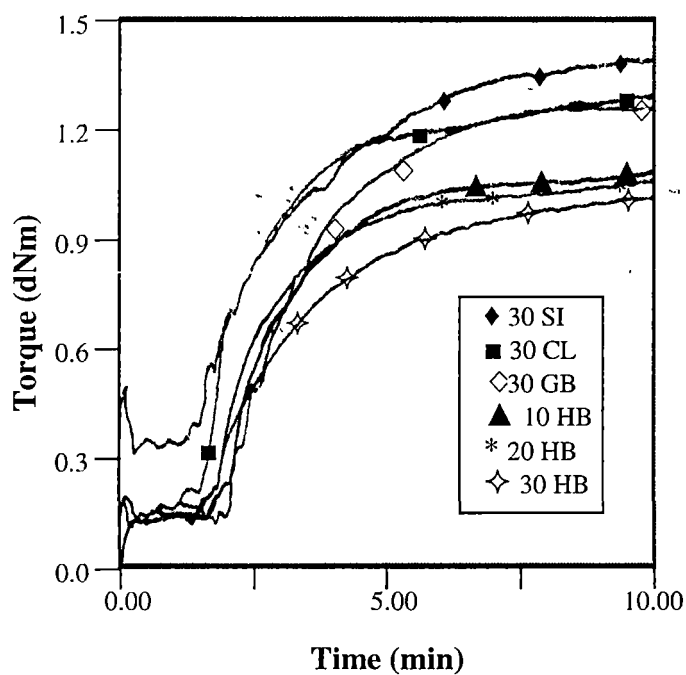


Figure 4.1 Rheographs of filled E₈₀S blends

4.2.2 Mechanical Properties

The physical properties of the filled blends such as modulus, elongation at break, tensile strength, tear strength and hardness have been studied. Figure 4.2 shows the effect of HAF black loading on the 300% modulus of the blend, E₈₀S. It is clear from the figure that the modulus increases progressively with increase in HAF black loading, even upto 80% carbon black loading.

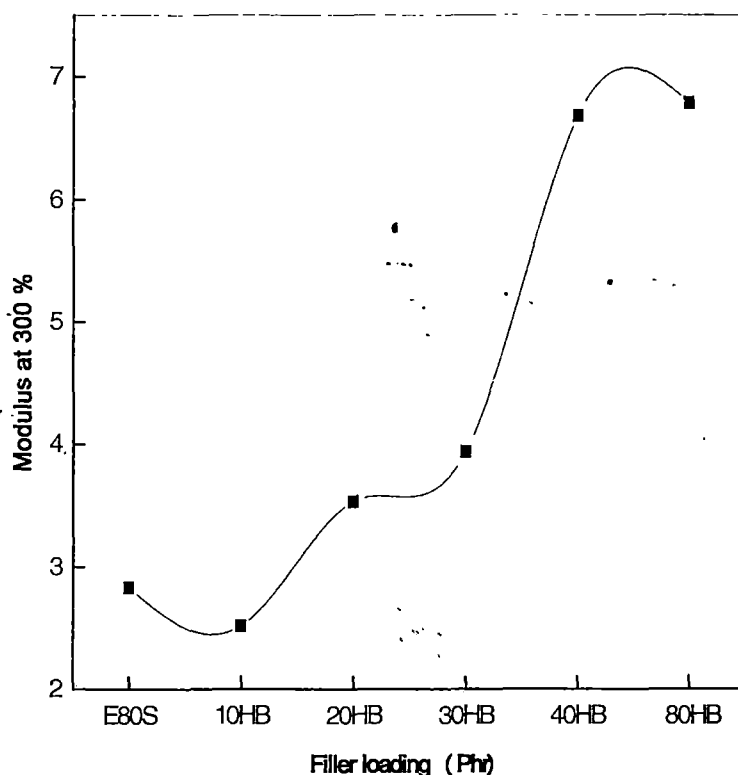


Figure 4.2 Effect of HAF loading on 300% modulus

Figure 4.3 shows the effect of higher HAF black loading on tensile strength. It is clear from the Figure that the Tensile Strength value is highest in 30 phr loading of HAF black. This shows that 30 phr is the optimum HAF loading for EPDM/SBR metrices. Further increment in filler loading can affect the macromolecular rearrangements during tension, resulting in lower tensile values.

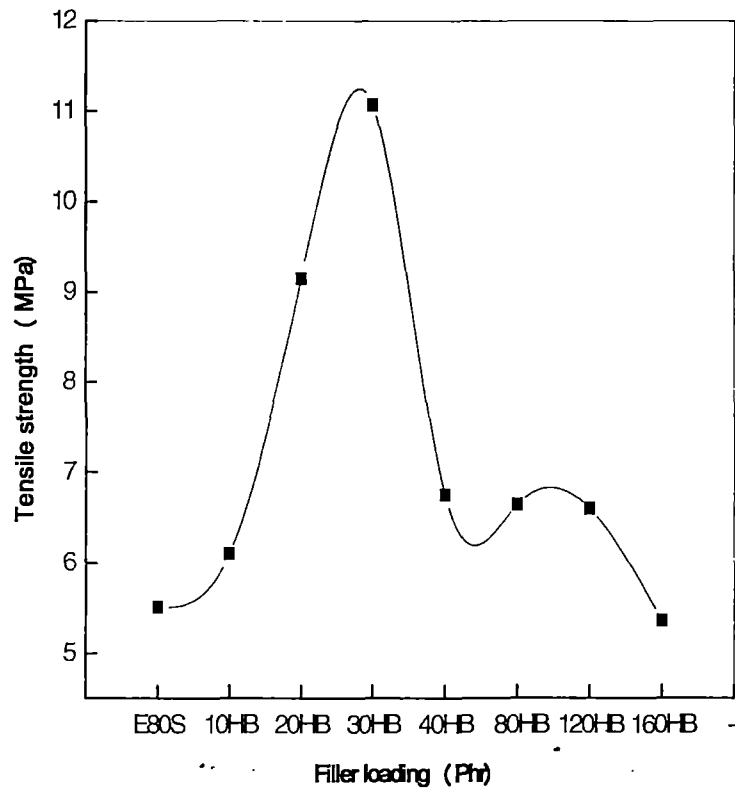


Figure 4.3 Effect of higher HAF black loading on the tensile strength

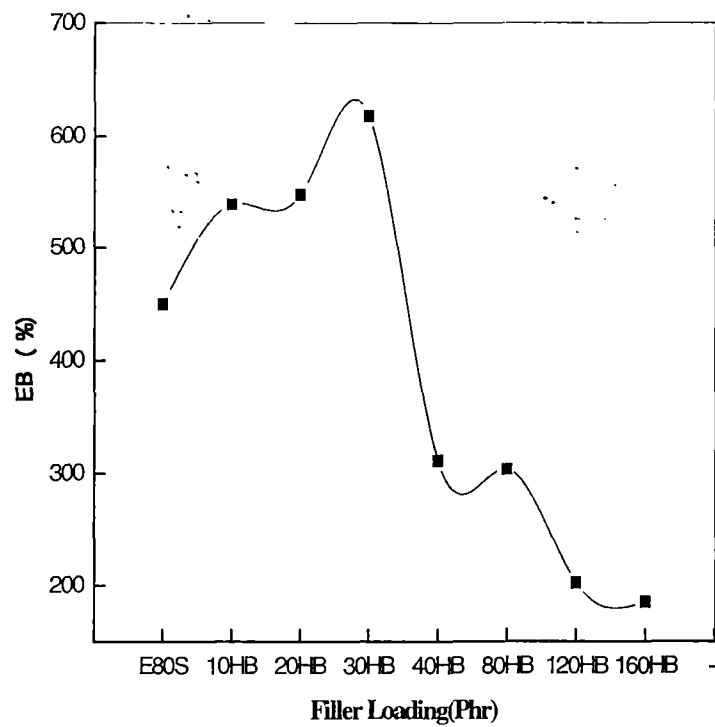


Figure 4.4 Effect of HAF black loading on EB (%).

Figure 4.4 represent the EB (%) of the given blend ratio, E₈₀S t higher HAF loadings. It can be seen that the EB values were decreased with increased crosslink density. In general, the EB of a vulcanizate with a high crosslink density is shorter than that of a vulcanizate with a low density because EB is a property inversely proportional to the degree of crosslink density [26].

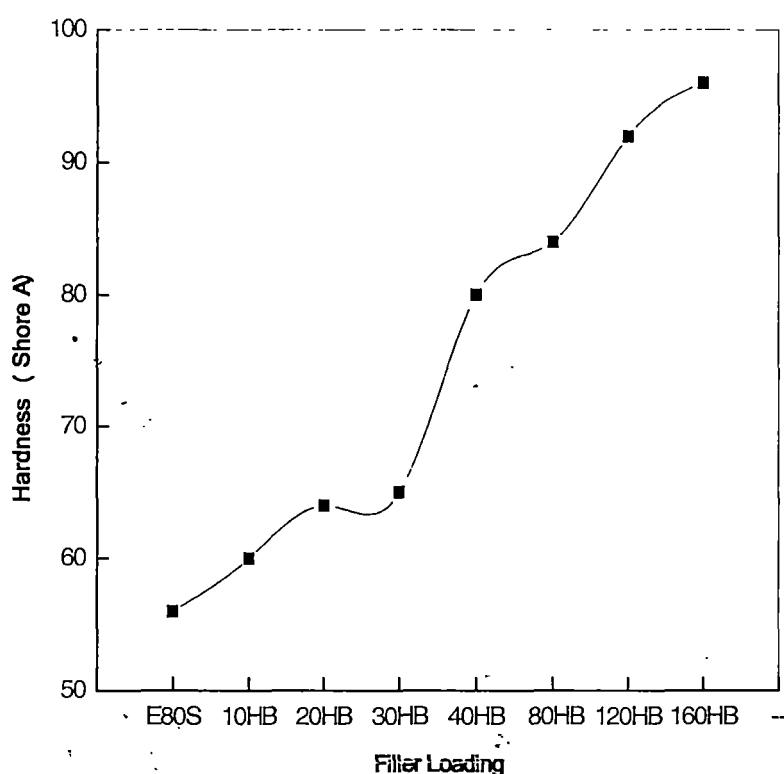


Fig 4.5 Effect of HAF black loading on hardness

It is also clear from the Figure 4.5 that the hardness increases progressively for every increase in the filler loading. Further it was noted that there was approximately a five point increase in hardness for every 10-phr HAF loading at the central part of hardness range (45-80 shore A).

Figure 4.6 represents the modulus at 300% of the filled blends for 30 phr filler loading of different fillers. All the fillers have been found to increase the modulus

of the matrix. It is also seen that the modulus is highest for HAF black filled blend and the values decrease in the order HB>GB> SI>CL. The increased modulus of HAF black filled blend clearly shows the better reinforcement effect.

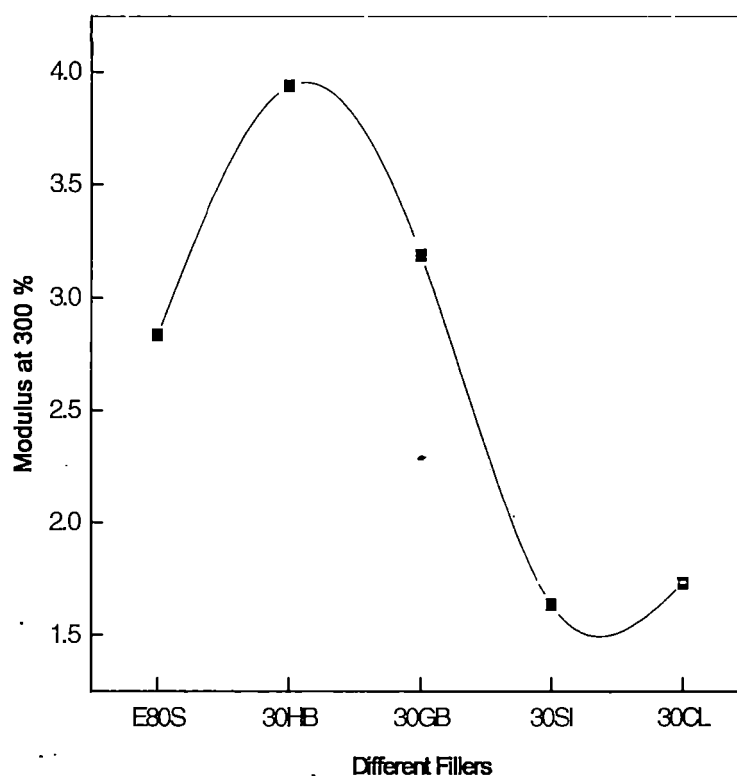


Figure 4.6 Effect of different fillers - 300 % modulus

Figure 4.7 shows the effect of 30 phr loading of black and non-black fillers on the tensile strength of E₈₀ blend. Among the various fillers, HAF black gives the highest TS values. The higher value of TS in HAF black filled blend can be attributed to the increased cross link density resulting from better reinforcement in addition to the discrete chemical cross linking formed through vulcanization. The filler effect on tensile values of the blends follow the order; HAF>GPF>clay>silica.

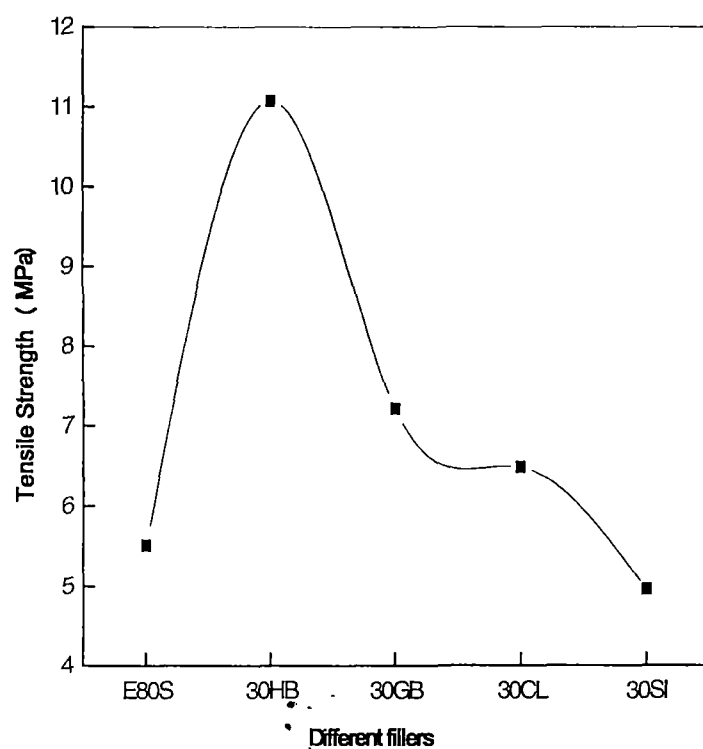


Fig 4.7 Effect of different fillers on the tensile strength

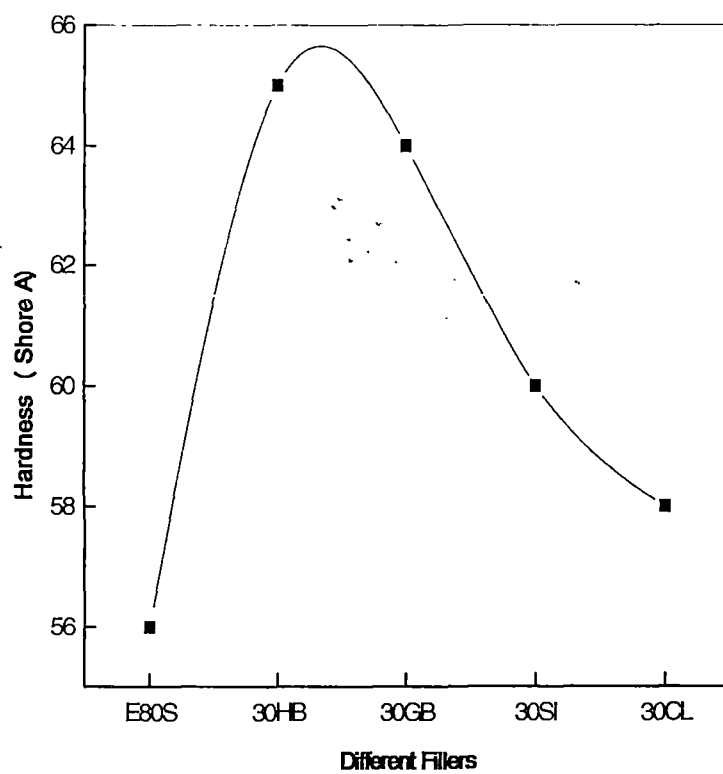


Fig 4.8 Effect of different fillers on hardness

From the Figure 4.8, it is clear that HAF black filled blend gives the highest hardness and the hardness among the blends with different fillers decreases in the order, HAF>GPF>SI>CL. To support the above observation, the crosslink densities of different filler loaded system were determined.

The effect of fillers on cross-link densities of E₈₀S has been given in Figure 4.9. The figure reveals that loading of blacks increase the crosslink density. The non-black fillers comparatively lack reinforcing effect and their contribution to cross-link densities is poor. However silica being reinforcing non-black filler, gives higher cross-link density compared to clay.

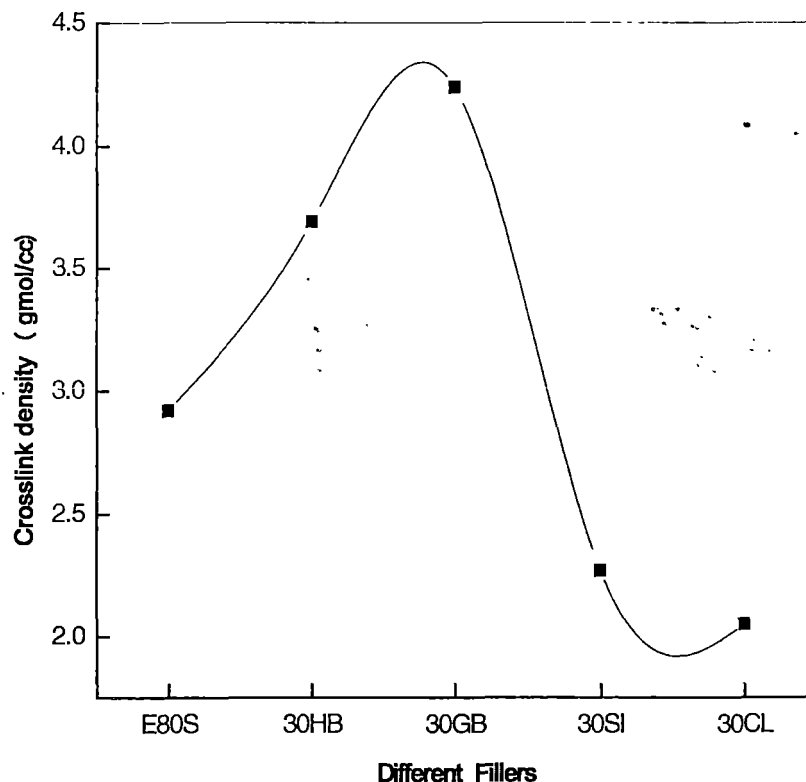


Figure 4.9 Effect of different fillers on crosslink density

4.2.3 Conclusion

The effect of two black fillers viz; HAF and GPF and two non-black fillers viz; silica and clay on the cure and mechanical properties of sulphur cured EPDM/SBR blend has been investigated. The black fillers showed better cure properties. The rate of cure was found to be higher in black filler loaded blends than in non-black filled systems. The t_{90} value was noted to be lowest for HAF black filled systems for a blend ratio. The scorch safety also was found to be good in HAF black filled system. Among the different fillers, the properties such as modulus, tensile strength and tear strength were observed to be highest in HAF black filled blends. The increase in properties by HAF black has been attributed to its better reinforcing effect. The cross-link density of the HAF filled blend was also found high. The other fillers also showed improved mechanical properties compared to the gum compound and followed the order; HB>GB>SI>CL.

References

1. A.R. Payne and R. E. Whittaker, *Rubber Chem. Technol.*, **45**, 1043 (1972).
2. J. A. C. Harwood, A. R. Payne, and R. E. Whittaker, *Rubber Chem. Technol.*, **44**, 690 (1971).
3. A. S. Hashim, B. Ashari, Y. Ikeda, S. Kohjiya, *Rubber Chem. Technol.*, **71**, 289 (1998).
4. S.S. Choi, *J. Appl. Polym. Sci.*, **79**, 1127, (2001).
5. U. Gori, A. Hunsche, Proceedings of the 150th Meeting of the *Rubber Division; American Chemical Society*: Washington, DC, Paper No. **76**, (1996).
6. P. K. Pal and S. De, *J. Appl. Polym. Sci.*, **28**, 3333, (1983).
7. F. L. Washough, *Rubber world*, Oct. 27 (1987).
8. F. F. Hanna, K. N. Abd- El- Nour, and S. L. Abd – EL- Messieh, *Polym. Deg. Stab.*, **35**, 49 (1992)
9. A. F. Younan, A. M. Gohneim, A. A. A. Tawfik and K. N. Abd-El- Nour, *Polym. Degrad. Stab.*, **49**, 251, (1995).
10. James E. Mark, Burak Erman, and Frederick R. Eirich, *Science and Technology of Rubber*, Academic Press Inc., USA, 1994.
11. W.M. Hess, *Rubber Chem. Technol.*, **64**, 386 (1991).
12. A.Y. Coran and J. B. Donnet. *Rubber Chem. Technol.*, **65**, 973 (1992).
13. A. Tubenkin, *Surface Topography*, **1**, 91, (1988).
14. A. E. Medalia, *Rubber Chem. Technol.*, **59**, 432, (1986).

15. W. A. Wampler, M. Gerspacher, and H. H. Yang, *Rubber World*, **210**, 1(1994).
16. J. Crank, G.S. Park, *Diffusion in Polymers*, Academic Press, New York, 1968
17. E. M. Daneberg, *Rubber Age* (N..Y) 85,431 (1959).
18. N. C. Das, T. K. Chaki, D. Khastgir, *Plastics Rubber and Composites*, **30**, 4, 162, (2001).
19. Sung- Seen Choi, *J. Appl. Polym. Sci*, **85**, 385, (2002).
20. DE.G. Hundiware, U.R. Kapadi, M. C. Desai, S. H. Bidkar, *J. Appl. Polym. Sci.*, **85**, 995, (2002).
21. W. M. Hess, R. A. Swor, P. C. Vegvari, *Kautsch Gummi Kunstst*, **38**, 1114, (1985).
22. E. Callan, W.M. Hess, C. E. Scott, *Rubber Chem. Technol*, **44**,814, (1971).
23. M. M. Chappius, M. H. Polley, R. A. Schultz, *Rubber Chem. Technol*, **28**, 253, (1955).
24. W.M. Hess, P. C. Vegvari, R. A. Swor, *Rubber Chem. Technol*, **58**, 350, (1985).
25. A. F. Younan, A. M. Gohneim, A. A. A. Tawfik, and K. N. Abd-el-Nour, *Polym. Deg. Stab.*, **49**,251(1995).
26. S.S. Choi, *J. Appl. Polym. Sci.*, **79**, 1127, (2001).

U. S. Patent & Trademark Office
Department of India
New Delhi

No: T1
11/10

Chapter 5

Thermal Analysis of EPDM/SBR Blends

Abstract

The thermal decomposition properties, the heat flow rate as a function of time and temperature and the glass transition temperatures of EPDM/SBR blends with respect to blend composition, cross-linking systems and fillers were studied. The thermogravimetric analysis (TGA) showed that the presence of EPDM in the blends reduced the rate of decomposition of SBR and enhanced the thermal stability of the blends. The blend with 80 wt % of EPDM showed the highest decomposition temperature. The TG and DTG curves of the filled blends indicated that both the initial and final decomposition temperatures of the blends increased by filler reinforcement. The weight losses of the filled blends were lower compared to unfilled ones. The thermal behaviour of uncross-linked and cross-linked blends also was studied by differential scanning calorimetry (DSC). It was observed that the introduction of cross-links shifted the glass transition temperature (T_g) towards higher temperatures. Among the different cross-linking systems, the blend with mixed system exhibited the highest T_g .

5.1 Introduction

A knowledge of the thermal decomposition process in polymers and their blends on heating is highly essential for developing many end products out of them. Thermogravimetry (TG) is an accepted technique in determining the thermal stability of polymers and polymer blends besides its use in compositional analysis. In thermogravimetric analysis, the analysis time is short and the sample weight required is small. The sample weight loss is measured as a function of temperature during the analysis. In differential scanning calorimetry (DSC) the energy difference (heat enthalpy) between the sample and the reference is measured. In DSC apparatus, the measured temperature difference is controlling the electrical power to the sample and the reference in order to keep them at the same temperature.

The thermal stability of polymers depends upon various factors. Schmidt et al [1] studied the thermal stability of the blends of polyaniline and EPDM, by TGA. The results indicated more than one stage of degradation and an improvement in the activation energy of degradation, after blending. Ahmed et al. [2] compared the thermal stability of sulphur, peroxide and radiation cured NBR/SBR vulcanizates, using TGA. They reported that the radiation cured formulation exhibited better thermal stability, compared to the other systems. Rocco et al.[3] used DSC and optical microscopy to determine the miscibility and crystallinity of blends of poly (ethylene oxide) (PEO) with poly (4-vinylphenol-co-2-hydroxyethyl methacrylate) (PVPh-HEM). A single glass transition temperature (T_g) was observed for all the blends, indicating miscibility. George et al. [4] reported that the oxidative degradation of cellulose took place in the amorphous region. They showed that less crystalline materials were degraded more rapidly by heat. The thermal stability of

component elastomers in blends is strongly influenced by the blend ratio. The increase in thermal stability in such blends can be due to the increased interaction between the constituent elastomers. Varghese et al. [5, 6] showed that the thermal stability of poly (vinyl chloride)/epoxidised natural rubber (PVC/ENR) was strongly influenced by the interaction between PVC and ENR. They also studied the miscibility of the components by measuring T_g , using DSC. A single T_g , between the T_g s of the components, revealed the miscibility of the systems. There are similar reports available in literature correlating T_g and miscibility [7, 8].

The present chapter discusses the effects of blend composition, cross-linking systems, and fillers on the thermal degradation behaviour of EPDM/SBR blends studied by thermogravimetry (TG) and differential scanning calorimetry (DSC). The total weight loss due to thermal decomposition, heat flow rate and the T_g of cross-linked and uncross-linked blends have been examined.

5.2. Results and Discussion

5.2.1 Thermogravimetric Analysis (TGA)

5.2.1.1 Effect of blend composition

The TG and derivative thermogravimetry (DTG) plots of sulphur cured SBR (E_{0S}) and EPDM (E_{100S}) are shown in Figures 5.1 and 5.2 respectively. The TG plot of SBR shows that the initial decomposition of the elastomer takes place at 330°C and that the final decomposition at 500°C. The weight loss observed during the initial and final decompositions were 4.85% and 95.59% respectively. The deflections noted in the curve around 300°C are attributed to the weight losses from highly volatile matters present in the elastomer. A residue of about 4.41% was obtained after the final decomposition, which contains metallic oxides as the chief

component. The weight losses at 350°C and 480°C were noted as 6.21 and 89.44 % respectively. In the DTG curve, the major peak has been found at 460°C, which corresponds to the highest decomposition temperature of the polymer.

Figure 5.2 shows that the initial decomposition of EPDM starts at 360°C and that the final decomposition completes at 510°C. The weight losses of the polymer noted at initial and final decomposition temperatures are 4.89 and 95.02 % respectively. A small deflection of the TGA plot in the beginning around 300°C can be due to the weight losses from highly volatile matters present as in the case of SBR.

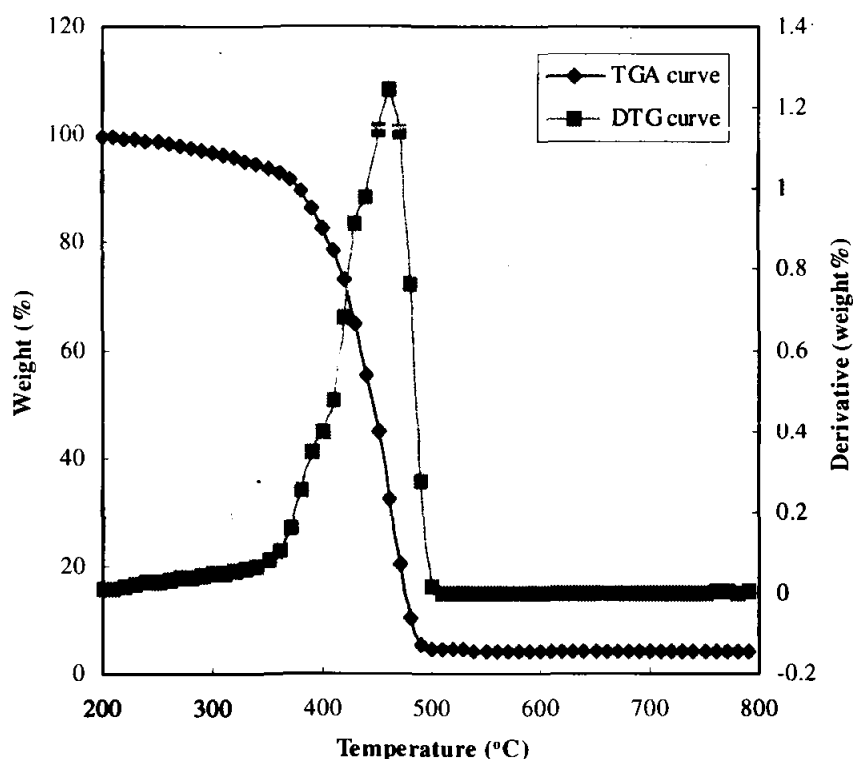


Figure 5.1 TG and DTG plot of sulphur cured SBR, E₀S.

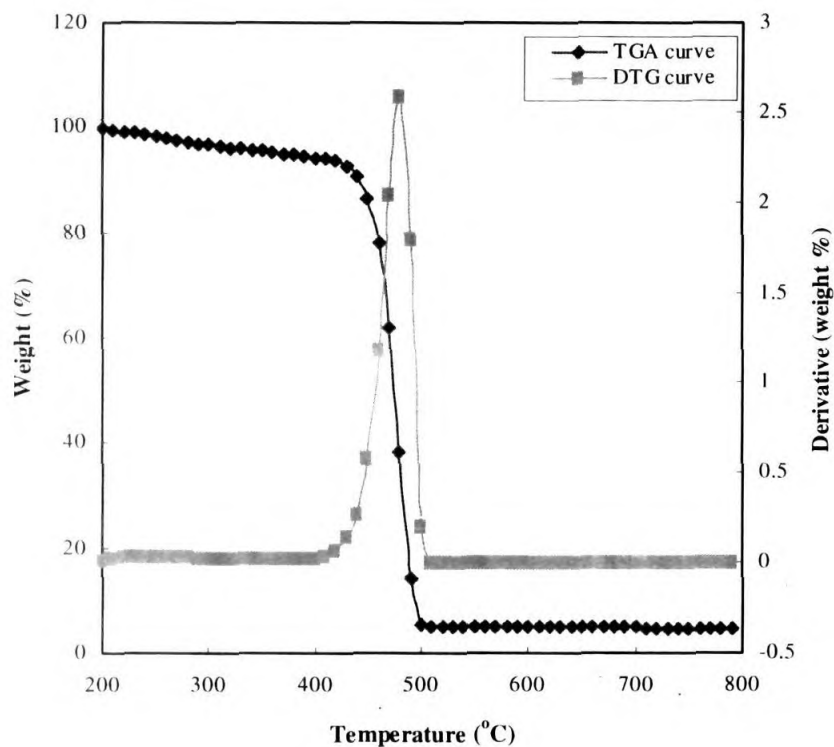


Figure 5.2. TGA plot of sulphur cured EPDM, E₁₀₀S

A residue of metallic oxides (4.98 %) was found after the final decomposition. The weight losses of EPDM at 350, 480 and 500°C were found to be 4.63, 61.87 and 94.83 % respectively. The major peak in the DTG plot shows that the maximum decomposition of the polymer occurs at 480°C.

The TG and DTG plots of sulphur cured EPDM/SBR blend in the blend ratio 40:60 (E₄₀S) are presented in Figure 5.3. The initial decomposition is observed at 340°C and the final decompositions at 500°C. The weight losses of the blend at initial and final decompositions are noted as 4.66 and 95.49 % respectively. The residue found after final decomposition was 4.5 %. The weight losses of the blend at 350

and 480 °C are noted as 5.25 and 79.04 % respectively. In the DTG curve, a major peak is observed at 480°C representing the maximum decomposition of the blend.

Figure 5.4 shows the TG and DTG plots of sulphur cured EPDM/SBR blend in the blend ratio, 80:20 (E₈₀S). The initial and final decomposition temperatures noted in this blend were 360 and 510°C respectively. The weight loss noted at initial decomposition temperature was 4.63 % and that at final decomposition temperature was 95.67%. A residue of 4.34 % was observed after final decomposition. The weight losses of the blends observed at 350, 480 and 500°C were 4.16, 67.27 and 95.40% respectively. A major peak has been noted in the DTG curve at 480° C, which corresponds to the maximum decomposition of the blend.

The TG and DTG plots of the unfilled EPDM/SBR blends show that the thermal behavior of the blends is not significantly different from that of the individual polymers. However, the initial and final decomposition temperatures of the blends are higher than that of pure SBR. Obviously, the thermal stability of SBR is improved by the incorporation of EPDM.

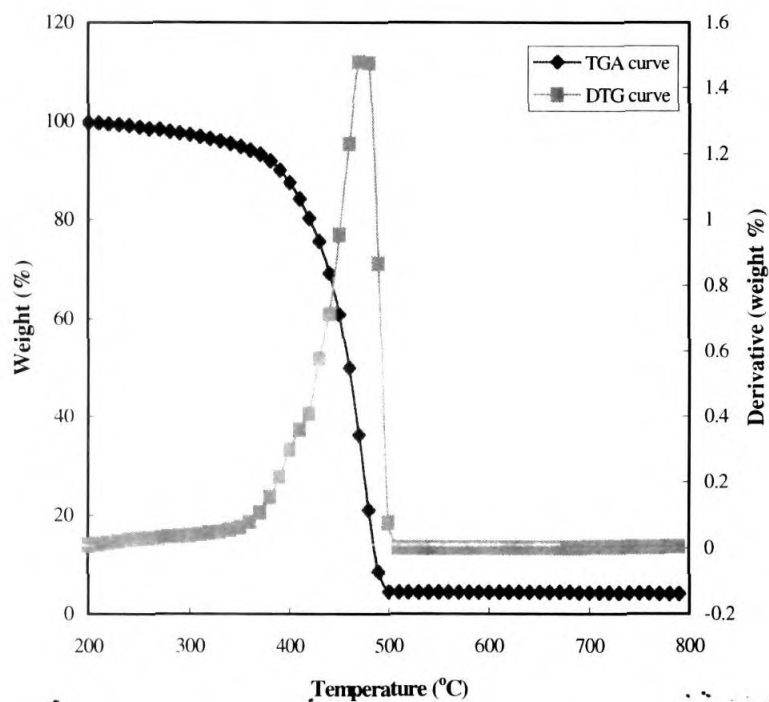


Figure 5.3 TG and DTG plot of sulphur cured EPDM/SBR blend, E₄₀S

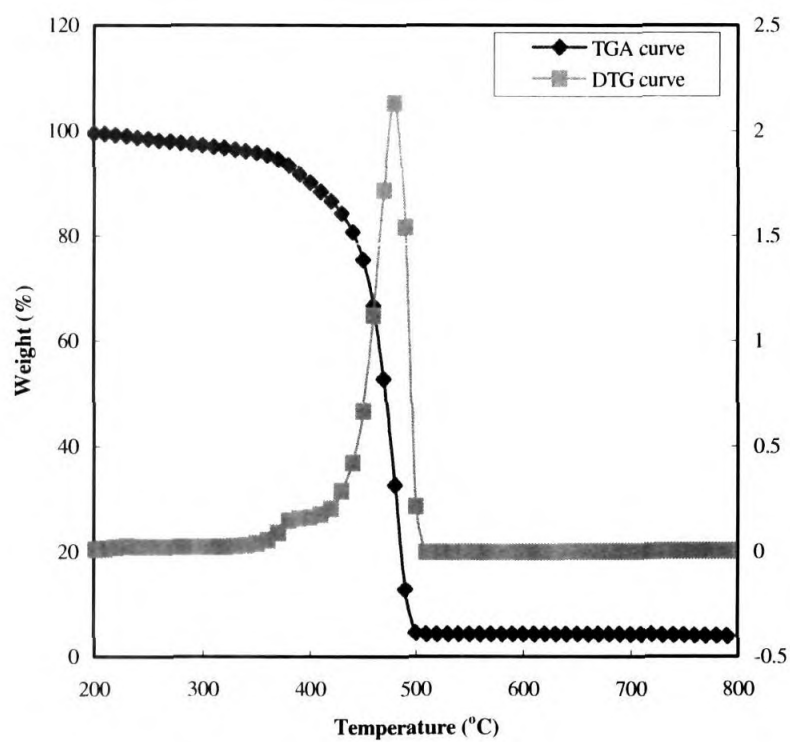


Figure 5.4 TG and DTG plot of sulphur cured EPDM/SBR blend, E₈₀S-

The decomposition temperatures of different blends at various stages are shown in Table 5.1 (a & b)

Table 5.1a Decomposition temperatures of different EPDM/SBR blends (unfilled)

Samples	Decomposition temperature (°C)		
	Initial	Maximum	Final
E ₀ S	330	460	500
E ₄₀ S	340	480	500
E ₈₀ S	360	480	510
E ₁₀₀ S	360	480	510
E ₈₀ P	370	470	500
E ₈₀ M	330	470	500

It is also noteworthy that the initial decomposition temperature of peroxide cured system is higher than those cured by the other two systems. A comparison of weight losses of the blends at 350, 480 and 500°C is given in Table 5.2. It is seen that the weight losses at each temperature significantly lowers with increase in weight % of EPDM. This again shows that the relative thermal stability of the blends depends on the weight % of EPDM in the blends.

Table 5.2 Weight losses of EPDM/SBR blends (unfilled and filled) at different temperatures

Samples	Weight loss (%)			Residue weight (%)
	350°C	480°C	500°C	
E ₀ S	6.21	89.44	95.59	4.41
E ₄₀ S	5.25	79.04	95.50	4.50
E ₈₀ S	4.16	67.27	95.40	4.60
E ₁₀₀ S	4.63	61.87	94.83	5.17
E ₈₀ P	3.77	75.85	94.67	5.33
E ₈₀ M	5.65	77.31	93.00	7.00
E ₈₀ S10HB	4.37	66.50	84.21	15.79
E ₈₀ S20HB	5.18	49.64	78.30	21.70
E ₈₀ S30HB	5.24	45.48	72.72	27.28
E ₈₀ S10GB	5.07	55.28	85.75	14.25
E ₈₀ S10SI	4.88	69.47	86.54	13.46
E ₈₀ S10CL	4.56	58.19	87.08	12.92

5.2.1.2 Effect of cross-linking systems

The effect of different cross-linking systems on the thermal behavior of the blends was also studied. The three cure systems used were sulphur (S), dicumyl peroxide, DCP (P), and a mixture of sulphur and DCP (M). The DCP cured system showed the highest initial decomposition temperature indicating its good thermal stability. The C-C linkages introduced between the macromolecular chains by DCP were less flexible with highest bond energy (Table 5.3).

Table 5.3 Bond length and bond energies of different types of chemical linkages

Bond type	Bond length ($^{\circ}\text{\AA}$)	Bond energy (Kcal/mol)
C-C	1.54	85
C-S	1.81	64
S-S	1.88	57

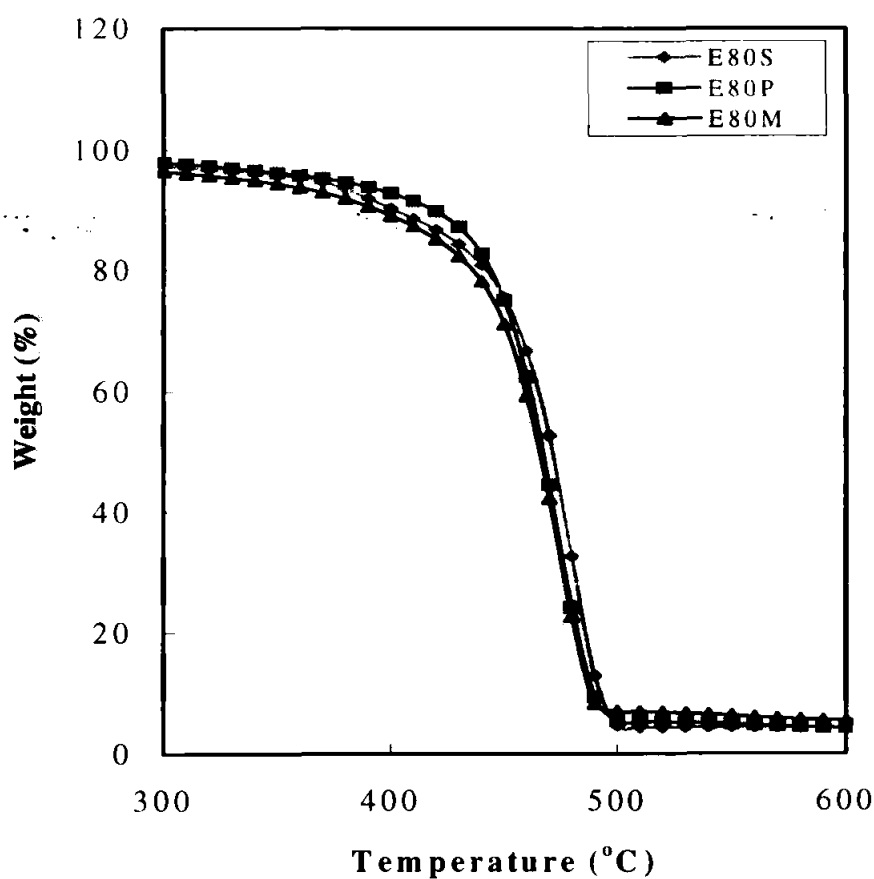


Figure 5.5 Influence of cross-linking systems on the thermal degradation properties of EPDM/SBR blends- Comparison of TGA plots

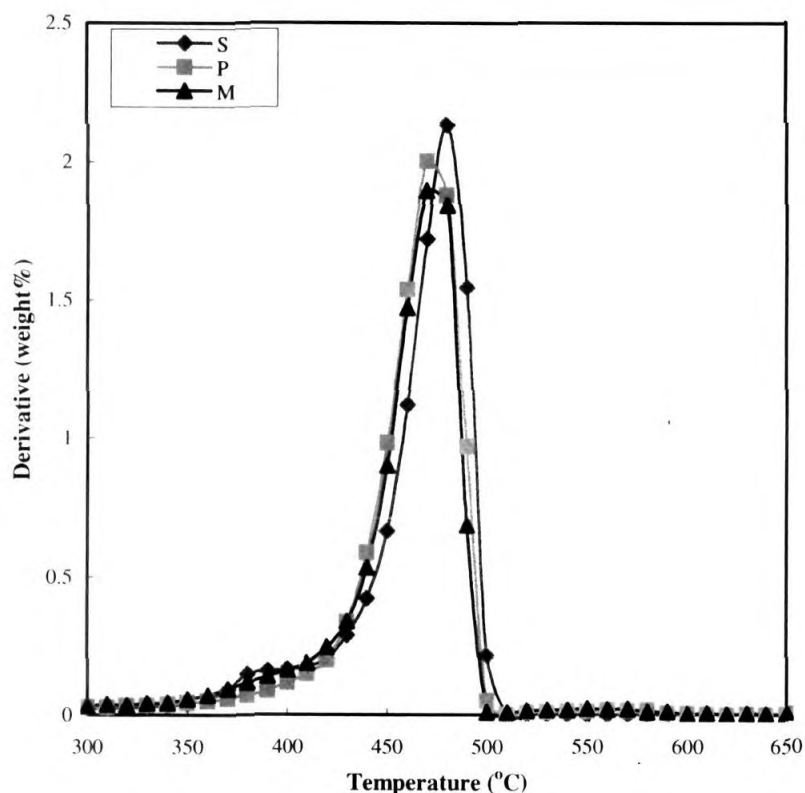


Figure 5.6 Influence of cross-linking systems in the DTG plots of EPDM/SBR blends.

A comparison of the TG and DTG curves of E₈₀S, E₈₀P & E₈₀M is given in Figures 5.5 & 5.6 respectively. The highest peaks correspond to the maximum decomposition temperature. It has been found that the decomposition temperature of peroxide cured blend is relatively higher than sulphur and mix cured blends. The weight losses at different temperatures for E₈₀S, E₈₀P and E₈₀M are also given in Table 5.2. The weight loss is lowest for 'P' at a given temperature which clearly indicates its thermal stability. The results showed that peroxide cured system has given the lowest weight loss at initial decomposition temperature indicating the better resistance towards thermal ageing. The weight losses observed for sulphur cured blends at 350, 480 and 500°C are given in Table 5.2.

5.2.1.3 Effect of fillers

Figures 5.7 to 5.12 show the TG and DTG plots of filled E₈₀S blend with different fillers. The initial decomposition temperatures show a decrease, compared to the unfilled E₈₀S. This can be due to the volatile matters in the fillers and the proportionate decrease in polymer volume in the vulcanizate, by the filler presence. However the final decomposition temperatures have been found to increase in all the filled blends. It is clear from the Figures 5.7, 5.8 and 5.9 that an increase in HAF black loading increases the final decomposition temperature. The peaks in the DTG curves are noted around 500°C in all the blends at which maximum decomposition occurs. The weight losses of the filled blends for the blend ratio, E₈₀S, at 350, 480 and 500°C are given in Table 5.2. The residue weight % of the blends are also given in the same Table. It is clear from these values that the weight losses decrease in all the filled blends with an increase in residue weight compared to the unfilled ones, indicating the increased thermal stability of the blends due to the effect of filler reinforcement. This can be further understood from the weight losses at a definite temperature, for example the weight losses at 480°C for E₈₀S, E₈₀S10HB, E₈₀S20HB and E₈₀S30HB are 67.27, 66.50, 49.64 and 45.48 % respectively.

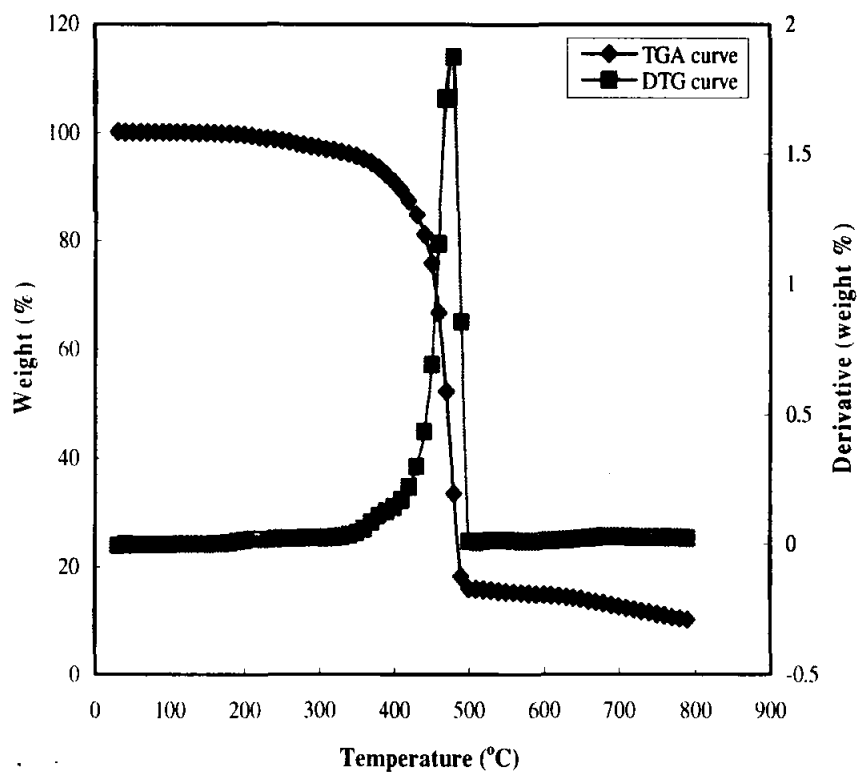


Figure 5.7 TG and DTG plots of EPDM/SBR blend, E₈₀S10HB

Table 5.1b Decomposition temperatures of different EPDM/SBR blends (filled)

Samples	Decomposition Temperature °C		
	Initial	Maximum	Final
E ₈₀ S10HB	350	480	500
E ₈₀ S20HB	340	480	510
E ₈₀ S30HB	330	490	510
E ₈₀ S10GB	340	480	510
E ₈₀ S10SI	350	480	500
E80S10CL	350	480	510

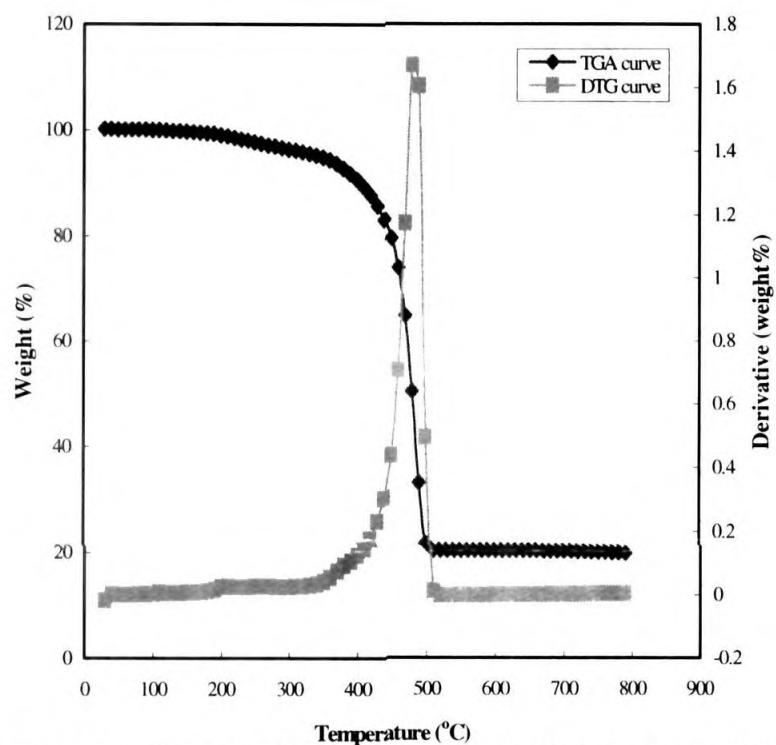


Figure 5.8 TG and DTG plots of EPDM/SBR blend, E₈₀S20HB

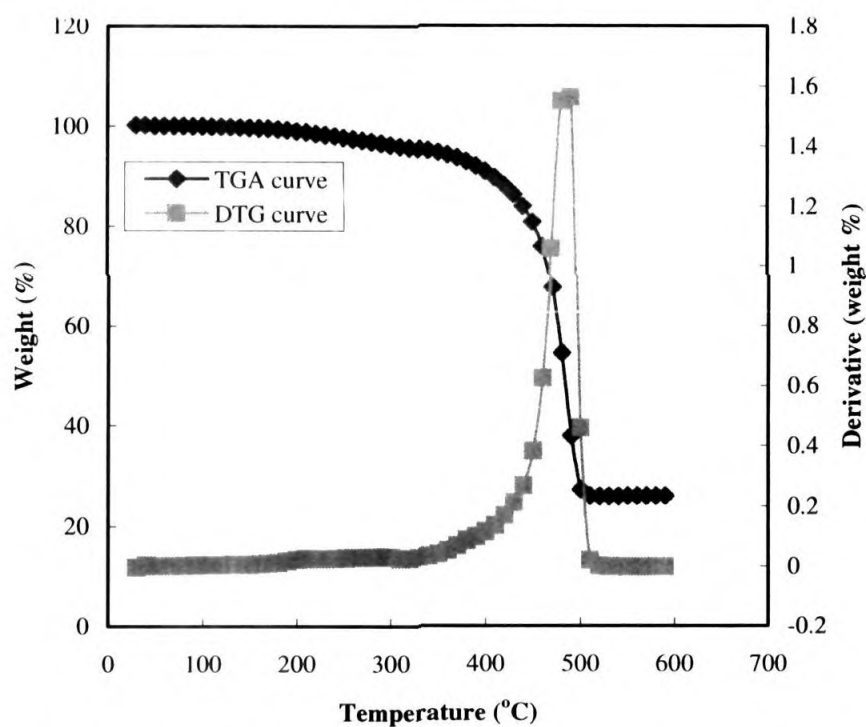


Figure 5.9 TG and DTG plots of EPDM/SBR blend, E₈₀S30HB

Figures 5.10, 5.11 and 5.12 show the extent of degradation of unfilled blends could also be reduced by the incorporation of fillers GB, silica and clay.

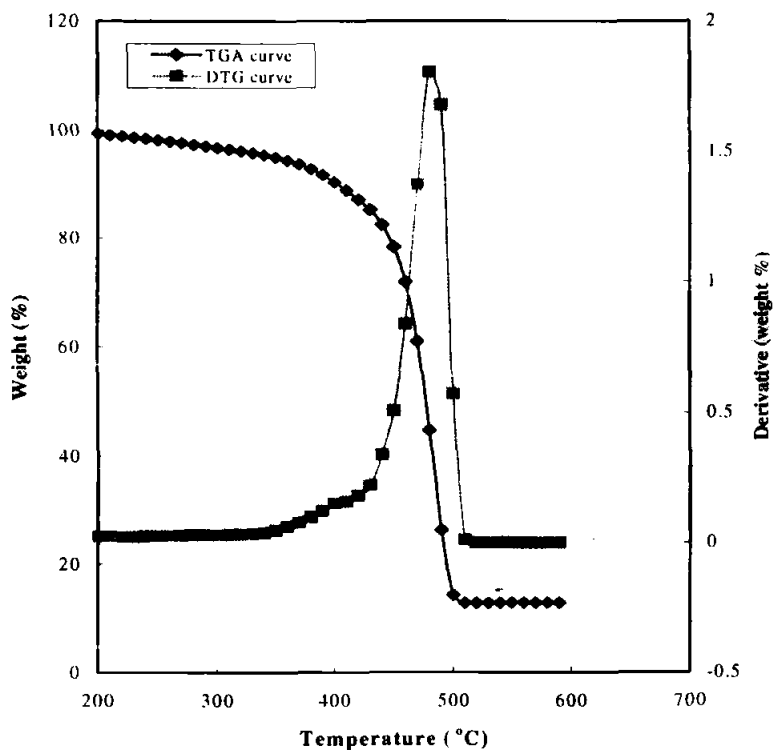


Figure 5.10 TG and DTG plots of EPDM/SBR blend, E₈₀S10GB

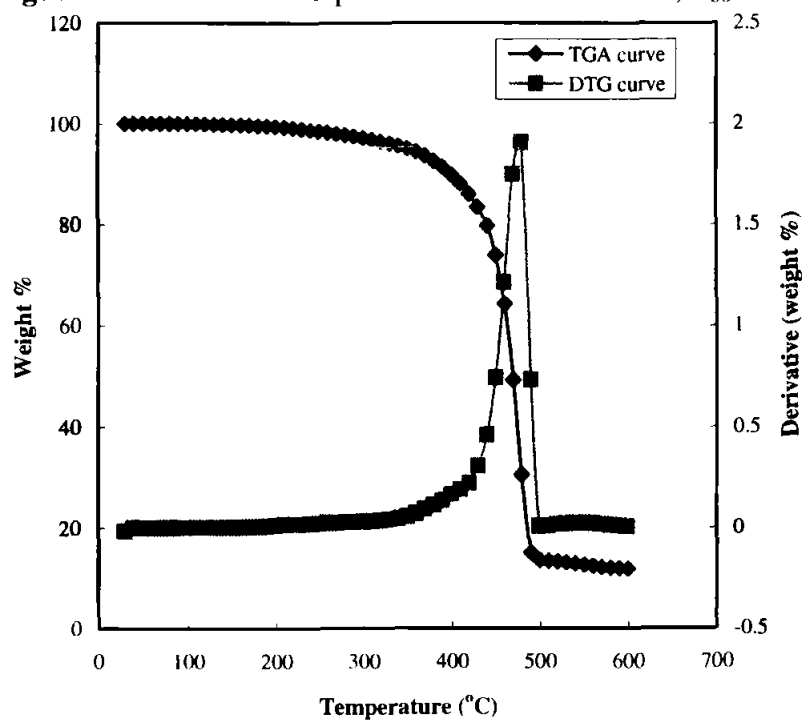
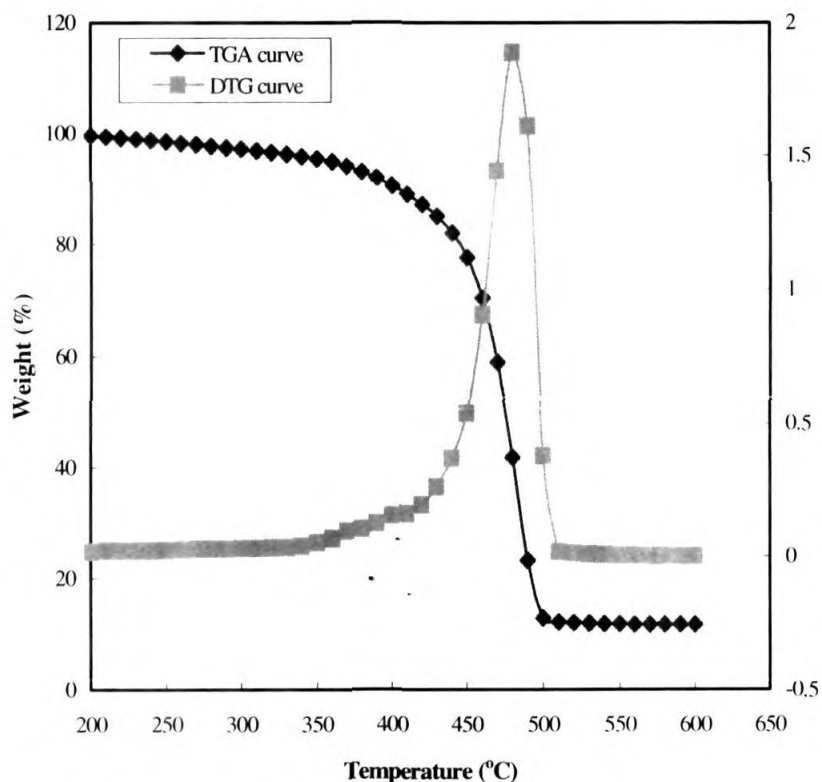


Figure 5.11 TG and DTG plots of EPDM/SBR blend, E₈₀S10SI**Figure 5.12** TG and DTG plots of EPDM/SBR blend, E₈₀S10CL

5.3 Differential scanning calorimetry (DSC)

The DSC plots of uncross-linked EPDM, SBR and EPDM/SBR blend (80:20) are shown in Figure 5.13. The mid point of the transition is recorded as the glass transition temperature (T_g). The T_g s of the raw polymers, SBR and EPDM are found to be -50.47 and -45.70°C respectively and that of E₈₀ blend is -46.75°C . It is interesting to note that for the blend, E₈₀, the T_g value comes in between those of SBR and EPDM indicating their better compatibility at this composition.

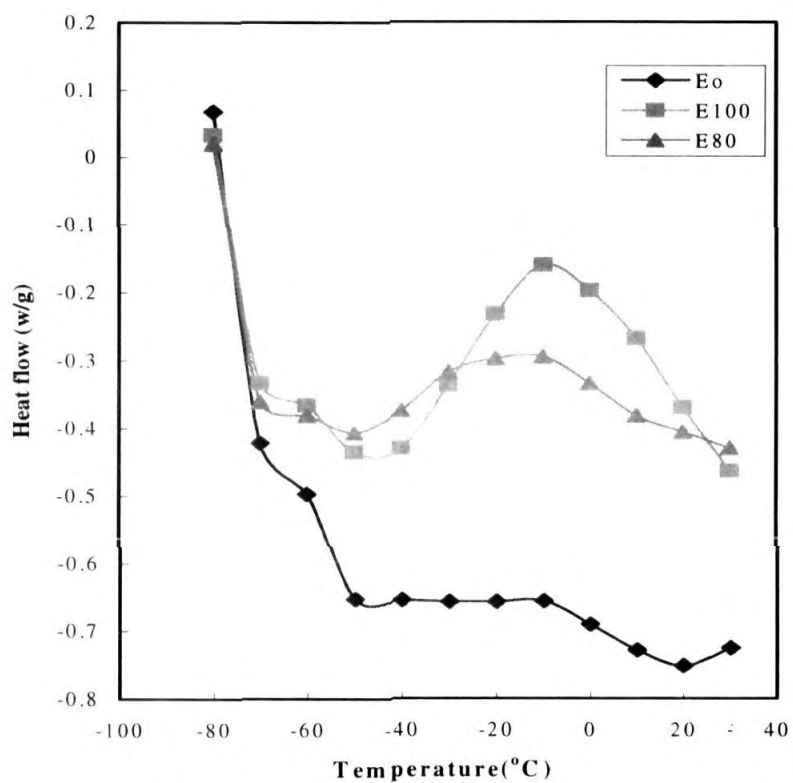


Figure 5.13 DSC plots of E₀, E₁₀₀ and E₈₀

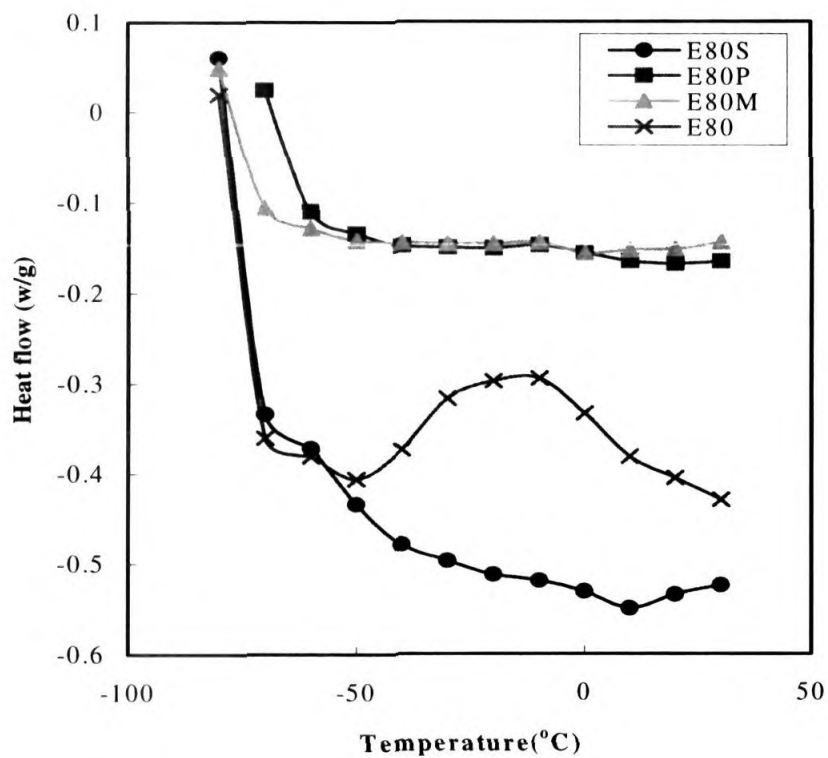


Figure 5.14 DSC plots of E₈₀S, E₈₀P, E₈₀M and E₈₀.

This result clearly supports the better mechanical properties exhibited by the 80/20 EPDM/SBR composition. Burfield and Lion [9] reported that for typical sulphur cures, using either a conventional or an efficient vulcanization systems the T_g of NR is increased by 3°C. It is also reported that a peroxide cure causes an increase of almost 1°C for each part of peroxide used per hundred parts of rubber. The DSC traces of uncross-linked E_{80} and cross-linked $E_{80}S$, $E_{80}P$ & $E_{80}M$ are presented in Figure 5.17.

Table 4 T_g of EPDM/SBR blends determined by DSC

Sample	T_g (°C)
E_0	-50.47
E_{80}	-46.75
E_{100}	-45.70
$E_{80}S$	-46.57
$E_{80}P$	-45.23
$E_{80}M$	-43.95

It is found that the introduction of cross-links shifts the T_g towards higher temperature. Among the three cure systems, the mixed system exhibits the highest T_g . T_g also increases with carbon black loading, but the increase is limited to about 2 to 6°C for 50 phr N330 carbon black. Carbon black and other fillers introduce a non-linear viscoelastic effect into the blends with different strains. This has tremendous implications for the elastomers dynamic mechanical properties.

5.4 Conclusion

The thermal properties of EPDM/SBR blends have been studied with special reference to the effects of blend composition, cross-linking systems and fillers, using TGA and DSC. The thermal analysis showed that the initial decomposition temperature increased with increase in EPDM content. The DTG peaks corresponding to the maximum decomposition also showed the same trend. This clearly established the increased thermal stability resulting from the blending of heat resistant EPDM with SBR. With reference to cross-linking systems, the initial decomposition temperature of DCP cured blend was higher than the initial decomposition temperatures of sulphur and mixed cured blends. It shows the higher stability of DCP cured blends due to the presence of strong C-C bonds. The comparatively lower initial decomposition temperatures of sulfur and mixed cured systems may be due to the weak C-S or S-S bonds. A comparison of the % residue of different blends at 350°C, 450°C and at 500°C showed that the % residue of EPDM rich blends was higher than the other blends. The studies on the influence of fillers on thermal stability showed that all the fillers; HAF black, GPF black, silica and clay increased the thermal stability. The decomposition temperatures and the % residue were found to be increased in all the filled systems. The better thermal stability was noted for HAF filled systems. The single T_g of the EPDM/SBR blend obtained from DSC measurements showed that the two polymers are compatible in the blend ratio 80:20. These results are complementary to the observations from DMA, morphology analysis, mechanical property measurements and ageing studies.

References

1. V. Schmidt, S.C. Domenech, M.S. Soldi, E.A. Pinheiro and V. Soldi, *Polym. Degrad. Stab.*, **83**, 519 (2004).
2. S. Ahmed, A. A. Basfar and M.M. Abdel Aziz, *Polym. Degrad. Stab.*, **67**, 319 (2002).
3. A.M. Rocco, C.E. Bielschowsky and R.P. Pereira, *Polymer*, **44**, 361 (2003).
4. J.George, S.S. Bhagavan and S.Thomas *J of Thermal analysis*, **47**, 1121 (1996)
5. K.T. Varghese, Kauts. *Gummi Kunst.*, **41**, 114 (1988)
6. K.T. Varghese, G.B. Nando P. P. De and S. K. De, *J. Mater. Sci.*, **23**, 3894 (1988)
7. P. P. Lizymol and S. Thomas, *Polym. Deg. Stab.*, **41**, 59 (1993)
8. P. P. Lizymol and S. Thomas, *Thermochimica Acta*, **233**, 283, (1994)
9. D.R. Burfield and K.L. Lim, *Macromolecules*, **16**, 1170 (1983).

Chapter 6

Dynamic Mechanical Analysis of EPDM/SBR Blends

Abstract

The effects of blend ratio, crosslinking systems, fillers and frequency on the viscoelastic response of EPDM/SBR blends were analysed over a temperature range of -70°C to 130°C . The storage modulus decreased with increase in SBR content. The loss modulus values and the tan delta results showed E₈₀S as the composition having the highest compatibility. Among the different curing agents used, the DCP cured blends exhibited the highest storage modulus. The reinforcing fillers were found to reduce the tan δ peak height. The experimental data on storage modulus have been compared with theoretical predictions.

6.1 Introduction

One of the remarkable features of polymers is their sharply expressed viscoelastic properties those give rise to a unique complex of fundamental physical and mechanical properties [1]. Polymers display properties of both elastic solids and liquids. This leads to a specific relationship between the stress σ , changing according to a periodic law for viscoelastic bodies, and the strain ε :

$$\sigma = E^* \varepsilon \quad (6.1)$$

Here E^* is the complex modulus of elasticity equal to

$$E^* = E' + i E'' \quad (6.2)$$

The real part of the modulus of elasticity E' is called the dynamic modulus of elasticity or the storage modulus, and the imaginary part E'' , the loss modulus. The phase shift between the sinusoidally varying stress and strain is expressed as

$$\tan \delta = E'' / E' \quad (6.3)$$

which is called the mechanical loss factor or the loss tangent. One of the simplest and most reliable ways of determining the above components is dynamic mechanical analysis.

Dynamic mechanical testing is a versatile and sensitive tool enabling a complete exploration of the relaxational mechanisms in viscoelastic materials [1,2]. The most common use of DMA is the determination of (T_g), where the molecular chains of a polymer obtain sufficient energy, usually from thermal sources, to overcome the energy barriers for segmental motion. This is also the region where the maximum loss of applied energy is observed, usually as a peak in the traces of

$\tan \delta$ or loss factor vs. frequency or temperature. Several interesting studies on the dynamic mechanical properties of various systems are available in literature [6-12].

6.2 Results and Discussion

6.2.1 Storage modulus

The magnitude and nature of changes in the dynamic storage moduli of elasticity are determined both by the intermolecular and intramolecular interactions, which are having significant influence on the different physical states of a polymer system [1-3].

6.2.1.1 Effect of blend ratio

Figure 6.1 shows the effect of blend ratio on the storage modulus of sulphur cured EPDM, SBR and their blends at different temperatures. At lower temperature below T_g , pure EPDM (E_{100}) shows the highest modulus while pure SBR (E_0) shows the lowest. This can be correlated with the different structural characteristics of EPDM and SBR. Modulus in the glassy region is the effect of intermolecular interactions [2, 3]. EPDM being crystalline and having better intermolecular interactions in the absence of any bulky groups such as the phenyl group as in SBR, shows the highest modulus. The blends $E_{80}S$ and $E_{40}S$ show intermediate values.

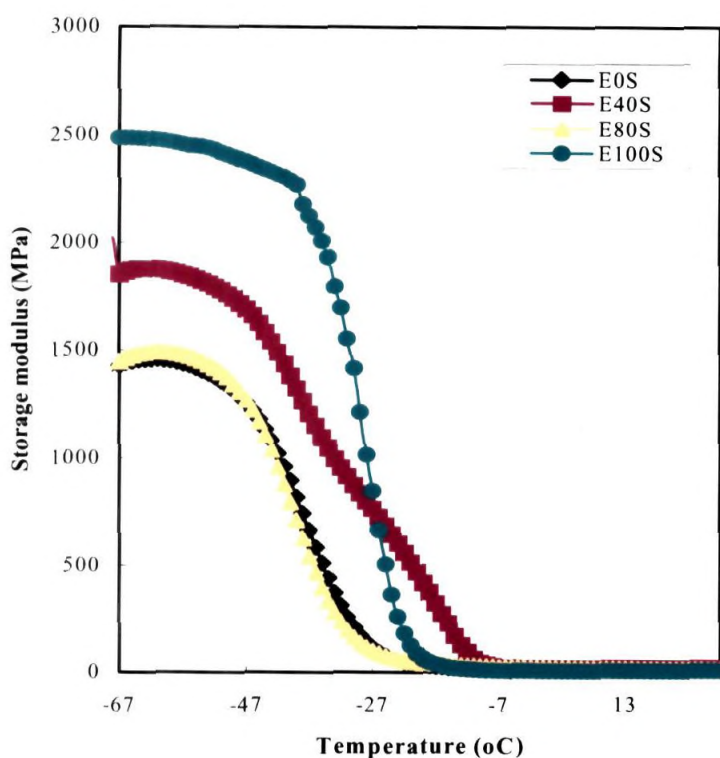


Figure 6.1 Effect of temperature (-67 to 30°C) on the storage modulus of sulphur cured EPDM, SBR and EPDM/SBR blends as a function of blend ratio at a frequency of 10 Hz

Both the rubbers and their blends show single transitions indicating the absence of immiscible phases. However, the blend E₄₀S shows a broad transition with a shoulder in the middle indicating the presence of heterogeneous zones in the blend. This indicates partial miscibility of this blend ratio [4]. This is also indicated in the lower mechanical properties of the blend, which is due to the poor interfacial adhesion, as discussed in chapter 3.

In the rubbery region (above T_g), E₀S shows the highest modulus followed by E₄₀S, E₈₀S and the lowest by E₁₀₀S. Modulus in the rubbery region is contributed by the ability of the macromolecules to resist the intermolecular slippage. As a result, SBR having stronger molecular interactions than the nonpolar EPDM shows the

highest modulus. The blends having SBR matrix (E_{40S}) again shows the higher modulus as compared to that having EPDM matrix (E_{80S}) for the same reason.

6.2.1.2 Effect of curing agents

The effect of curing agents on the storage modulus of E_{80S} composition cured by different agents viz; sulphur, DCP and mixed are shown in the Figure 6.2. The peroxide cured blend (E_{80P}) exhibits a higher storage modulus in the glassy region as compared to the sulphur-cured blend (E_{80S}). This is attributed to the stiff C-C crosslinks in E_{80P} vis-à-vis the more flexible C-S_x-C bonds in E_{80S} . Figure 6.3 shows the influence of temperature on the storage modulus of E_{80} , cured with three curing agents viz., sulphur, DCP and mixed above ambient conditions (30-120°C). It has been noted that the storage modulus is highest for sulphur-cured systems compared to DCP and mixed cured systems.

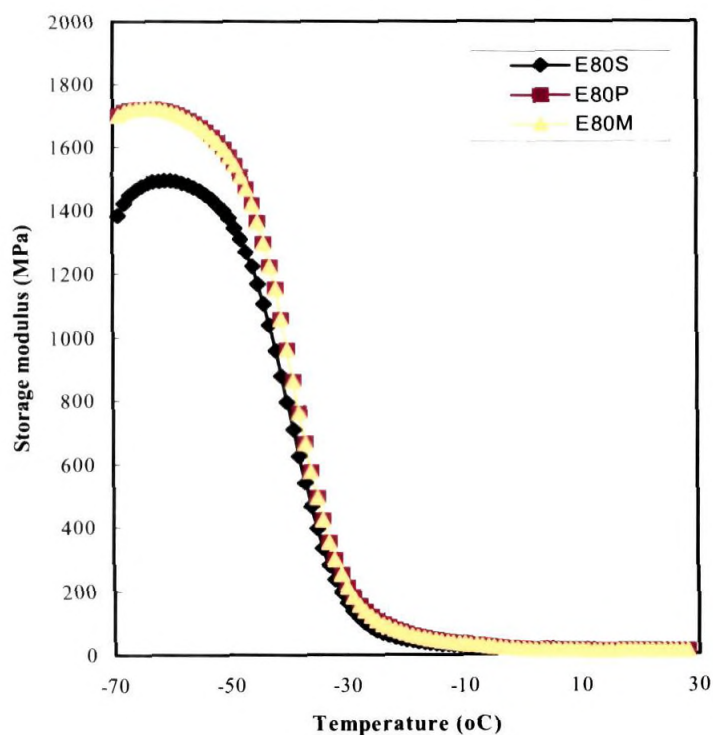


Figure 6.2 Effect of temperature (-70 to 30°C) on storage modulus of E_{80S} , E_{80M} and E_{80P} at a frequency of 10Hz

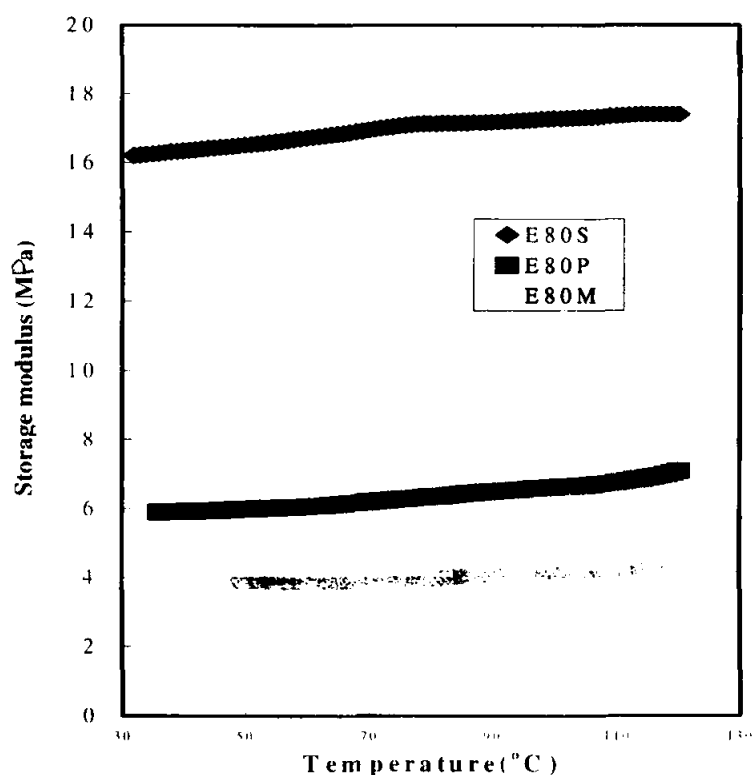


Figure 6.3 Effect of temperature (30-120°C) on the storage modulus of E₈₀ cured by sulphur, DCP and mixed systems at a frequency of 10 Hz

6.2.1.3 Effect of fillers

Figures 6.4 and 6.5 represent the effect of fillers on the storage moduli of EPDM/SBR blend, E₈₀S. The incorporation of reinforcing fillers has been found to increase the modulus and the effect is visible in the various plots of E₈₀S. Among the black fillers, HAF has been found to exhibit higher modulus compared to GPF. This is attributed to the reinforcing effect of HAF which provides the highest modulus in the blend followed by GPF, silica and clay. [5] HAF a better reinforcing agent interact well with the blends and shows a high modulus. Among the non-black fillers examined, clay has been found to exhibit lower modulus compared to silica. This has been due to the non-reinforcing nature of clay, as it has no interaction with the rubber matrix. Though silica is also reinforcing filler, in this case, its effect is less because of the fact that the interaction between the polar silica filler and the mostly

nonpolar EPDM or SBR matrix is very poor. GPF is a semi- reinforcing filler and hence shows a modulus in between HAF and silica.

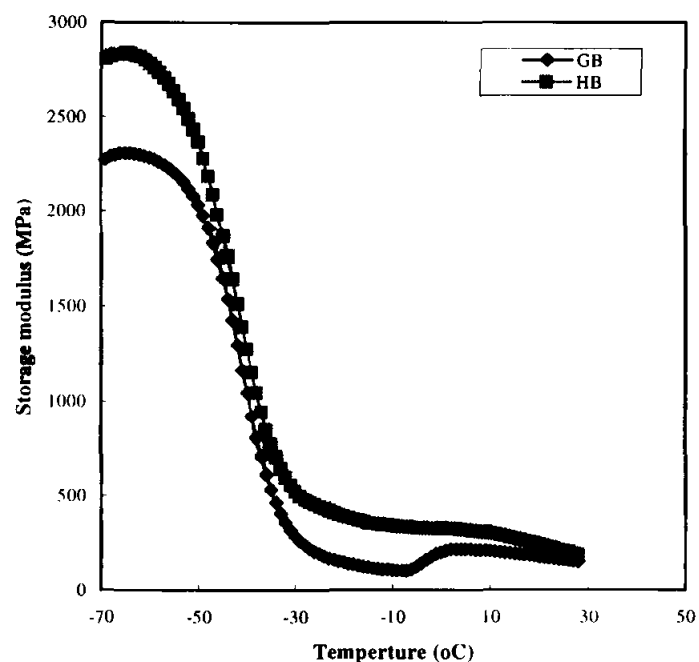


Figure 6.4 Effect of temperature (-70 to 30°C) on the storage modulus of E₈₀S10HB and E₈₀S 10GB at a frequency of 10 Hz

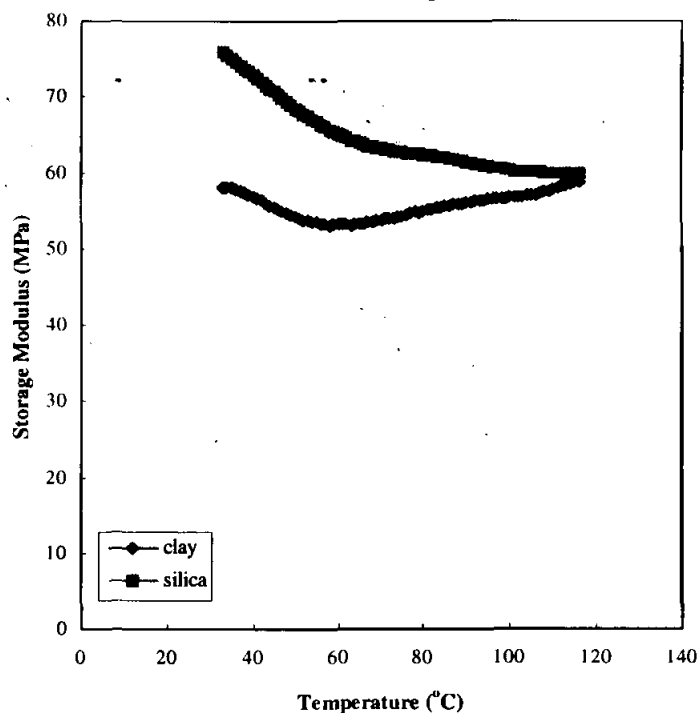


Figure 6.5 Effect of temperature (30-120 °C) on the storage modulus of clay and silica filled EPDM/SBR blend, E₈₀S at a frequency of 10Hz

6.2.2 Loss Modulus

6.2.2.1. Effect of blend ratio

The effect of blend ratio on the loss modulus of sulphur cured EPDM, SBR and their blends in different ratios are shown in Figure 6.6. The pure rubbers and the blend E₈₀S except E₄₀S show single glass transition peaks in the loss modulus vs temperature peaks indicating again the presence of a homogeneous phase in the blends. E₄₀S exhibits two peaks at -36°C and -15°C indicating again the presence of two phases. The peak at -36°C corresponds to SBR (pure SBR also have the transition at -36°C) and the one at -15°C relates to EPDM. Pure EPDM has the glass transition at -28°C. The difference may be

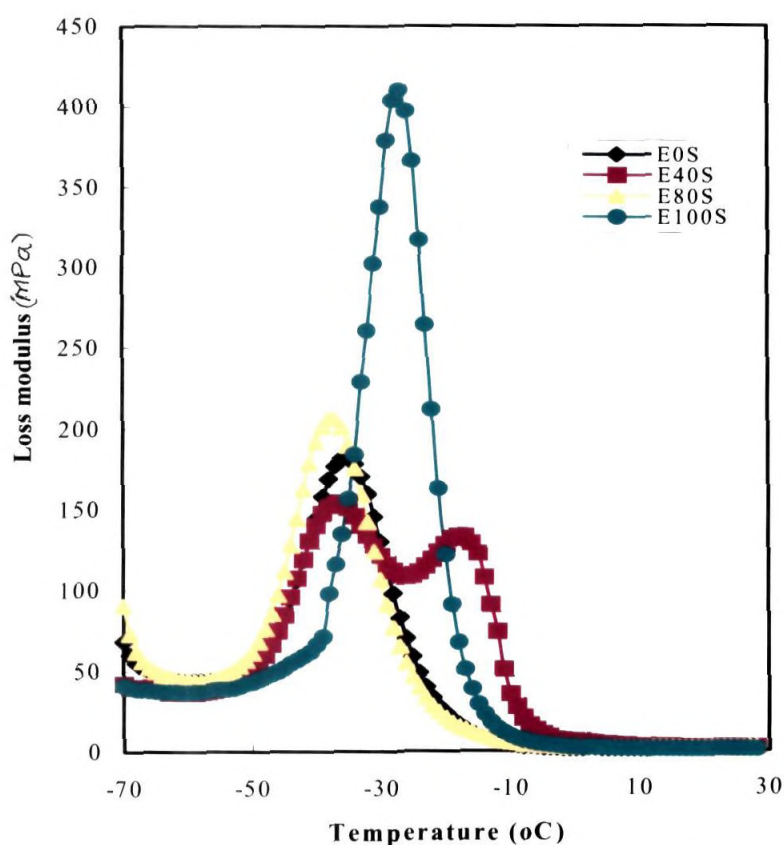


Figure 6.6 Effect of temperature (-70 to 30°C) on the loss modulus of sulphur cured EPDM, SBR and EPDM/SBR blends at a frequency of 10Hz

due to the compacting of the EPDM macromolecules dispersed as particles in the SBR matrix, which restricts the molecular movement. Any type of molecular interactions that affects the molecular motion leads to a shift in the transition to higher temperature, as more energy is needed to overcome the interactions [3,4]. The influence of temperature (30-120 °C) on the loss modulus of unvulcanized blend components EPDM, SBR and the blend E_{80} were determined and have been shown in the Figure 6.7. The Figure shows that pure EPDM has given an increase in loss modulus while the values of SBR and the blend almost remain constant with increase of temperature.

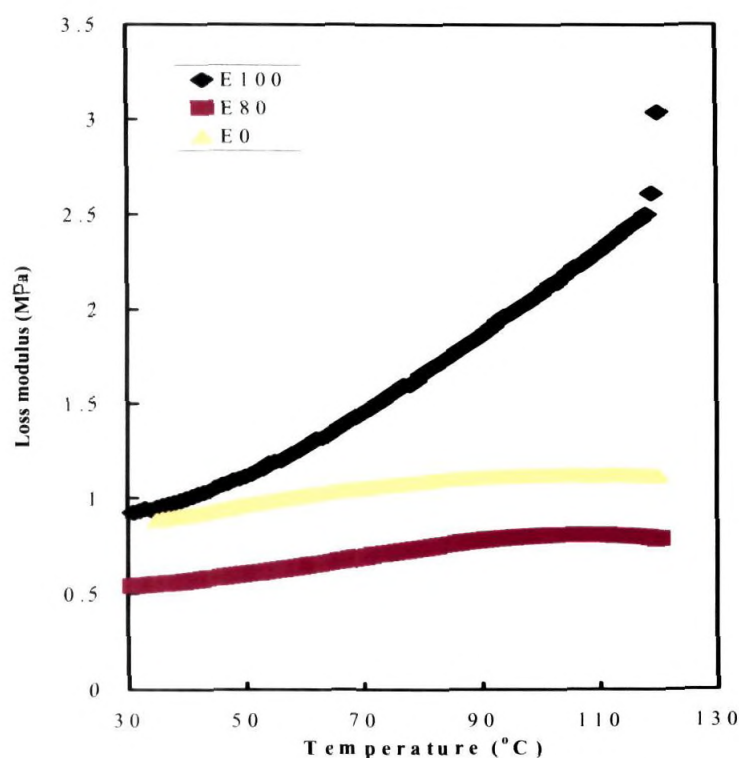


Figure 6.7 Effect of temperature (30-120°C) on the loss modulus of unvulcanized blend, E_{80} , EPDM and SBR at a frequency of 10 Hz

6.2.2.2 Effect of curing agents

Figure 6.8 shows the influence of curing agents on the loss modulus of the blend E_{80} as a function of different curing agents viz sulphur, DCP and mixed. The E_{80} blend does not show any significant effect in the loss modulus behaviour on changing the curing agents, as compared to the storage modulus value.

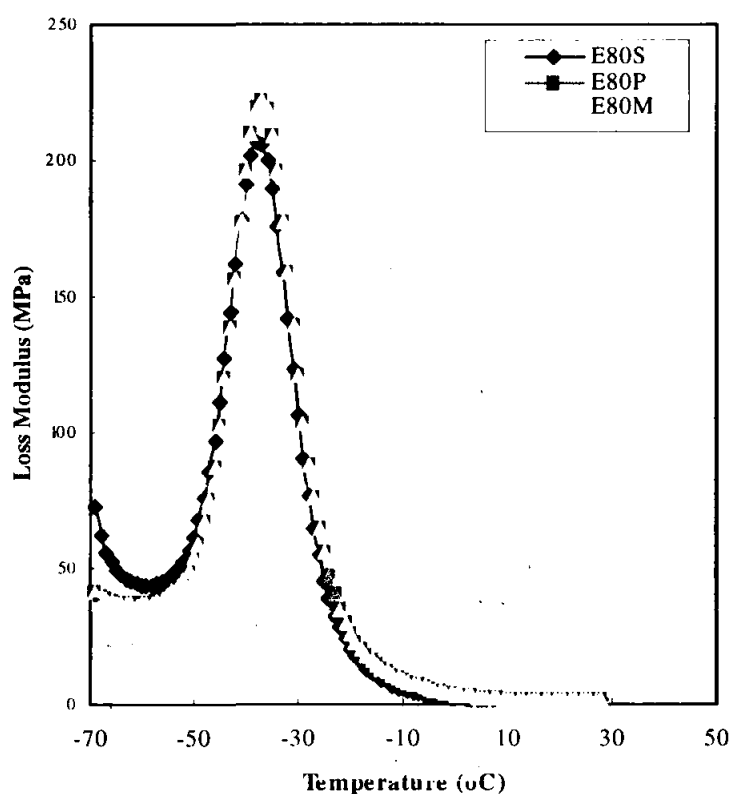


Figure 6.8 Effect of temperature (-70 to 30 °C) on the loss modulus of sulphur, DCP and M systems at a frequency of 10 Hz

6.2.2.3 Effect of fillers

The effect of temperature on the loss modulus of filler loaded EPDM/SBR blend, $E_{80}S$ is presented in Figures 6.9 and 6.10. As observed in the case of E' , the blend containing the reinforcing filler HAF shows highest loss modulus compared to GPF. This has been attributed to the energy loss occurring at the rubber-filler

interface consequent to the good rubber-filler interaction [5]. At room temperature, the loss modulus remains low and more or less constant for all filled systems. The loss modulus values and the corresponding T_g 's of the filled and unfilled blend, E_{80} cured in different curing systems are presented in the Table 6.1. It can be seen that the T_g values are not affected by different curing systems while carbon blacks have changed the T_g from -37 to -40 in HAF.

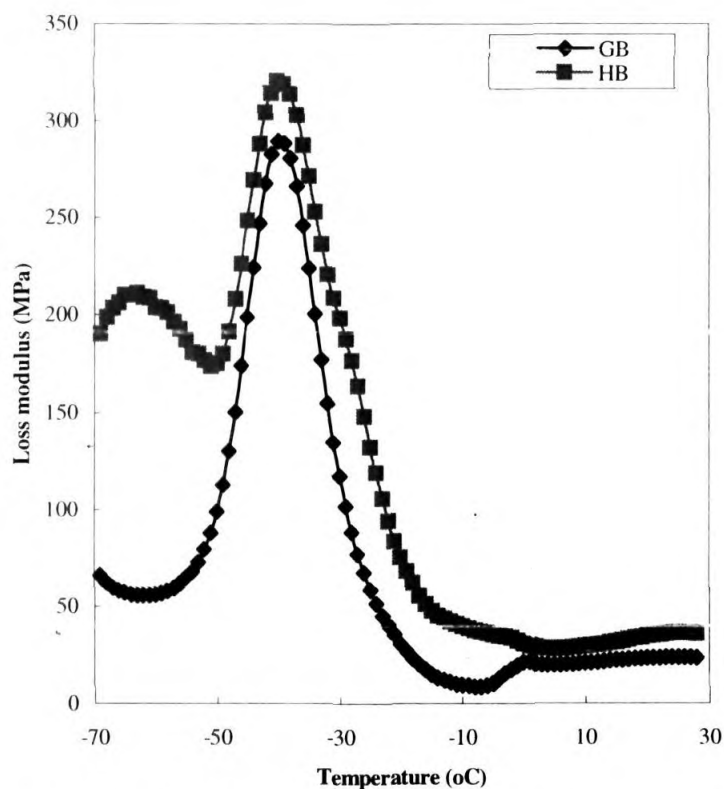


Figure 6.9 Effect of temperature (-70 to 30°C) on the loss modulus of carbon black filled $E_{80}\text{S10HB}$ and $E_{80}\text{S10GB}$ at a frequency of 10 Hz

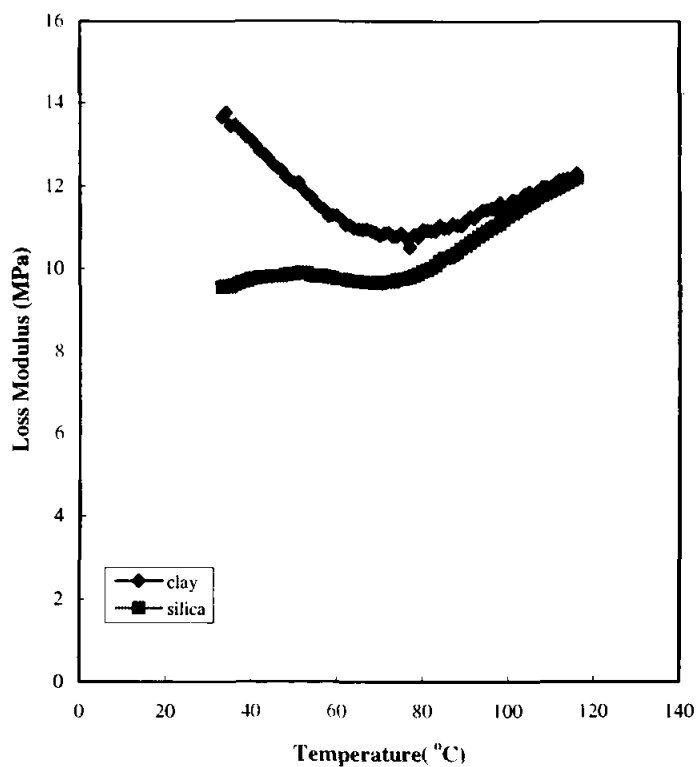


Figure 6.10 Effect of temperature (30 to 120°C) on the loss modulus of E₈₀S10HB and E₈₀S10GB at a frequency of 10 Hz.

Table 6.1 Values of loss modulus and T_g of filled and unfilled E₈₀ blend cured with sulphur, DCP and mixed systems at 10 Hz

Sample code	Loss modulus (MPa)	T _g (°C)
E ₈₀ S	205.7	-37
E ₈₀ P	221.8	-37
E ₈₀ M	221.8	-37
E ₈₀ S 10HB	320.5	-40
E ₈₀ S10GB	288.5	-39

6.2.3 Loss tangent

The loss tangent is a ratio and corresponds to the energy lost as heat per energy absorbed and returned by the system per unit cycle. As the temperature is increased, the damping goes through a maximum in the transition region and then

decreases in the rubbery region. The damping is low below T_g since the chain segments are frozen in that region. Below T_g , the deformations are primarily elastic and the molecular motions resulting in viscous flow are less. Above T_g , the damping is low because the molecular segments are free to move and there is no resistance to flow. The damping is high in the transition region because of the initiation of micro Brownian motion of the macromolecules and their stress relaxation, although not all the segments will be able to take part in such relaxation together.

6.2.3.1 Effect of blend ratio

The effect of blend ratio on loss tangent has been shown in the Figure 6.11. Pure EPDM and SBR show the glass transition peaks at -18° and -24°C respectively (Table 6.3). The blend E_{80} also shows a single transition at -28°C indicating miscibility between the components. When the EPDM/SBR blend ratio is 40/60, there is a large peak at -11°C , followed by a small shoulder at -35°C , which are attributed to SBR and EPDM as described earlier in the case of loss modulus plots. The presence of a shoulder rather than a clear peak indicates partial miscibility than true immiscibility [4]. Though SBR is the matrix in this case, its transition is rather suppressed by EPDM, as observed in many blends, due to the compact EPDM particles dispersed in the matrix. A comparison of T_g of sulphur cured EPDM/SBR blends based on peak values of $\tan \delta$ and loss modulus (E'') at 10Hz is given in Table 6.2

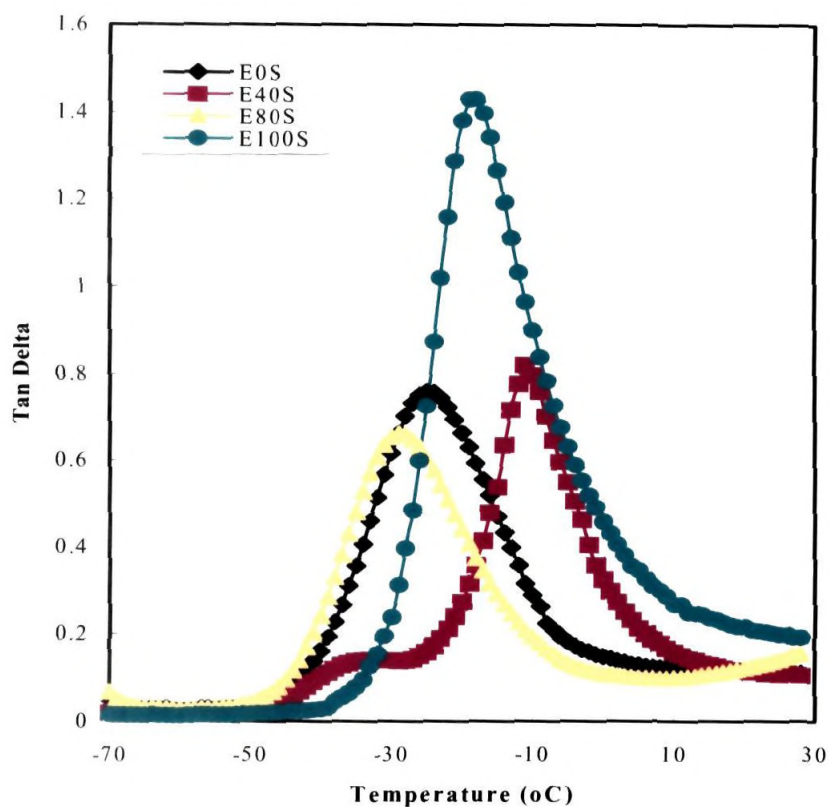


Figure 6.11 Effect of temperature on the $\tan\delta$ values of EPDM/SBR blends as a function of blend ratio at a frequency of 10 Hz

Table 6.2 Comparison of T_g of sulphur cured EPDM/SBR blends based on peak values of $\tan\delta$ and loss modulus (E'') at 10Hz

Blend ratio	$T_g (^{\circ}\text{C})$	
	$\tan\delta$ peak	E'' peak
E ₁₀₀ S	-18	-27
E ₈₀ S	-28	-37
E ₄₀ S	-11	-36 & -17
E ₀ S	-24	-35

Figure 6.12 shows that with increase of temperature above ambient conditions, the $\tan\delta$ values increase in all the three uncured systems of EPDM, SBR and the blend E₈₀. The $\tan\delta$ values in all these systems seems to be closer with increase of

temperature but SBR has given higher values in the early stages of heating but the values continuously increased in the blend, E₈₀ with hike in temperature.

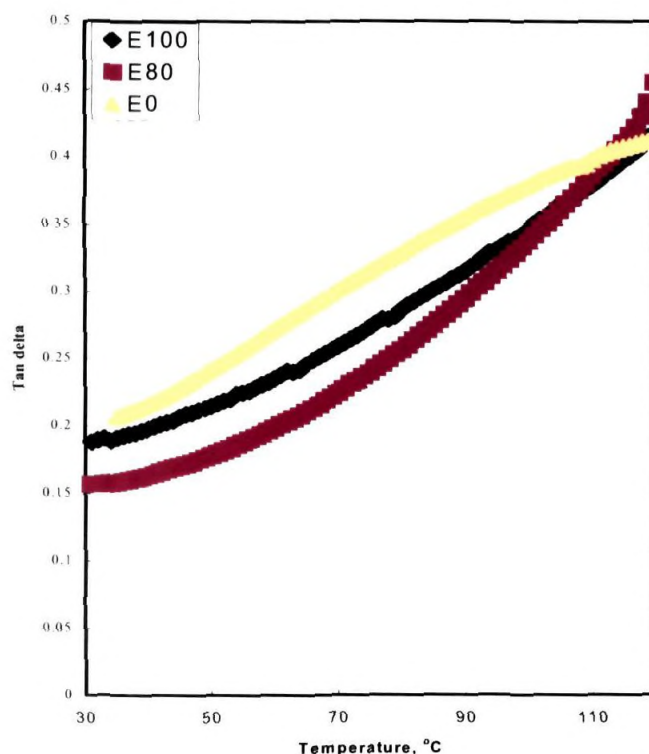


Figure 6.12 Effect of temperature (30-120°C) on the tan δ values of unvulcanized blend components EPDM, SBR and the blend E₈₀ at frequency of 10 Hz

6.2.3.2 Effect of curing agent

The effect of temperature on the loss tangent of E₈₀ blend cured by different curing agents is presented in Figure 6.13. The E₈₀ blend, when cured with sulphur, shows single transition indicating a homogeneous composition. However, E₈₀P and E₈₀M exhibit a shoulder at -7°C after the primary transition at -28°C , the latter corresponding to SBR. The shoulder may be due to some heterogeneous phases of crosslinked EPDM where crystallisation is effected consequent to peroxide curing in E₈₀P and E₈₀M. Peroxide curing is known to improve the chances of crystallization in EPDM as compared to sulphur curing, as the macromolecules are aligned and brought closer due to the intermolecular C-C bond formation.

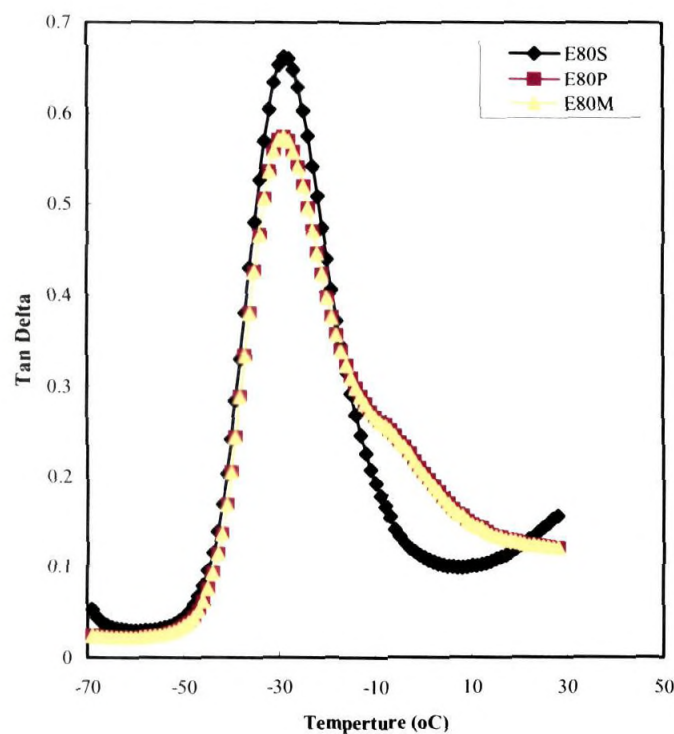


Figure 6.13 Effect of temperature on the $\tan\delta$ values of $E_{80}S$, $E_{80}P$ and $E_{80}M$

6.2.3.3 Effect of fillers

The effect of temperature on loss tangent of the filled (black and non- black) EPDM/SBR blend, $E_{80}S$ has been shown in Figures 6.14 and 6.15. The addition of reinforcing fillers reduces the loss tangent peak height, whereas non-reinforcing fillers increases the value. As the $\tan \delta$ value at T_g is 0.66 for pure $E_{80}S$ blend, whereas the values are 0.38 and 0.43 respectively for the highly reinforcing HAF and semireinforcing GPF filled blends.

The $\tan \delta_{\max}$, T_g and v for the filled blend systems are given in Table 6.3. The $\tan \delta_{\max}$ and T_g for EPDM/SBR blends in different vulcanizing systems are shown in Table 6.4.

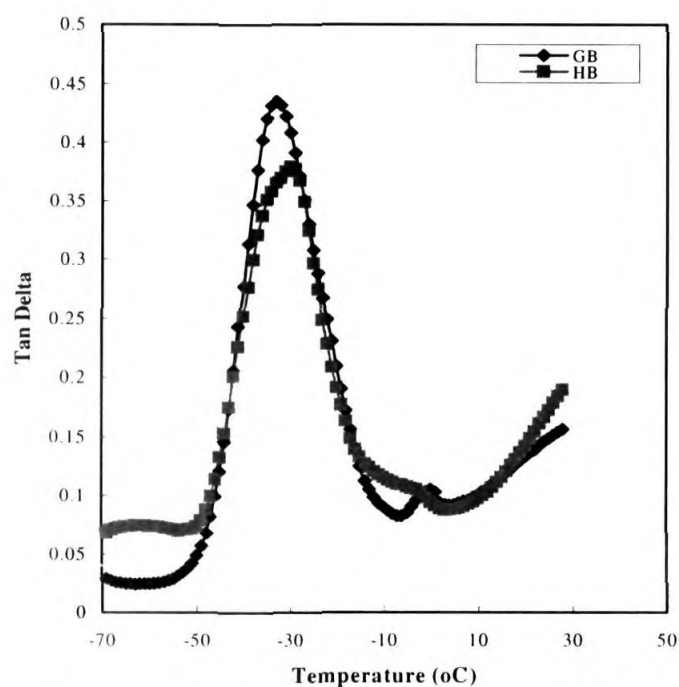


Figure 6.14 Effect of temperature (-70 to 30°C) on the $\tan \delta$ values of the $E_{80}S_{10}HB$ and $E_{80}S_{10}GB$ at a frequency of 10 Hz

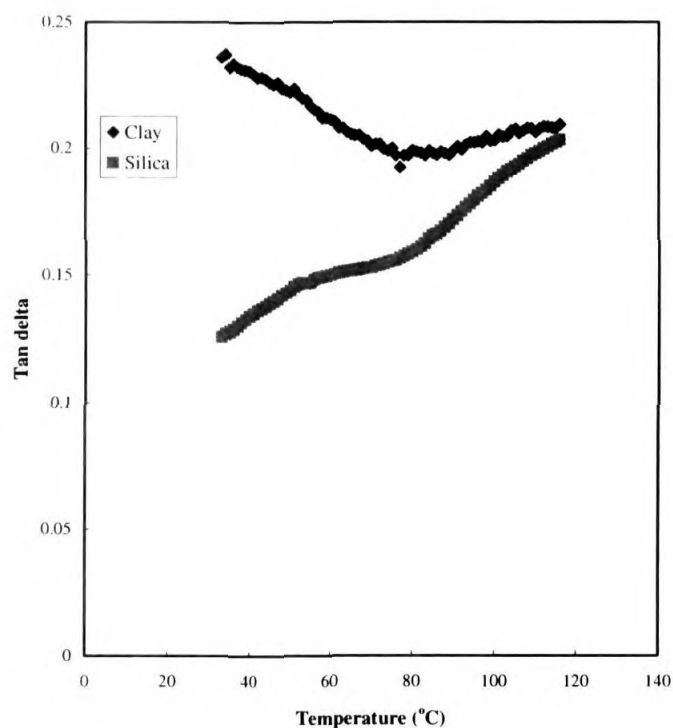


Figure 6.15 Effect of temperature (30 to 120 °C) on the $\tan \delta$ values of $E_{80}S_{10}Cl$ and $E_{80}S_{10}SI$ at a frequency of 10 Hz

Table 6.3 Values of $\tan \delta_{\max}$, T_g and ν for the EPDM/SBR blends and its components at 10 Hz

Sample code	Tan δ_{\max}	T_g	Crosslink density (gmol/cc)
E ₁₀₀ S	1.429	-18	-
E ₈₀ S	0.6599	-28	2.92×10^{-4}
E ₄₀ S	0.8193	-11	2.87×10^{-4}
E ₀ S	0.7565	-24	0.22×10^{-4}

Table 6.4 Values of $\tan \delta$ and T_g of filled and unfilled E₈₀ blend cured with sulphur and mixed systems at 10 Hz

Sample code	$\tan \delta$ values	T_g
E ₈₀ S	0.6599	-28
E ₈₀ P	0.5737	-29
E ₈₀ M	0.5737	-29
E ₈₀ S10HG	0.379	-30
E ₈₀ S10GB	0.4351	-33

6.2.4 Effect of frequency

The effect of different frequencies on the dynamic mechanical properties of E₈₀S above room temperature has also been examined. Figure 6.16 shows the influence of different frequencies, 0.1, 10, 20, 30 and 100 Hz on $\tan \delta$ of E₈₀S. It has been observed that $\tan \delta$ values, except those at 100 Hz frequency have been found to be parallel to the temperature axis. This has been attributed to the fact that at higher frequencies polymer chain will not get sufficient time for molecular relaxation.

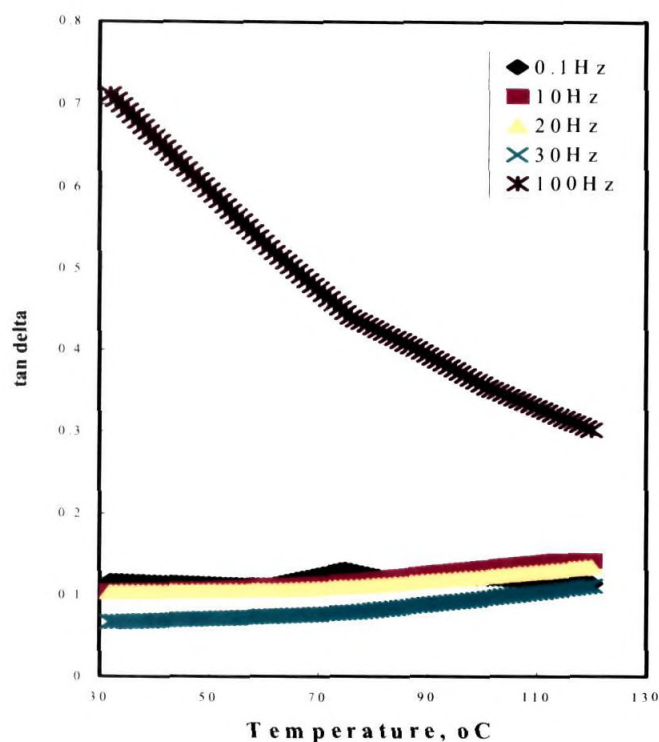


Figure 6.16 Effect of various frequencies on the loss modulus of E₈₀S above ambient temperature (30-120°C)

6.2.5 Theoretical modelling

To assess the behaviour of the EPDM/SBR blends from the DMA data, different theoretical models have been used. The various models applied include parallel, series and Halpin Tsai. The $\tan \delta$ of sulphur cured EPDM/SBR blends and its components was calculated applying equations 3.3 to 3.5 of Chapter 3.

The curves resulting from the theoretical models and that of the experimental data, for the variation of $\tan \delta$ at 30°C with the volume fraction of EPDM, are given in Figure 6.17. The experimental value of $\tan \delta$ has been found to be lower than that of the theoretical predictions. This has been due to the presence of extraneous materials present in the blends. The experimental model has been found to fit well

with the series model. The parallel model and Halpin Tsai model show the upper bound over the entire compositions.

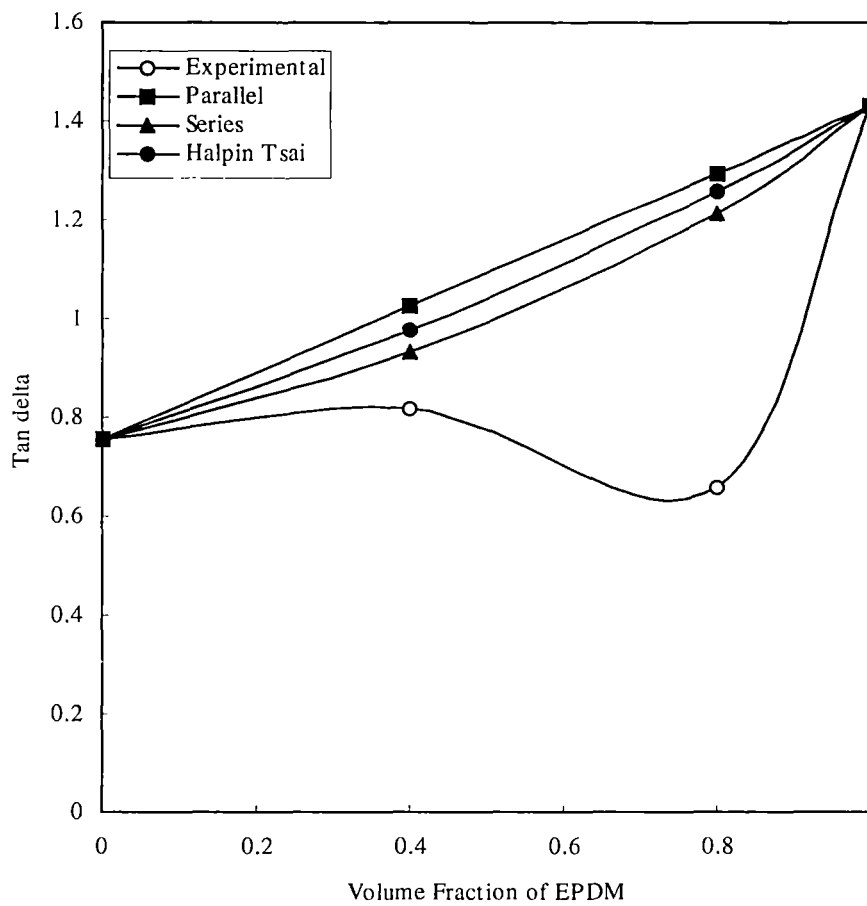


Figure 6.17 Experimental and theoretical curves of $\tan \delta$ peak of sulphur cured EPDM/SBR blends

6.3 Conclusion

Dynamic mechanical analysis is an effective tool for evaluating the miscibility of polymer blends. The DMA of EPDM/SBR blends has been carried out as a function of blend composition, cross-linking systems and fillers over a wide range of temperature and frequency. The single T_g obtained from the $\tan\delta$ peak for the blend E₈₀S showed that the system is miscible. The two separate $\tan\delta$ peaks, obtained during DMA, in the blend ratio E₄₀S indicate that miscibility of the system is decreased with increased SBR content.

Reinforcing black fillers have been found to increase the modulus and decrease the $\tan \delta$ peak.

References

1. I. Perepechko., *Acoustic Methods of Investigating Polymers*” Mir Publishers: Moscow, (1975).
2. T. Murayama., *Dynamic Mechanical Analysis of Polymeric Materials*. Materials Science Monograph 1, Elsevier Science: New York, (1978).
3. JD Ferry., *Viscoelastic Properties of Polymers*. John Wiley: New York, (1980).
4. W.J. MacKnight and F.E. Karasz and J.R. Fried in D.R. Paul and S. Newman Ed., “*Polymer Blends*”, Vol.1, Chapter 5, 185, Academic Press, (1978).
5. AR Payne, “*Reinforcement of Elastomers*”, (Ed.) Kraus, Interscience, New York, (1965).
6. T. Murayama., *Dynamic Mechanical Analysis of Polymeric Materials*, Elsevier, New York (1977).
7. P. M. Kevin P.M., *Dynamic Mechanical Analysis- A Practical Introduction*, CRC Press, New York (1999).
8. B. E Read. and G. D Brown., *The Determination of Dynamic Mechanical Properties of Polymers and Composites*, Wiley, New York (1978).
9. J. Ferry., *Viscoelastic Properties of Polymers*, Wiley, New York (1980).
10. A. Karger-Kocsis A. and Kiss L., *Polym. Eng. Sci.*, **27**, 254 (1987).
11. H. A Khonakdar., U.Wagenknecht.,S. H., Jafari., R. Hassler. and H. Eslami., *Adv. Polym. Technol.*, **23**, 307 (2004).

12. J. Mas., A. Vidaurre., J. M. Mesegner., F. Romero., M. M. Pradas., J. L. G. Ribelles., M. L. L. Maspoch., O.O Santana., P. Pages. and J. Perez-Folch., *J. Appl. Polym. Sci.*, **83**, 1507 (2002).

Chapter 7

Ageing Studies on EPDM/SBR Blends

Abstract

The ageing behaviour due to the effects of heat, ozone, γ - radiation and water on EPDM/SBR blends was studied. It has been observed that an increase in EPDM in the blends improves the ozone resistance of the blends. Crack initiation was noted only in blends with lesser amount of EPDM and the cracks in such blends were found deeper, wider and continuous. Tensile strength of blends of different compositions increased after thermal ageing for 96 hrs at 100°C probably due to the continued cross-linking. With 15 kGy irradiation dose, the tensile strength of the blends found to be decreased while it increased with 80 kGy dosage of γ - radiation. The elongation at break showed a decreasing trend with increased dosage of γ -radiation. It has also been observed that the EPDM rich blends showed negligible water uptake.

Results of this chapter have been communicated to *Polymer Degradation and Stability*

7.1 Introduction

The demand for high temperature, ozone and weather resistant rubbery materials has increased during the last decade. Rubber blends are becoming preferred materials to meet these requirements. Earlier studies on accelerated ageing of rubber vulcanizates show that the properties such as elongation at break, tensile strength and modulus undergo changes due to deterioration [1]. It is well known that for many unsaturated rubbers, the hydrogen atom of α -methylenic carbon is abstracted in the presence of oxygen and an oxidative reaction chain is initiated which propagates auto-catalytically and ends in chain scission. Besides scission of the main chain and of the cross-links, depending upon polymers, ageing causes the formation of more cross-links of the same type as those already present or of a different type, which may be inactive to further scission. Introduction of antioxidants and antiozonents helps to reduce the property loss of rubber vulcanizates due to ageing though these chemicals have many limitations in performance. With the introduction of weather resistant rubbers such as EPDM, hypalon and polysulfide, the efforts to modify the ageing characteristics of highly unsaturated rubbers gained a new momentum, through blending techniques [2].

The effects of degrading agents on each type of polymer will be different and they depend mainly on the chemical structure of the polymer and the type of crosslinking system used. For SBR, the resistance to thermal, gamma and ozone ageing is poor due to the presence of double bonds in the main chain. In EPDM as the reactive carbon-carbon double bond is located on a side chain, the polymer backbone structure is completely saturated and not subject to molecular breakdown via ozone attack or oxidation. Therefore the behaviour of blends of these elastomers against the action of various degrading agents is worth examining.

Excellent reports on the ageing characteristics of rubbery systems exist. For example, Bhowmick and White [3] investigated the thermal, UV- and sunlight ageing of thermoplastic elastomeric NR/PE blends. They found that thermal ageing of the blends caused the tensile properties to deteriorate, especially at longer times, or higher temperatures of ageing after an increase of properties in the initial stage. Deuri et al.[4] investigated the ageing behaviour of IIR/EPDM blends and found that the ageing resistance increased with increase in EPDM content. Koshy et al [5-6] studied the ageing of different rubber-rubber blends. Sulekha et al.[7] reported that the use of oligomer bound antioxidants was an effective means of protecting non-resistant rubbers against surface cracking. Vinod et al.[8] investigated the effects of heat, ozone and high energy radiation on the degradation behaviour of aluminium powder filled NR composites. They found that resistance to degradation was improved, when NR was reinforced with aluminium powder. Many other interesting works have also been reported on the ageing characteristics of polymeric systems [9-19].

SBR is an elastomer extensively used for a wide variety of products, viz., tires and related products, belts, hoses, foot wears, foamed products, mechanical goods etc. SBR, in general, has high resilience, better flex life, lower heat build up and better abrasion resistance. However, with unsaturation sites, it is prone to attack by ozone or oxygen. EPDM is a rubber having excellent temperature and ozone resistance. Furthermore, depending up on the molecular weight, molecular weight distribution, % of ethylene content and % of diene, EPDM gives better tensile/tear strength, hot green strength, higher cure rate, flow at high temperature, higher modulus and lower compound cost.

This chapter examines the ageing characteristics of EPDM/SBR blends with special reference to the effects of heat, ozone, radiation and water. Ageing studies

were conducted on sulphur cured EPDM/SBR blends along with the component elastomers.

7.2 Results and Discussion

7.2.1 Thermal ageing

The mechanical properties of the blends before and after thermal ageing were compared. Figure 7.1 shows a comparison between the tensile strength of the blends before and after aging at 100°C for 96 hours. It is clear from the graph that the tensile strength values were increased with increased weight percentage of EPDM in the blend. Figure 7.2 shows the percentage increase in tensile strength of EPDM/SBR vulcanizate after ageing at 100°C for 96 hrs. The increase in tensile strength of the blends might be due to the continued cross-linking of the blend components by thermal ageing. The effects of temperature and environmental conditions on the performance of polymers, including the degradation mechanisms are available in the literature [20-26]. Generally, the retention of properties depends up on the degradation behaviour of the component elastomers. Amorphous polymers degrade faster than crystalline polymers by heat. This is evident from the crosslink density values given in Table 7.1. The table shows that the crosslink density of the blends increased with increased EPDM composition, which ultimately enhanced the TS. Rubber vulcanizates are cured only at t_{90} . The remaining 10% is kept at an allowance during service. Thermal ageing completes this 10 % curing as clear from the crosslink density values, which subsequently enhance the TS.

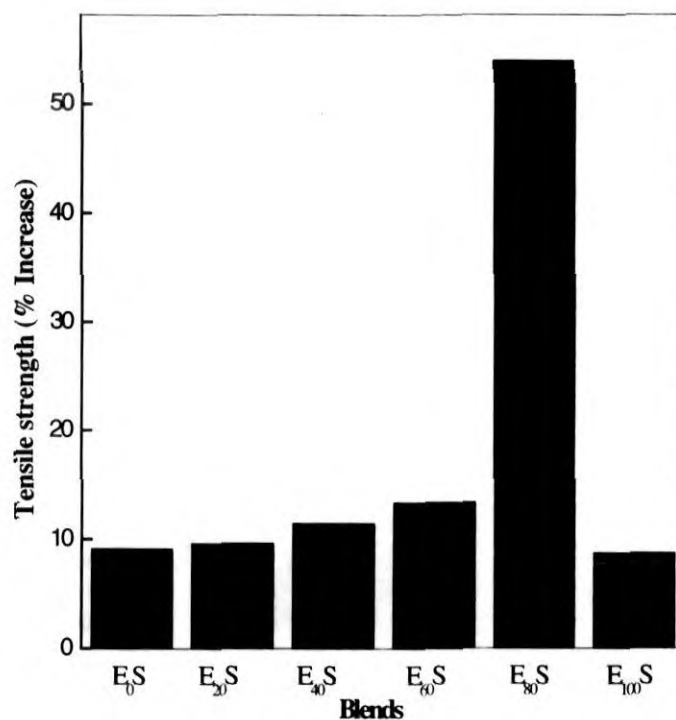


Figure 7.1 Thermal ageing at 100°C: % Increase in tensile strength

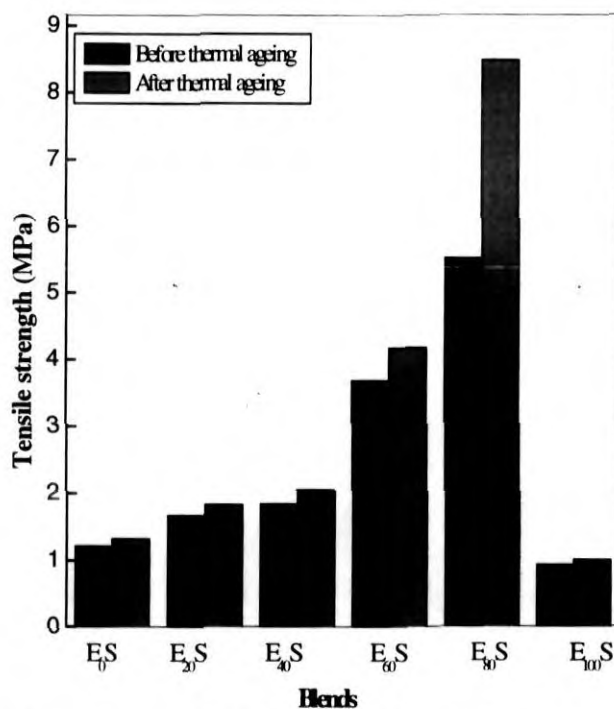


Figure 7.2 Thermal ageing at 100°C - Comparison of tensile strength before and after ageing

Table 7.1 Crosslink density of unaged and aged EPDM/SBR blends

Sample	Crosslink density $\times 10^4$ (gmol/cc)	
	Before thermal ageing	After thermal ageing
E ₀ S	0.22	0.48
E ₂₀ S	2.83	4.04
E ₄₀ S	2.87	3.36
E ₆₀ S	2.91	3.33
E ₈₀ S	2.92	3.18
E ₁₀₀ S	-	0.15

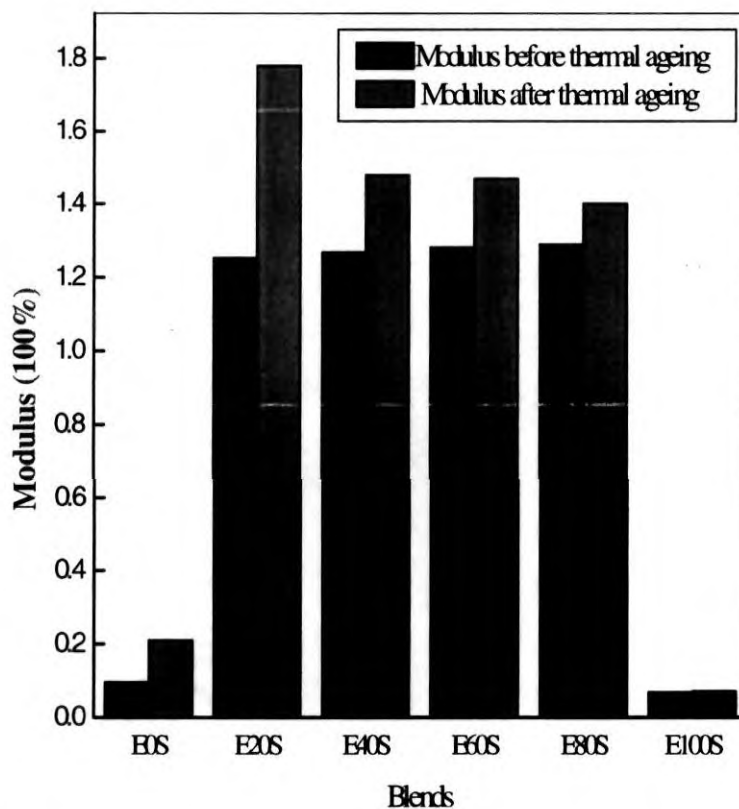


Figure 7.3 Comparison Modulus at 100% - Before and after thermal ageing of EPDM/SBR blends at 100°C

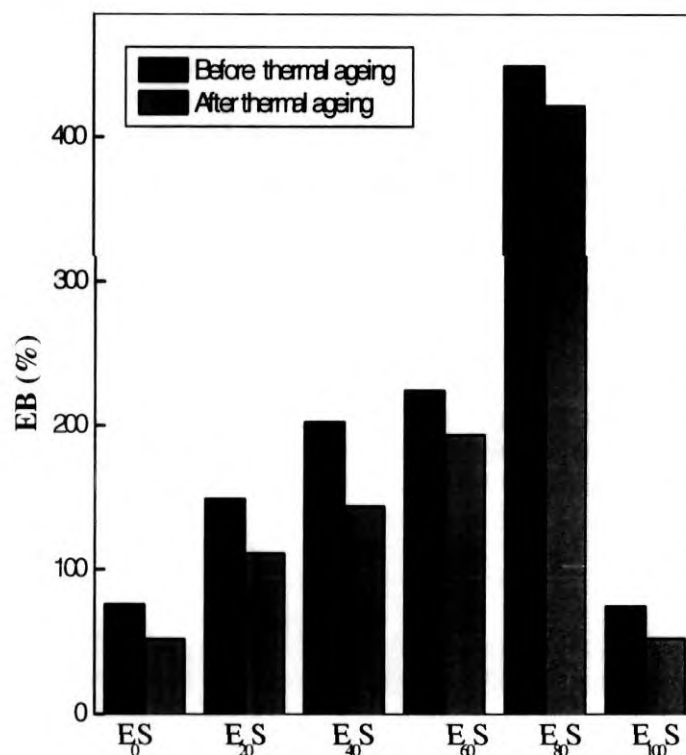


Figure 7.4 Comparison of EB (%) – Before and after thermal ageing at 100°C

Table 7.2 Percentage retention of elongation at break – Effect of thermal ageing on EPDMSBR blends at 100°C

Elongation at break (%)	% Retention
E ₀ S	67.94
E ₂₀ S	74.73
E ₄₀ S	71.01
E ₆₀ S	86.19
E ₈₀ S	93.82
E ₁₀₀ S	70.20

Figure 7.3 illustrates the percentage increase in modulus (100%) of the EPDM/SBR blends after thermal ageing at 100°C for 96 hrs. The graphs show that the modulus of all the blend compositions increases after thermal ageing. The variations in the elongation at break values of the blends after thermal ageing are

presented in Figure 7.4. It has been found that the elongation at break of the vulcanizate decreases due to thermal ageing. Thermal ageing leads to the formation of additional cross-links in the blends. It is clear from Table 1 that the crosslink densities increase after ageing. In general, the elongation at break of a vulcanizate with higher crosslink density is shorter than that of a vulcanizate with a lower density [27]. The trends of EB among the blends are in the order $E_{80}S > E_{60}S > E_{40}S > E_{20}S > E_0S$ which is in agreement with the above observation.

Figure 7.5 reveals that the hardness of all the EPDM/SBR blends increases after thermal ageing. This increase is also associated with the increase in crosslink density.

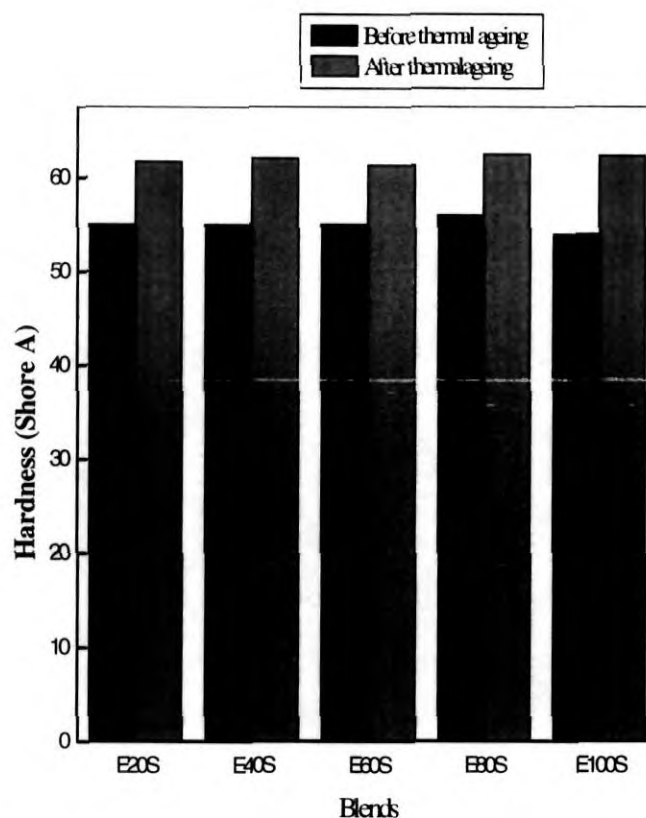
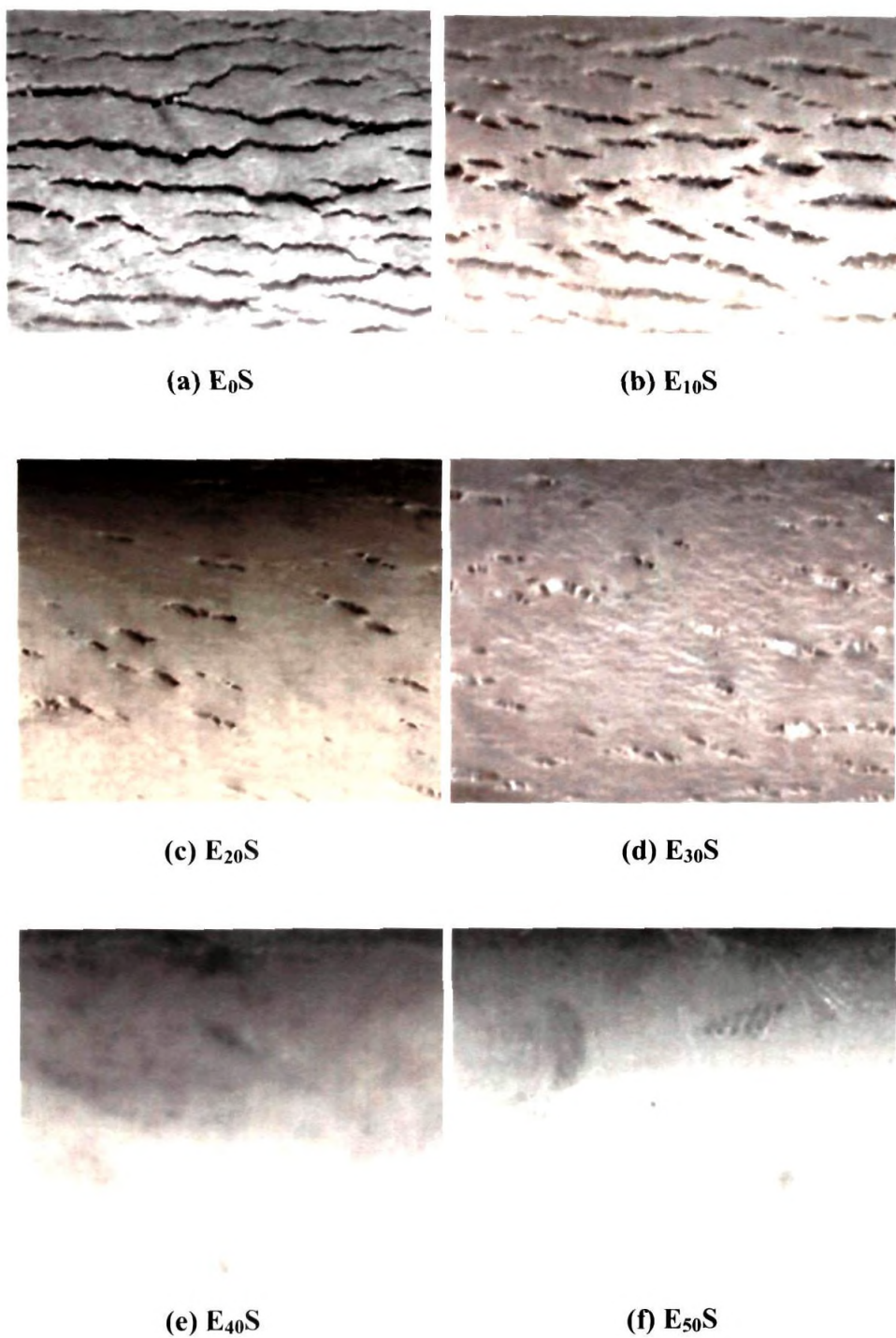


Figure 7. 5 Comparison of hardness (shore A) – Before and after thermal ageing at 100°C

7.2.2 Ozone ageing

The optical photographs of the surfaces of the ozone aged samples presented in Figure 7.6 shows that no cracks were developed on the EPDM rich blends. However, cracks were seen initiated on the surfaces of SBR rich blends, E₀S, E₁₀S, E₂₀S and E₃₀S at lesser exposure of time. In blend E₃₀S, shallow type cracks were appeared after 17 hrs of ageing. Moderate cracks were developed in blend E₂₀S after 7 hrs of ozone ageing. Deep cracks were noted in E₀S after 4 hrs of ageing while cracks were noted in E₁₀S only after 6hrs of ageing. However blend compositions, E₄₀S, E₅₀S, E₆₀ S, E₇₀S, E₈₀S E₉₀S and E₁₀₀S were not affected by ozone ageing even for 120 hrs. Obviously, the crack growth in SBR due to ozone attack is effectively controlled and prevented by the highly ozone resistant EPDM in these blends.



**Figure 7.6 (a) to (f) Optical photomicrographs of ozone exposed (120 h)
Sulphur cured EPDM/SBR blends**

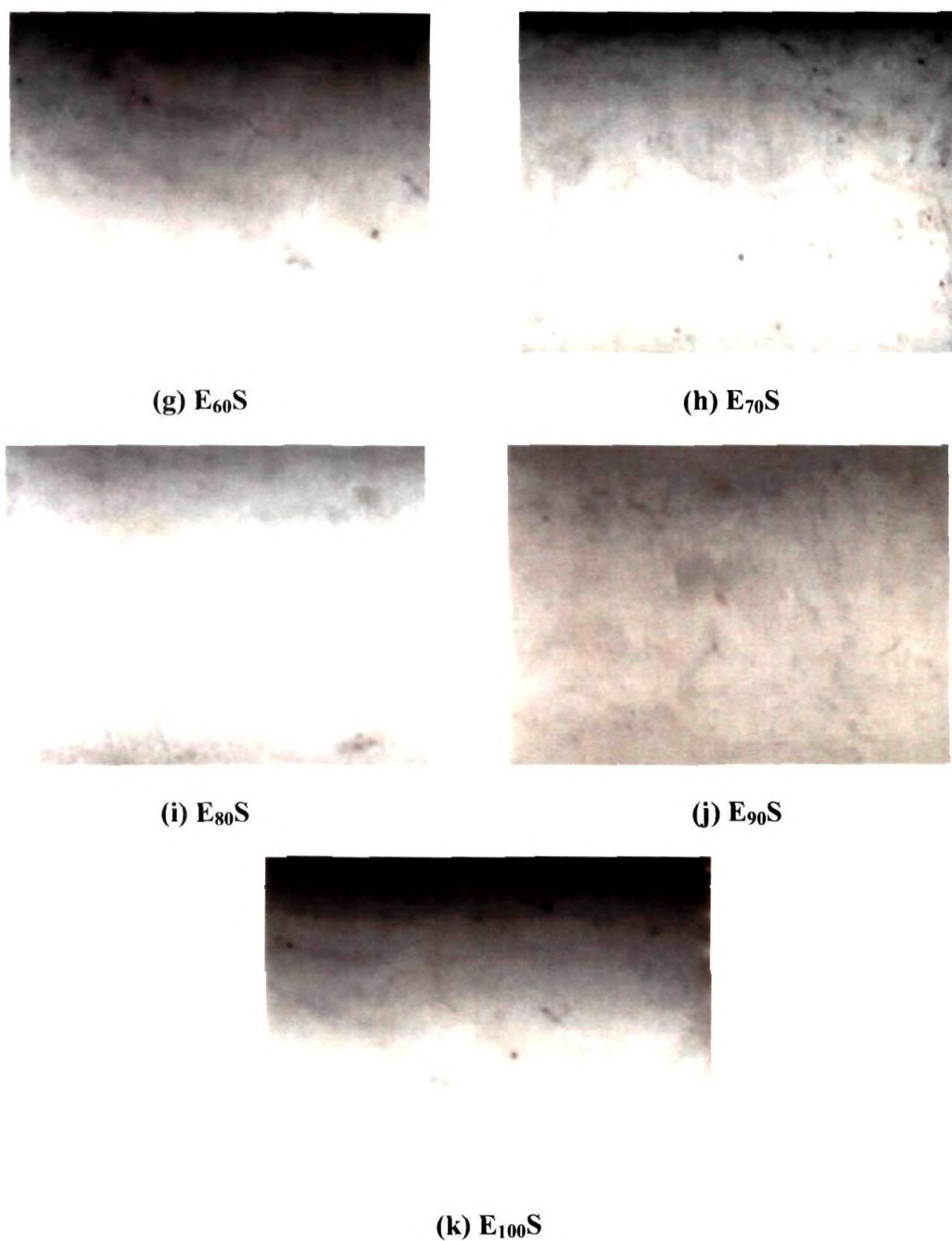


Figure 7.6 (g) to (k)

**Figure 7.6 (g) to (k) Optical photomicrographs of ozone exposed (120 h)
Sulphur cured EPDM/SBR blends**

Figure 7.7 shows the trends in ozone crack initiation and crack resistivity EPDM/SBR blends with respect to time.

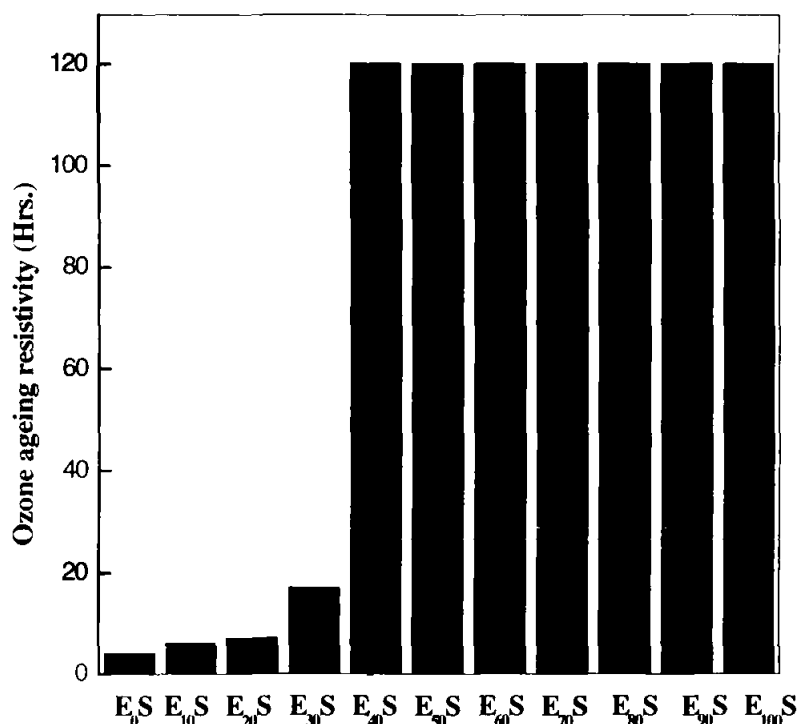


Figure 7.7 Ozone ageing resistivity of EPDM/SBR blends

7.2.3 Gamma [γ] irradiation

The γ -radiation interacts with polymers in two ways; chain scission, which results in reduced tensile strength and elongation, and cross linking, which increases tensile strength but reduces elongation. Generally, polymers containing aromatic ring structures are resistant to radiation effects. The radiation resistance in aliphatic polymers depends upon their levels of unsaturation and substitution.

Figure 7.8 shows that the γ -irradiation at 15-kGy doses lowered the tensile strength of EPDM rich blends compared to the un- irradiated blends (control samples). This indicates.

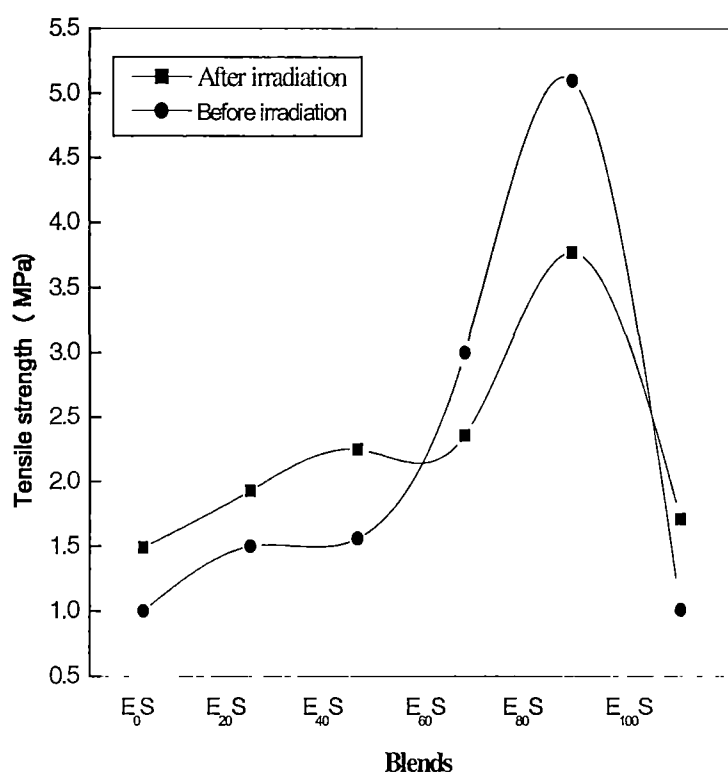


Figure 7.8 Effect of gamma irradiation on the tensile strength of EPDM/SBR blends at 15-kGy irradiation dose.

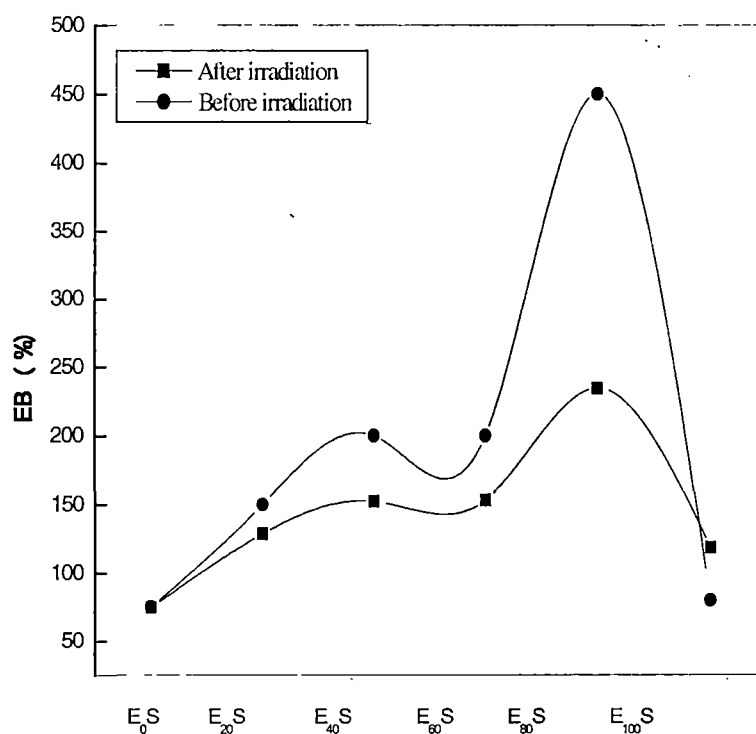


Figure 7.9 Effect of gamma irradiation on the EB (%) of EPDM/SBR blends at 15-kGy irradiation dose.

that lower dose rate of irradiation performed under oxygen leads to a rapid decrease of the gel content due to chain scission and decrease in cross-linking . Meanwhile the increase in TS of SBR rich blends at lower level irradiation might be due to the presence of aromatic rings in the polymer, which are relatively degradation resistant. However, higher dosage of radiations enhances additional cross-linking, which increases tensile strength but reduces elongation [28]. The elongation at break was found to be lowered by chain scission due to the radiation effect, as shown in Figure 7.9. Figures 7.10 and 7.11 illustrate the comparison of tensile strength and elongation at break respectively of the blend, with a control sample, containing 80 wt % of EPDM at 80 kGy irradiation. It is clear from Figure 7.10 that tensile strength was increased at 80-kGy dosages compared to the EPDM/SBR blend at 15 kGy dose and also to the unirradiated control sample.

When SBR is the continuous phase, the matrix is more γ -resistant and at lower dosages, the cross-linking reaction predominates over chain scission and in such blends the TS increases. However, EPDM having an aliphatic chain is weak to resist γ -radiation of lower doses where chain or cross-link degradation is dominating over additional cross-link formation. However, when dosage is enhancing, the cross-link formation can get activated and a dominance of cross-linking reaction where scission can give better results. Similar observations exist in literatures [29]

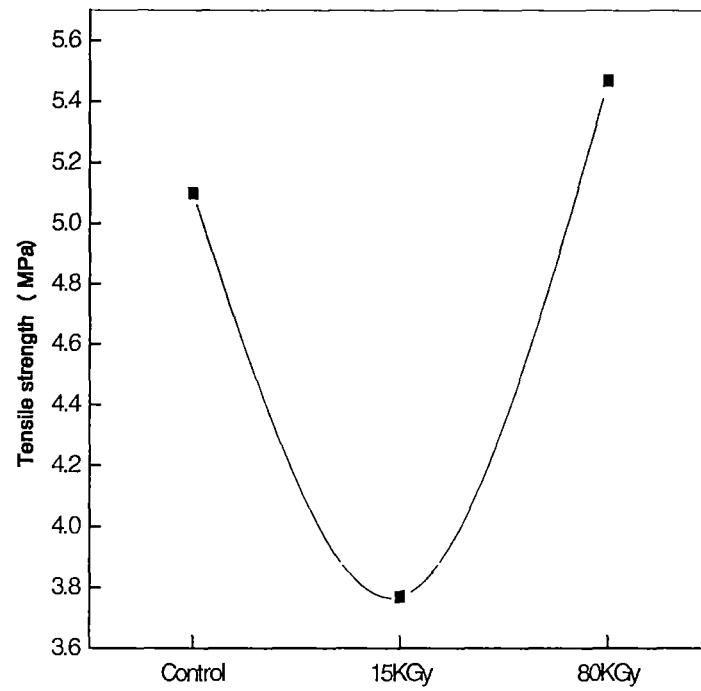


Figure 7.10 Effect of γ irradiation dose on the TS of the effective blend E₈₀S - Comparison with control sample

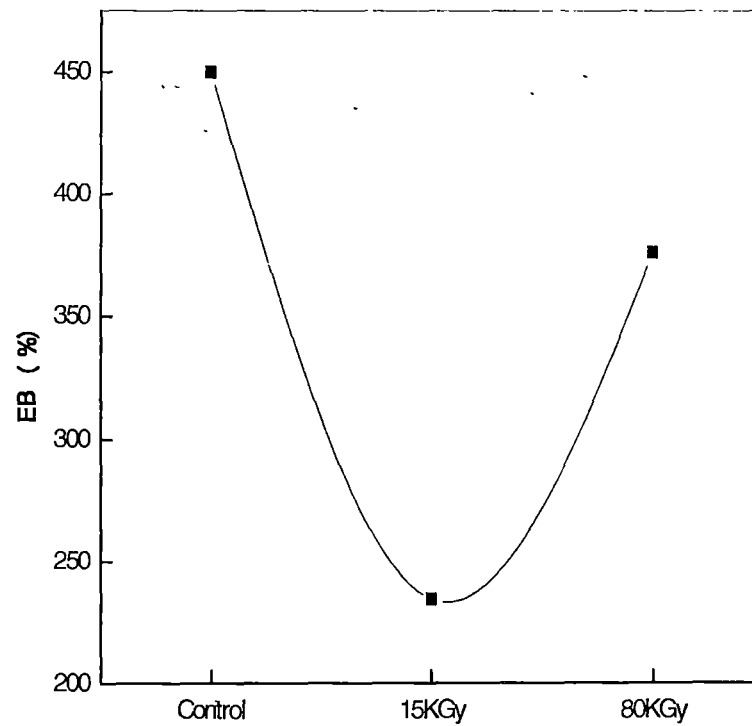


Figure 7.11 Effect of γ irradiation dose on the EB of the effective blend E₈₀S - Comparison with control sample

7.2.4 Water ageing

Figure 7.12 illustrates the water uptake (mass %) of various EPDM/SBR blends after water immersion. The results show that the water uptake was negligible in majority of the blends due to the presence of water resistant EPDM. For instance, in blend E₈₀S, the percentage of water uptake after 7, 14, 21 and 42 days of water ageing have been noted only as 1.63, 2.09, 2.87 and 3.19 % respectively.

Table 7.3 Distilled water uptake by EPDM/SBR blend vulcanizates

Samples	Water Uptake (%)			
	After 7days	After 14days	After 21days	After 42days
E ₁₀₀ S	+0.07	+0.25	+0.331	+0.44
E ₈₀ S	+0.48	+0.70	+0.726	+1.12
E ₆₀ S	+0.48	+0.87	+0.938	+1.32
E ₄₀ S	+0.99	+1.31	+1.549	+2.23
E ₂₀ S	+1.63	+2.09	+2.499	+3.05
E ₀ S	+2.09	+2.58	+2.898	+3.26

7.3 Conclusion

Thermal, ozone, gamma and water ageing studies were conducted on EPDM/SBR blends with special reference to the effects of blend ratio. A comparison of the mechanical properties of the blends before and after thermal ageing showed an increase in the tensile strength due to the continued cross-linking while a decrease in the elongation at break. The percentage increase in tensile strength of the blends was found to increase with increase in EPDM content because of its relatively crystalline nature. The ozone ageing studies showed that cracks were initiated only in few blends in which the amount of EPDM was lesser to prevent crack growth.

No ozone cracks were noticed in blends with EPDM level above 30-wt %. The γ -

irradiation studies showed that the radiation interacts with polymers by chain scission and cross-linking. The chain scission resulted in reduced tensile strength and elongation and the cross-linking added an increased tensile strength and reduced elongation. The negligible water uptake in the blends showed that the EPDM/SBR blends could be successfully applied in any severe outdoor weathering applications.

References

1. Davies K.M., Lloyd D.G., in *Developments in Polymer Stabilisation* Vol. 4, Scott G. (Ed.), Applied Science Publishers, London (1981).
2. M.G. Oliveira, B.G. Soares. *Polymers & polymer composites*, **9**, 7, 459, (2001).
3. A.K. Bhowmick and J.R. White. *J. of Material Science- Springer*; **37**, 5141, (2002).
4. Deuri A.S., Adhikari A. and Mukhopadhyay R., *Polym. Degrad. Stab.*, **41**, 53 (1993)
5. Koshy A.T., Kuriakose B. and Thomas S., *Polym. Degrad. Stab.*, **36**, 137 (1992).
6. Varghese H., Bhagawan S.S. and Thomas S., *J. Therm. Anal. Calorim.*, **63**, 749 (2001).
7. Sulekha P.B., Rani J., Madhusoodhanan K.N. and Thomas K.T., *Polym. Degrad. Stab.*, **77**, 403 (2002).
8. Vinod V.S., Varghese S. and Kuriakose B., *Polym. Degrad. Stab.*, **75**, 405 (2002).
9. Dunn J.R., *Rubber Chem. Technol.*, **41**, 182 (1968).
10. Razumorskii S.D. and Zaikor G.E, in *Developments of Polymer Stabilisation*, Vol. 6, Scott G. (Ed.), Applied Science Publisher, London (1982).

11. Ishiaku U.S., Lim F.S., Ishak Z.A. M. and Perera M.C. S., *Polym. Plast. Technol. Eng.* **38**, 939 (1999).
12. Ismail H., Mohamad Z. and Bakar A.A., *Polym. Plast. Technol. Eng.*, **42**, 81 (2003).
13. Sirisinha C., Saeoui P. and Guaysomboon J., *Polymer*, **45**, 4909 (2004).
14. Brown R.P., *Physical Testing of Rubbers*, Third Edition, Chapman and Hall, London (1996).
15. Lewis P.M., *Polym. Degrad. Stab.*, **15**, 33 (1986).
16. Ambelang J.C., Kline R.A., Lorenz O.N., Parks. C.R., Wadelin C. and Shelton J.R., *Rubber Chem. Technol.*, **36**, 1497 (1963).
17. Layer R.W. and Lattimer R.P., *Rubber Chem. Technol.*, **63**, 426 (1990).
18. Solanky S.S. and Singh R.P., *Prog. Rubber Technol.*, **17**, 13 (2001).
19. Thomas S., Gupta B.R. and De S.K., *Polym. Degrad. Stab.*, **18**, 189 (1987)
20. S. S. Bhagawan. *Polym Degrad stab*, **23**, 1 (1989)
21. D.G. Clint, K.D. Naba and R.C. Namitha, *Polym Degrad stab*, **80**, 525 (2003)
22. A.C. Thiang, K. Makuuchi, F.J.Yoshi. *J Appl Polym Sci*, **54**, 525 (1994)
23. N.L. Hancox. *Plast Rubber Comp process Appl*, **27**, 97 (1998)
24. M.S. Sambhi. *Rubber Chem Technol*, **55**, 181 (1982)
25. J.R. Sheltin. *Rubber Chem Technol*, **45**, 359 (1972)
26. D. Barnard, M.E. Cain, J.I. Canneen, T.H. Housema. *Rubber Chem Technol*, **45**, 381 (1972)

27. N.J. Morison, M. Porter., *Rubber A. Buttfava*, G. Consalati, M. Mariani, F. Quasso, U. Ravasio. *Polym Degrad Stab*; **89**, 133, (2005).
28. N. Celette, I. Stevenson, Devenas, L. David, G. Vigier. IRAP 2000; *Nucl Instr and Meth B*, 185, 305, (2001).
29. AAMI Recommended Practice-“Process control Guidelines for Gamma Radiation Sterilization of Medical Devices”, ISBN-0-910275 1984; 38-6: pages 7-21.

Chapter 8

Conclusion and Future Outlook

Abstract

The major findings of the present investigation have been summarized in this Chapter. The scope of future work based on EPDM/SBR blends has also been discussed.

8.1 Conclusion

The development and characterisation of blends of EPDM and SBR have been done with emphasis on blend ratio, cross-linking systems and fillers. The morphology studies of the blends showed the existence of increased inter-facial adhesion between EPDM and SBR in the blend ratio 80:20. The properties such as tensile strength, tear strength, abrasion resistance and hardness increased with increase in EPDM content up to 80%. Among the different vulcanizing systems, the tensile and tear strength were highest for mixed systems compared to sulphur and DCP systems. The elongation at break with sulphur cured blends was found to be higher compared to the other two systems possibly due to flexible polysulphidic linkages. The abrasion resistance of the sulphur-cured blends was examined and it was found that the properties increased with EPDM content and the values were highest for E₈₀ system. The mechanical properties of the filled EPDM/SBR blends in a selected ratio, E₈₀S, were studied. Among the different fillers, the blends filled with HAF black gave the highest tensile strength and elongation at break at 30-phr levels. The enhancement in the tensile properties of E₈₀S blend at 30 phr level followed the order, HAF black > GPF black > clay > silica.

Thermogravimetric properties of EPDM/SBR blends have been studied with special reference to the effects of blend composition, cross-linking systems and fillers. The thermal analyses showed that the initial decomposition temperature of the blends increased with increase in EPDM content, which gave the evidence that the thermal stability of the blends increased due to the presence of EPDM. The final decomposition of all the blends occurred around 500°C. The initial

decomposition temperature of DCP cured blends was noted as 384.9°C which was higher than the initial decomposition temperatures of sulphur and Mixed cured blends.

The dynamic mechanical analysis (DMA) of the uncross-linked and cross-linked EPDM/SBR blends has been carried out as a function of blend composition at varying frequencies, 0.1 to 100 Hz at -70 to 120°C. The DMA results below ambient temperatures showed a single T_g for the blend E₈₀S exhibiting better compatibility. Two separate $\tan \delta$ peaks were noted for the blend E₄₀S which indicates the decrease in miscibility of the blend with increased SBR content. This has also been corroborated with the SEM photographs.

Thermal, ozone, gamma radiation and water ageing studies were also conducted on EPDM/SBR blends. The thermal ageing of the blends at 100°C for 96 hrs increased the tensile strength; attributed to continued cross-linking in the blends. The percentage increase in tensile strength of the blends was found to increase with increase in EPDM content and the values were found to be highest for 80/20 EPDM/SBR blend ratio. The ozone ageing studies showed that cracks were initiated only in a few blends in which the amount of EPDM was not sufficient enough to prevent crack growth. It was found that, no ozone cracks were found in blends with EPDM level above 30-wt %. The γ -irradiation studies showed that the radiation interacted with polymers by chain scission and cross-linking. It was also observed that the main factors, which determine the cross linking/chain scission, are the presence of oxygen together with the irradiation dosage and the initial

cross-link density of EPDM. The EPDM/SBR blends have been found to exhibit, in general, good water resistance.

The blends of EPDM and SBR developed by this study could be successfully used in place of EPDM in various fields in the form of products such as windshield gaskets, washing machine gaskets, steam hose, automotive radiator hose, air-conditioning hose, roof sheeting and tire flaps.

8.2 Future Outlook

The work carried out so far on EPDM/SBR blends gives interesting scope for further research on several related areas. Typically, the following studies are proposed.

8.2.1 Use of compatibilisers

The effect of different compatibilisers on the physical properties of EPDM/SBR blends can be studied.

8.2.2 Examination of electrical properties

The need for dielectric data such as volume resistivity, dielectric strength, dielectric constant and loss factor of polymeric systems becomes essential if they are to be used in wires and cables. It is worth attempting to study the electrical properties of EPDM/SBR blends with reference to blend composition, cross-linking systems and compatibilization.

8.2.3 Effects of other types of fillers

The effective reinforcement of fillers in blends depends on their affinity towards the blend components and also on their distribution and dispersion in each phase of

the blends. It will be exciting to examine the effect of various powderous and fibrous fillers especially nano fillers on the physical properties of SBR/EVA blends.

8.2.4 Oil resistant and heat resistant polymers

The examination of the possibility of increasing the oil resistant properties of the blends by incorporating an oil resistant elastomer, such as NBR is an extension to the present work. Treatments with fire resistant chemicals for enhanced fire resistant behaviour can also be done.

8.2.5 Fabrication of useful products

The optimization of formulations and processing characteristics to develop different products, in consultation with industry, based on the present blend system can be tried.

List of publications in international journals:

1. “Mechanical and Ageing properties of cross linked Ethylene Propylene Diene Rubber/ Styrene Butadiene Rubber Blends” T. Muraleedharan Nair, M.G. Kumaran and G. Unnikrishnan Published in *Journal of Applied Polymer Science*, vol-93 2606-2621 (2004).
2. “Thermogravimetric (TGA) and Differential Scanning Calorimetric (DSC) Analyses of EPDM/SBR Blends” T. Muraleedharan Nair, M.G. Kumaran, G.Unnikrishnan, and Sam Kunchandy *Journal of Thermal Analysis and Calorimetry (Communicated)*.
3. “Ageing Studies on EPDM/SBR Blends; Effects of Ozone, Heat, Gamma Radiation and Water” T. Muraleedharan Nair, M.G. Kumaran, G. Unnikrishnan and Sam Kunchandy *Polymer Degradation and Stability (Communicated)*.
4. “Effects of higher non-black filler loadings on the mechanical properties of Ethylene propylene diene monomer-Natural rubber blends” Sam Kunchandy and T. Muraleedharan Nair Published in *Asian Journal of Chemistry*, vol. 18, 3017-3021 (2006).

भारतीय विज्ञान संस्थान
भारत
मुंबई

संख्या: T162
दिनांक: 11/11/08

CURRICULUM VITAE

Name	MURALEEDHARAN NAIR T.
Age and Date of Birth	49, 08.02.1957
Address for correspondence	<i>Technical Assistant (CT), Department of Industries and Commerce, Common Facility Service Centre, Industrial Nagar P.O, Changanacherry – 686 106, Kerala, India. Phone: 0481-2400526, 9388479254 Email: mdnair@yahoo.com</i>
Permanent Address	PARVANENDU, Vidya Nagar, Perunnai East, Changanacherry-686 102, Kerala, India.
Sex	Male
Nationality	Indian
Educational Qualification	M.Sc in Chemistry
Research Interest	<ol style="list-style-type: none">1. Polymer Blends: Development & Characterization2. Compound Development3. Testing4. Problem Solving5. Reverse Engineering
Work Experience	<ol style="list-style-type: none">1. Possess 22 years of experience in polymer field under the Industries Department, Govt. of Kerala and continuing in Govt. Service.2. Worked as Manager (Compound Development & Testing) in a US based Laboratory (ARDL-India, Kakkanadu, Cochin).
03-04-2006	Muraleedharan Nair T.